BIOGEOCHEMICAL AND HYDROLOGIC CONTROLS ON SOLUTE SOURCES AND CYCLING IN A BIOLOGICALLY PRODUCTIVE KARST RIVER

By

MARIE JULIETTE KURZ

A DISSERTATION PRESENTED TO THE GRADUATE SCHOOL
OF THE UNIVERSITY OF FLORIDA IN PARTIAL FULFILLMENT
OF THE REQUIREMENTS FOR THE DEGREE OF
DOCTOR OF PHILOSOPHY

UNIVERSITY OF FLORIDA

2013

To Mom and Dad

ACKNOWLEDGMENTS

I would like to thank my advisor, Jon Martin, my co-authors, Matt Cohen, Veronique de Montety, Rachel Douglass, and Chad Foster, and my additional committee members, Liz Screaton, Pete Adams, and Mark Brown for their invaluable support of this research. Thanks also go to Jason Curtis, George Kamenov, Jin Jin, Amy Brown, Mitra Khadka, John Ezell, and Carolyn Ball for their support in the lab and field. I would like to acknowledge the Ichetucknee Springs State Park for the support of their staff, and the United States Geological Survey and Florida Automated Weather Network for the data they provided. This research was supported by the National Science Foundation through research grant EAR0838360, and the Integrated Graduate Education and Research Traineeship program # 0504422, Adaptive Management of Water, Watersheds & Wetlands.

TABLE OF CONTENTS

page

LIST OF TABLES

LIST OF FIGURES

Abstract of Dissertation Presented to the Graduate School
of the University of Florida in Partial Fulfillment of the
Requirements for the Degree of Doctor of Philosophy

BIOGEOCHEMICAL AND HYDROLOGIC CONTROLS ON SOLUTE SOURCES AND CYCLING IN A BIOLOGICALLY PRODUCTIVE KARST RIVER

By

Marie Juliette Kurz

August 2013

Chair: Jonathan B. Martin
Major: Geology

Multiple, coupled physical, chemical and biologic processes control the sources and cycling of solutes in streams; however, the relative magnitude and temporal variability of individual processes can be difficult to differentiate in large river systems. Understanding timing and magnitudes of these processes is critical to preserving water quality and ecological health of stream systems and predicting their responses to environmental change. This dissertation investigates the hydrologic and biogeochemical controls on the sources and cycling of solutes, particularly trace metals, within the Ichetucknee River, a large, spring-fed river in north-central Florida. The stable chemical composition and discharge, high clarity and biologic productivity, and minimal hyporheic exchange of the Ichetucknee River provides a model system for distinguishing the processes controlling solute sources and cycling.

High-frequency river and synoptic pore-water sampling, combined with measurements of submerged vegetation stoichiometry and long-term records of river and pore-water hydrology were used to investigate the biogeochemical controls on in-stream solute cycling at diel (24-hour) frequency, the relationship between solute cycling and aquatic vegetation stoichiometry and functioning, and the significance of

diffuse groundwater discharge as a unique source of solutes to the river ecosystem. Multiple overlapping inorganic processes, indirectly and directly the result of solar radiation and submerged plant metabolism control the in-river cycling of Ca, Mn, Ba, Fe, U, and Sr at diel frequencies. Plant metabolism also directly controls the diel variations of trace metal concentrations via assimilatory uptake, although the exact timing of assimilation relative to the other inorganic controls remains uncertain. Diffuse groundwater discharge passing through the chemically distinct hyporheic zone provides a unique source of additional Fe, Mn, P, Ca and Cl to the river, partially offsetting the solute removal by the diel processes. By mediating the availability of nutrients to the aquatic ecosystem, diel variation and diffuse groundwater inputs in turn affect the productivity and relative abundance of benthic algae and submerge macrophytes. These results illustrate the reciprocal interactions between the sources and cycling of solutes in streams and the elemental requirements of submerged aquatic vegetation, and highlight the significance of these interactions even to systems where the individual effects are indistinguishable.

CHAPTER 1
INTRODUCTORY REMARKS

Controls on the Sources and Cycling of Solutes in Streams

Understanding the processes controlling the transport and cycling of solutes to and within streams is critical to preserving the water quality, ecological health, and ecosystem services of stream systems and anticipating their response to environmental change. The processes controlling solute dynamics can be physical, chemical and biologic and can be coupled over a wide range of temporal and spatial scales. The transport of solutes through catchments and into streams is inherently linked to the sources and physical flowpaths of water (Figure 1-1). Climate and landscape characteristics, including land use patterns and surface hydrology, control the recharge of water and solutes to the groundwater system. Within the groundwater system the flow path, mixing, residence time and interactions with the aquifer material can all influence the transport of water and solutes (e.g. Moore et al., 2009; Perrin et al., 2007). The delivery of water and solutes to streams can occur either at sites of point discharge at springs, or diffusely through the stream channel. Once in the stream, water and solutes are transported downstream although this transport may be retarded by processes such as cycling through the stream bed hyporheic zone. In addition to processes controlling the physical transport of solutes into and within streams, numerous biogeochemical processes also control the chemical exchange of solutes between reactive sites, including changes in speciation and phase, sorption/desorption, and biological uptake (Stream Solute Workshop, 1990).

Reciprocal Interactions with Stream Ecosystems

Stream ecology, in particular in-stream vegetation, both responds to and controls the physical and biogeochemical transport and cycling of solutes within streams (Clark, 2002). The environmental availability of nutrients required for metabolism controls the productivity, distribution and species abundance of vegetation within stream ecosystems. In return vegetation controls the biogeochemical cycling of solutes, and act as ecological engineers to modify the hydrologic controls on solute transport and cycling. Hyporheic exchange and diel variations are two examples of processes where clear reciprocal feedbacks exist between aquatic vegetation and in-stream biogeochemical cycling and/or physical solute transport. Although these feedbacks between vegetation and solute dynamics should exist in almost all streams, the magnitude of the effects, and therefore the ability to distinguish them relative to other controls on solute transport and cycling, should be most apparent in systems with high aquatic biomass and autotrophic productivity.

The Hyporheic Zone

The hyporheic zone occurs at the boundary between the surface water of a stream and the underlying groundwater, where infiltrating stream water mixes with shallow groundwater. The chemical and biological alteration of solutes within the hyporheic zone coupled with the physical exchange of of water and solutes control the functional significance of the hyporheic zone with respect to solute sourcing and cycling in streams. Localized upwelling of hyporheic water and solutes can influence both the distribution and productivity of aquatic vegetation in streams. For example, localized upwelling of water from the hyporheic zone has been shown to enhance localized species richness and productivity, when the upwelling water is enriched in N and P (e.g.

Mouw et al., 2009; Claret and Fontvielle, 1997; Valett et al., 1994; Grimm et al., 1991), but also to be toxic to localized growth when the upwelling and/or hyporheic pore water is oxygen-depleted (Sand-Jenzen et al., 1982). In return, the presence of aquatic vegetation can control both the chemical exchange and physical transport of solutes into and out of the hyporheic zone. For example, oxygen released from macrophytes roots controls the speciation and sorption reactivity of solutes beneath the streambed (Clark, 2002), and dense beds of vegetation can act as obstacles on the streambed surface and drive local advective subsurface exchange (Salehin et al., 2003).

Diel In-Stream Variations

Many of the biogeochemical processes that can control the cycling of solutes in streams operate on diel (24-hour) time scales in response to the solar photocycle (e.g. Nimick et al., 2011 and references therein). The metabolism of submerged aquatic vegetation, responding to this photocycle, can control the cycling of solutes directly, via biological uptake (e.g. Heffernan and Cohen, 2010; Cohen et al. 2013), and indirectly by controlling the contribution of dissolved oxygen and carbon dioxide to the stream and as a result the speciation and adsorptive reactivity of solutes. Depending on the timing of the changes in stream water composition related to biological processes, the phase of diel variations in element concentrations may shift relative to the solar cycle. Changes in speciation and reactivity can affect the environmental bio-availability of dissolved solutes within the river and therefore the composition, productivity and functioning of aquatic vegetation with relatively constant nutrient requirements.

Although processes controlling diel variation do not depend on the solute concentration, much of the existing work on diel variation in streams has, not surprisingly, focused on systems with elevated concentrations of the solutes being

investigated. I.e. spring-fed streams in karst terrains for studies in diel carbonate cycles (e.g. de Montety et al., 2011; Lui et al., 2008; Drysdale et al., 2003), and streams draining mining lands in diel metals studies (Gammons et al., 2007; Nimick et al., 2003; Schwartz and Ploethner, 2000). Although the metabolism of submerged vegetation may be significant in these systems, the direct effects of assimilatory uptake are likely minor compared to the abiotic controls on diel variation.

Florida's Spring-Fed Rivers

The abundant spring-fed rivers of northern Florida provide model systems to study the interactions between hydrologic, geochemical and ecological processes that control the sources and cycling of solutes within streams. Most of Florida's springs are sourced by the Floridan Aquifer, an eogenetic (Vacher and Mylroie, 2002) carbonate karst aquifer characterized by high matrix storage (Budd and Vacher, 2004; Florea and Vacher, 2006) and active conduit-matrix exchange (e.g., Martin and Dean, 2001; Bailly-Comte et al., 2010). These properties result in low temporal variability in discharge, temperature and chemical compositions over diel to longer (month – year) timescales. Long-term variation that does occur can generally be attributed to major climatic and weather events, such as tropical storms and, prolonged drought and excess evaporation occurring with the El Nino Southern Oscillation. These changes in precipitation can alter the relative contribution of groundwater from shallower and deeper flowpaths (Florea and Vacher, 2006; Martin and Gorden, 2000; Toth and Katz, 2006).

Florida's spring-fed rivers are, by definition, sourced entirely from groundwater and primarily from individual or groups of springs with characterizable source chemistry. Since this source chemistry is constant over time periods of weeks to years (e.g., Martin

and Gordon, 2000), element budgets can be constrained based on the characteristic composition of the springs, aiding in quantifying the temporal and longitudinal changes in river chemistry. This stability provides an ideal setting to study fine spatial and temporal scale variations in solute dynamics resulting from in-stream cycling and diffuse inputs at a resolution not possible in most river systems. Lastly, the hydrologic and chemical stability of the rivers, coupled with abundant solar radiation and high water clarity also allows Florida's spring-fed rivers to support dense, highly productive communities of aquatic macrophytes (Kurz et al., 2004; Odum, 1957). This high productivity enhances the effect that reciprocal feedbacks, between the aquatic vegetation and in-stream hydro-geochemical processes, have on the availability and cycling of solutes.

The Ichetucknee River, an entirely spring-fed system in north-central Florida, has been the focus of a number of studies investigating the biogeochemical processes, in particular aquatic plant metabolism, controlling the transport and cycling of solutes. Heffernan and Cohen (2010) and Heffernan et al. (2010) examined the nitrate dynamics in the river and found that nitrate removal was the result of denitrification, and assimilatory uptake by aquatic vegetation occurring with diel frequency. The high magnitude of denitrification was attributed to flow across the benthic surface and/or hyporheic exchange from the subsurface, although it was noted that the magnitude and distribution of hyporheic exchange within Florida's spring-fed rivers remained poorly understood. de Montety et al. (2011) examined the diel variation in carbonate within the river and determined that these were the result of the CO_2 consumption by submerged vegetation altering the pH and therefore the solubility of carbonate in the river. de

Montety et al. (2011) further suggested that the diel precipitation of calcite should affect the cycling of metals which co-precipitate with calcite, but did not identify this effect or its implications for control on the vegetation.

This Research

This dissertation addresses the processes controlling the cycling and sources of solutes, particularly trace metals, within the Ichetucknee River (e.g., Figure 1-1), giving particular focus to the feedbacks between these solute dynamics and submerged vegetation in the river. Chapter 2, in revision for *Chemical Geology*, investigates the direct and indirect control that the metabolism of submerged vegetation has on diel variation in trace metal chemistry of the river. Carbonate (co-)precipitation, pH-dependent adsorption reactions, and changes in redox state, all controlled by diel variation in dissolved oxygen and pH produced by submerged plant metabolism, in turn control the diel variation of Ca, Mn, Ba, Fe, U and Sr. Photo-reduction and temperature-dependent adsorption, unrelated to plant metabolism, may also control these metal cycles. Aquatic plant metabolism also directly control, to varying degrees, the diel variation in these metals via assimilatory uptake of metals as nutrients.

Chapter 3, in preparation for submission to *Limnology and Oceanography*, follows from work presented in chapter 2 on which metal exhibit diel cycles, and focuses on the relationship between the elemental requirements of the submerged vegetation, the availability of nutrients to the aquatic ecosystem, and the magnitude and timing of diel variations in river geochemistry. The stoichiometry of the submerged vegetation in the river is markedly similar to the average composition of terrestrial leaf biomass. There are, nonetheless, distinct differences between the average stoichiometry of the vascular and algal species, and systematic differences in the tissue stoichiometry of

both species which can be correlated to changes in the ambient water chemistry. These differences suggest that the two vegetation types may respond differently to changes in elemental availability and, conversely, that changes in the relative abundance of algae vs. vascular plants will lead to corresponding changes in the magnitude of assimilatory uptake and its control on the in-stream diel variation. Determining the timing of assimilation is confounded by limited understanding of the timing of biological demand for elements. Evaluating assimilatory uptake relative to the other inorganic controls on diel variation may be useful in determining the timing of uptake and improving our understanding of ecosystem function.

Finally, chapter 4, in preparation for submission to *Freshwater Science*, investigates the role of diffuse groundwater discharge passing through the hyporheic zone as a source of solutes to the river that is distinct and different from the source from springs. The hyporheic pore-waters of the river are enriched in Fe, Mn, P, and Ca, and depleted in N as the result of organic carbon remineralization, which alters the redox conditions, pH, and thus mineral solubility in the subsurface. Diffuse groundwater discharge to the river, the magnitude of which increases with stage and during the winter, provides a mechanism for transporting these enriched solutes into the river. This advective flux, in addition to varying amounts of diffuse flux, of solutes contributes to the downstream increase observed in Fe, P and Ca, and partially offsets the removal of Mn from the river by the diel processes. Together these three studies illustrate how the functioning of aquatic vegetation both controls the cycling of solutes in streams and is, in turn, controlled by this cycling which mediates the biological availability of elements in streams.

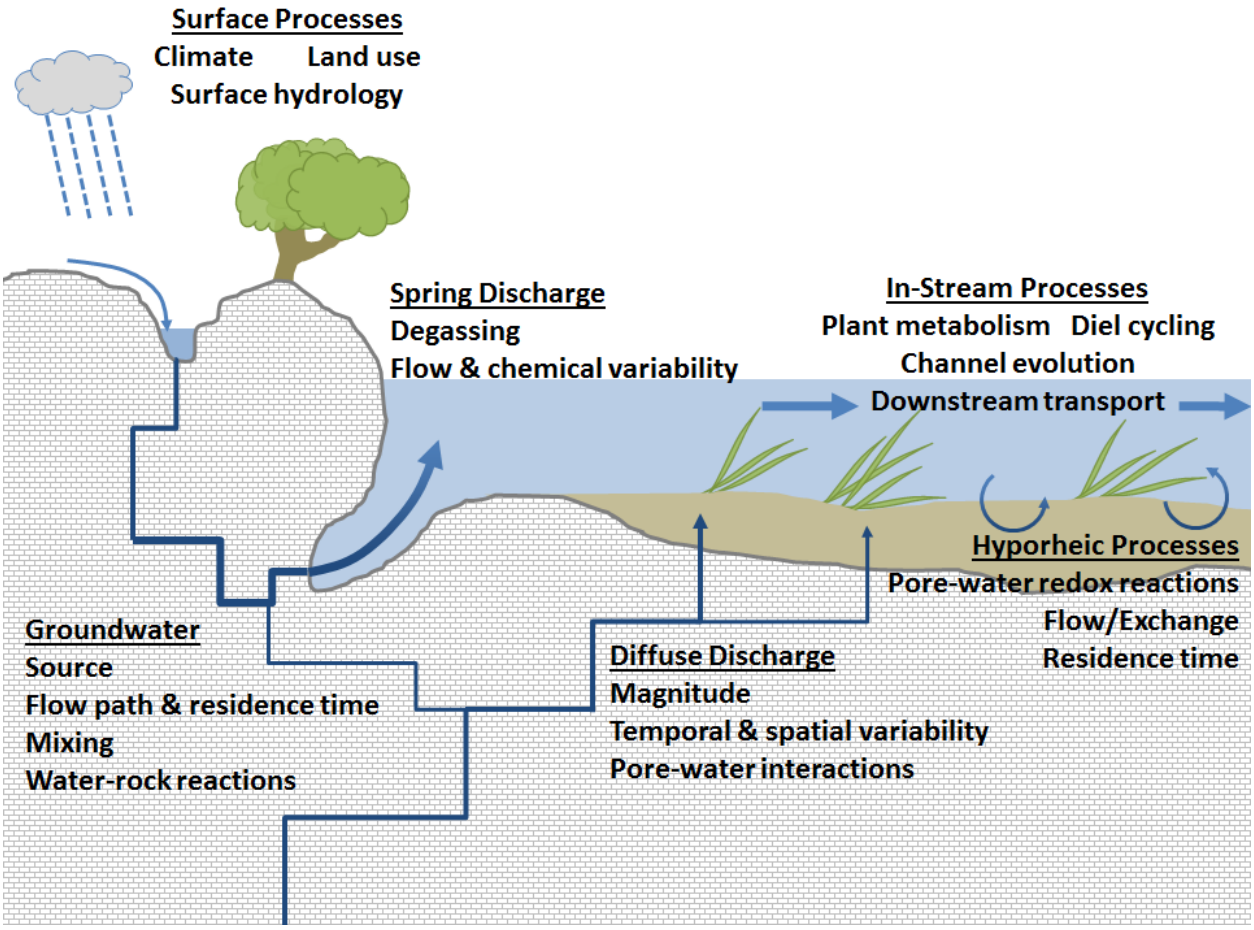

Figure 1-1. Processes controlling the sources and cycling of solutes within Florida's spring-fed rivers.

CHAPTER 2
CONTROLS ON DIEL METAL CYCLES IN A BIOLOGICALLY PRODUCTIVE CARBONATE-DOMINATED RIVER

Introduction

The chemical compositions of streams vary with diel (24-hr) periodicity as a result of the solar photo-cycle and associated biogeochemical processes. The most common and best understood of these processes is the photosynthesis and respiration of submerged aquatic vegetation which alternately produce and consume O_2 and CO_2, resulting in diel cycles in dissolved oxygen (DO) concentrations and pH (Clarke, 2002; Desmet et al., 2008; Odum, 1956; Simonsen and Harremoës, 1978). These processes change pH, mineral saturation state, and redox conditions thereby possibly indirectly controlling the diel cycling of metals. Diel metal cycles may also be directly controlled if assimilated as micronutrients by aquatic plants during primary productivity. Consequently, diel cycles of metal concentrations in streams, if present, are likely the result of multiple geochemical and biological processes, which may be out of phase with each other and with solar radiation, thereby complicating our ability to determine which processes affect metal concentrations (e.g., Cohen et al., in press).

Diel metal cycles exhibit the highest variability in streams with elevated metal concentrations, such as those draining abandoned mine lands, and consequently much prior research has focused on this type of system (e.g., Gammons et al., 2005 & 2007; Nimick et al., 2003; 2011; Schwartz and Ploethner, 2000). In these systems abiotic processes, such as variability in metal speciation and solubility controlled by photo-reactions, can be sufficient to explain observed diel metal cycles (e.g., Borman et al., 2010; McKnight et al., 2001), although, biofilms and submerged macrophytes have

been shown to indirectly enhance or control these inorganic processes (e.g. Jones et al., 2004; Morris et al., 2005; Shope et al., 2006).

Considerably less work has focused on non-polluted streams with naturally low concentrations of metals. In these systems the direct and indirect effects of submerged plant metabolism may be critical in controlling the availability and diel cycling of metals. The primary production of aquatic vegetation responds to, and in turn alters, environmental availability of elements (Sterner and Elser, 2002). Plants require certain elements, both macro- and micro-nutrients, in particular and generally constrained proportions during growth for metabolic functions (Elser et al., 2003) and to maintain compositionally homeostatic biomass (Frost et al. 2005, Kerkhoff et al. 2005). However, biomass stoichiometry (commonly assessed as elemental/C ratios) may also adjust in response to changes in element availability and light (Persson et al., 2010; Sterner et al., 1998), as may the relative abundance of plant species with varying elemental requirements (Hall, 2004). A better understanding of the reciprocal interactions between biological and geochemical processes controlling the cycling and availability of metals is therefore critical not only for managing water quality, assessing trace metal mobility, but also to evaluating the structure and health of stream ecosystems, particularly in systems where low concentrations may create micronutrient limitation.

Precipitation and dissolution of carbonate minerals may control diel metal cycling, particularly in high pH systems at or near carbonate mineral saturation. Ecosystem metabolism regulates the saturation state of carbonate minerals, by increasing pH during the day in response to autotophic assimilation of bicarbonate, and decreasing pH at night due to respiration (de Montety et al., 2011; Liu et al., 2006; 2008; Spiro and

Pentecost, 1991). Carbonate precipitation should decrease, and dissolution increase, Ca^{2+} concentrations, although these changes are not always observed in supersaturated streams (Neal et al., 2002; Parker et al., 2007; Usdowski et al., 1979). Nonetheless, precipitation and dissolution of calcite could influence concentrations of divalent metals that partition strongly with calcite, such as Cd, Mn, Fe, and Zn (Dromgoole and Walter, 1990; Lorens, 1981; Nimick et al., 2003; Parker et al., 2007; Tesoriero and Pankow, 1996). This co-precipitation has been observed to remove Cd, Cu, Mn, Pb and Zn with distance downstream (Schwartz and Ploethner, 2000) and to create simultaneous cycles of Cd concentrations and carbonate precipitation and dissolution in a eutrophic lake (Cicerone et al., 1999). At low concentrations, adsorption of divalent metals to calcite surfaces may also affect dissolved metal concentrations (Mettler et al., 2009; Zachara et al., 1991). Diel cycles of some dissolved metals may therefore be linked to variations in saturation state and resulting precipitation or dissolution of calcite, caused by photosynthesis and respiration.

Previous work has identified a number of other inorganic processes which can control diel cycling of metals in streams, many of which are also regulated by metabolism. In systems with elevated metal concentrations, redox state has been shown to control diel cycles in dissolved Fe and Mn through both photochemical reactions and metabolically enhanced oxidation processes. Daytime increases in Fe and Mn concentrations have been attributed to photo-reduction of Fe- and Mn-oxides (Gammons et al., 2005; McKnight et al., 1988; Sullivan et al., 1998; Sunda and Huntsman, 1994). However, photo-reduction reaction rates are pH controlled and photo-reduction is not expected to be a major control on diel Fe cycles in pH-neutral to

basic streams (Borman et al., 2010; McKnight et al., 2001; Parker et al., 2008). Instead, dissolved Fe and Mn concentrations typically decrease during the day in streams with high pH, suggesting the diel cycles of these metals may be primarily controlled by increased daytime oxidation as a result of photosynthesis or microbially mediated oxidation (Brick and Moore, 1996; Parker et al., 2007; Scott et al., 2002), the rate of which is further enhanced by daytime increases in pH (Stumm and Morgan, 1996).

Adsorption reactions are also pH- as well as temperature-dependent and can be influenced by the metabolically pH produced by submerged macrophytes and biofilms (e.g. Jones et al., 2004; Shope et al., 2006). Cation adsorption to substrates such as metal oxides and biofilms should increase with pH and temperature (Nimick et al., 2003 and references therein) and thus the concentrations of absorbing cationic species should decrease during the day. Conversely anionic absorption decreases with pH and temperature producing increased daytime concentrations in anionic species. Adsorption and sequestration of metals into biofilms has even been shown to control in-stream diel metal cycles in the absence of diel pH changes in the bulk water column by providing microenvironments unique from the bulk stream chemistry (e.g. Morris et al., 2005; 2006).

The phase and amplitude of diel cycles as well as seasonal changes in the cycles are critical to assess overlapping geochemical and biological processes that may be controlling diel metal cycling (e.g., Cohen et al., in press). The connection that diel cycling has to solar radiation, both indirectly through the co-precipitation with carbonate minerals and productivity of submerged vegetation and directly through photic-reactions, suggests that seasonal changes in solar radiation could affect both the timing

and magnitude of diel metal cycles. Variations at seasonal frequencies may help distinguish relative controls on diel cycling through comparison with changes in solar radiation and plant metabolism at annual periodicities. Such an evaluation requires observing a model system with little seasonal changes in flow to minimize complications caused by changes in hydrologic characteristics including variations in discharge and water compositions (e.g. Nimick et al. 2005; Sullivan and Drever, 2001).

In this study, we assess the presence of and controls on diel metal cycles across a range of seasons in the Ichetucknee River, an entirely spring-fed river in north-central Florida characterized by neutral to basic pH, low metal concentrations, and high primary productivity. Florida's karstic, spring-fed rivers, including the Ichetucknee River, have stable chemical compositions and discharge, extreme water clarity and thus high productivity, which make them ideal for this study. We hypothesized that diel cycles of metals in the Ichetucknee River may be controlled directly by metabolism of submerged vegetation via autotrophic assimilation (e.g., Heffernan and Cohen, 2010; Cohen et al., in press; Roberts and Mulholland; 2007) and indirectly via co-precipitation with calcium-carbonate (e.g., de Montety et al., 2011). To test this hypothesis, we compare observations of magnitude and phases of the metal cycles with calculations of predicted removal due to these processes, as well as changes in redox chemistry and adsorption. Because multiple processes may control metal concentrations, we are unable to uniquely identify the magnitude of each process, but we are able to show which processes are likely to have primary or secondary affects, or have no effect, over diel metal cycles. This improved understanding of the controls on metal cycling in pristine streams will be important for monitoring of water quality and assessing the potential

effects of metals as micro-nutrients on primary production in streams with abundant submerged vegetation.

Methods

Study Site

The Ichetucknee River is fed by eight named springs and numerous small unnamed springs. The river flows approximately eight kilometers before discharging into the Santa Fe River, a tributary of the Suwannee River. The springs feeding the river are sourced from the Floridan Aquifer, an eogenetic carbonate karst aquifer (Vacher and Mylroie, 2002) characterized by high matrix storage (Budd and Vacher, 2004; Florea and Vacher, 2006) and active conduit-matrix exchange (e.g., Martin and Dean, 2001; Bailly-Comte et al., 2010). The springs drain an estimated 960 km^2 springshed (Champion and Upchurch, 2006) that includes both confined and unconfined areas of the Floridan Aquifer (Figure 2-1A & B). The Ichetucknee River, in the southern, unconfined portion of the springshed, flows directly on top of the Ocala Limestone, which comprises the Floridan Aquifer. The gradient along the entire river is less than 2 m/km and, although there is little evidence for physical erosion, bedrock is increasingly exposed downstream in and along the channel. The entire study area is within the boundaries of Ichetucknee Springs State Park and thus land use immediately surrounding the river is pristine, although much of the springshed is improved pasture. The downstream end of the study area is marked by the US 27 highway bridge (Figure 2-1C), which in this study is referred to as the US27 Bridge sampling site and is also the location for a USGS gaging station (# 02322700). This gaging station, as well as ones at the largest spring (Blue Hole) and midway down the river (Dampier's Landing; Figure 2-1C) provide stage and discharge data at 15-minute increments. The four next largest

springs were similarly monitored from February 2002 to March 2010. River discharge at the US27 Bridge has ranged from 5.7 to 14.3 m^3/s over the eight-year monitoring period but exhibits no diel trends in the 15-minute data.

Although each spring has unique chemistry, reflecting sources from different portions of the aquifer, the individual springs exhibit relatively little change in chemical composition through time (Martin and Gordon, 2000). Water quality of the river is excellent (FDEP, 2006), with high water clarity (horizontal secchi distances of tens of meters; Anastasiou, 2006), low turbidity (<1 NTU; Heffernan and Cohen, 2010) and low to negligible dissolved organic carbon (DOC) concentrations (1.6 ± 1 mg/L). Warm waters (> 19°C) and abundant light result in dense submerged vegetation (submerged macrophytes and filamentous algae), which cover up to 78% of the river bed (Kurz et al., 2004). High primary productivity results in distinct diel fluctuations in nitrate (Heffernan et al., 2010), carbonate (de Montety et al., 2011) and phosphate (Cohen et al., in press). Heffernan et al. (2010) found productivity was greater than other rivers with similar discharge because of the clarity of the water. The water remains consistently at or above saturation with respect to calcite throughout the day and night (de Montety et al., 2011). Authigenic calcite has not been found in the river although diel variations in Ca^{2+} concentrations, corresponding to the variations in saturation index, suggest that calcite precipitates during daylight hours.

Water Sampling Procedure

Three sampling surveys were conducted at the US27 Bridge sampling site in March 2009, November 2009, and May 2010 to assess diel cycles in river chemistry across different seasons. USGS stream discharge measurements were available at the US27 Bridge during all three surveys. Solar intensity and precipitation data were

obtained in continuous 15-minute increments from the Florida Automated Weather Network (FAWN; http://fawn.ifas.ufl.edu) site in the town of Alachua, ~20 km from the field site. The March 2009 survey was conducted during cloudy weather conditions, with hourly sampling frequency for 24 hours from 3/26/2009 16:00 to 3/27/2009 16:00. The November 2009 survey was conducted during clear conditions, with 2-hr sampling frequency for 30 hours, from 11/2/2009 00:00 to 11/3/2009 6:00. The May 2010 survey was conducted during clear conditions, at hourly frequency for 48 combined hours from 5/12/2010 17:00 to 5/13/2010 10:00 and 5/14/2010 11:00 to 5/15/2010 13:00.

The field parameters (temperature, specific conductivity, pH, and DO concentration) were recorded in the river at 1-hour intervals by a YSI 6920 sonde and NO_3^- concentrations at 15-minute intervals by a SUNA (Submersible UV Nitrate Analyzer; Satlantic Corporation, Halifax, Nova Scotia) in-situ nitrate sensor. Both sensors were calibrated in the lab prior to deployment and the calibration was verified in the lab after deployment. River samples were collected by an ISCO autosampler in 1 L bottles triple washed with deionized water prior to sampling and reuse. Autosampler bottles were kept chilled with ice to preserve the samples during storage in the ISCO. ISCO samples were filtered and preserved for analysis, in the order they were collected, with a maximum delay between collection and preservation of 15 hours for the first sample. To test for possible changes in concentration during ISCO storage, grab samples were collected simultaneously with samples stored for the longest period of time in the ISCO. The grab samples were preserved immediately and their concentrations were compared with those samples collected and stored by the ISCO.

With the exception of Cu and Zn the difference between these ISCO duplicates was within analytical error (Table 2-1).

Unfiltered samples for inorganic carbon concentrations and carbon stable isotope ($\delta^{13}C_{IC}$) analysis were preserved with three drops of saturated $HgCl_2$ solution in 30 ml glass vials. Although these samples were not filtered, duplicate filtered and unfiltered samples show no difference in inorganic carbon concentrations or $\delta^{13}C$ values. Samples for metal, cation, anion, and alkalinity analysis were filtered through trace-metal grade 0.45 µm cellulose acetate membranes and stored in separate, high density polyethylene (HDPE) vials. Samples for cation and metal analysis were collected in acid washed 20 ml vials and the samples were preserved with 3 drops of concentrated trace-metal grade HNO_3^-. Filtered samples were also collected for dissolved organic carbon (DOC) (collected only in November 2009 and May 2010) in ashed 40 ml amber glass vials and preserved with three drops of HCl. The six main springs of the river were manually sampled during each survey using these same methods. The field parameters of the springs were measured with a calibrated YSI 556 MPS. All samples were kept chilled until analysis.

Water Sample Analytical Methods

Samples were analyzed for alkalinity, major and selected trace element concentrations, including Cl^-, Ca^{2+}, total dissolved Al, Mn, Fe, Cu, Zn, Sr, Ba, and U, DOC, inorganic carbon, and $\delta^{13}C_{IC}$. Total alkalinity was titrated within 24 hours of sampling using 15 ml of sample and 0.1 N HCl with a precision of 3% based on replicates of 7 different samples. The difference between duplicate grab samples titrated in the field and ISCO samples titrated 20-24 hours after collection was <1%. Major element chemistry was measured with an automated Dionex DX500 Ion

Chromatograph with precision of better than 3% for all runs and elements based on repeated measurements of internal standards. Charge balance errors were less than 3%, except for the May survey when charge balance could not be determined due to errors in the alkalinity data. DOC samples were analyzed on a Shimadzu TOC-5000A total organic carbon analyzer after sparging for 2 minutes with carbon-free air to remove inorganic C. Three to five injections of a 60 µL sample were measured and the mean of the injections was reported. Replicates of each sample had <5% coefficient of variance. Inorganic carbon concentrations were measured on CO_2 extracted by acidifying samples using an AutoMate Prep Device coupled with a UIC (Coulometrics) 5011 carbon coulometer. The method was standardized with dissolved $KHCO_3$. Data accuracy was better than ±0.015 mM for all runs. $\delta^{13}C_{IC}$ samples were acidified in Labco Exetainer tubes and the liberated CO_2 analyzed using a Thermo-Finnigan GasBench II coupled with a Thermo-Finnigan DeltaPlusXL isotope ratio mass spectrometer. Dissolved $KHCO_3$ was again used for isotopic standardization, with a precision of better than 0.09‰ for all runs. The isotopic data are reported in the conventional delta notation (‰) versus V-PDB. Metal concentrations were measured using a HR ICP-MS Element 2 (Thermo Finnigan). The precision and accuracy of the technique were calculated by comparing multiple measurements of the external standard SLRS4 (Canadian river water standard) (Table 2-1).

Speciation of the dissolved metals, as well as the saturation indices of major metal-carbonate and metal-oxide minerals were estimated based on the field parameters and the measured major element, trace metal and inorganic carbon concentrations using the geochemical modeling program PHREEQC (Parkhurst and

Appelo, 1999). Inorganic carbon concentration measurements were used in the place of alkalinity measurements for these calculations because of the lack of alkalinity data for some samples.

A simple analytical model was developed to test for the presence of diel cycles in the river time-series data and to quantify the phase, amplitude, and significance of those cycles. The model fits a sine function with 24-hr periodicity to the time-series data providing the mean, amplitude and phase of the cycle:

$$E_t = M + A \cdot \left[\cos\left(t \cdot 360 \cdot \pi \cdot 180^{-1}\right) - \left(P \cdot \pi \cdot 180^{-1}\right)\right] \quad (2\text{-}1)$$

where E_t is the model estimate at time t, t is the hour of the day, M is the mean value of the time series, A is the amplitude of the diel cycle, and P is the time phase of the cycle. The 3 parameters (M, A, and P) were adjusted using a generalized reduced gradient approach (Solver function in Microsoft Excel) to minimize the sum of squared errors between the model and measured data. For statistical comparison a second 1 parameter null model was calculated fitting the measured values to the mean value of the time series, M, e.g.:

$$E_t = M \quad (2\text{-}2)$$

The statistical significance of each diel cycle was determined by calculating the F-statistic for the sine model in comparison with the null model:

$$F = \frac{\left(RSS_N - RSS_S\right) \cdot df1^{-1}}{RSS_S \cdot df2^{-1}} \quad (2\text{-}3)$$

where RSS_N is the sum of the squared errors from the null model, RSS_S is the sum of the squared errors from the sine model, *df1* is the difference in the number of parameters in the two models and *df2* is the number of observations, n, minus the

number of parameters in the sine model. The statistical significance (p-value) of the sine model was evaluated using an F-distribution with *df1* = 2 and *df2* = *n*-3. The time-series was considered to have a significant diel cycle if the p-value was < 0.1.

Plant Tissue Sampling Procedure and Analytical Methods

Plant tissue samples were collected at 10 sites on the river, located roughly every 500m from the source springs to the US27 Bridge. Tissue material was collected from the vascular plant (*Sagittaria kurziana*) and algal (*Vaucheria* sp.) species that dominated benthic cover at all sites. To the extent possible only new growth tissue was collected as this should most closely reflect current water chemistry and was the least colonized by epiphytic mineral and algal growth. For the vascular plant species *S. kurziana,* whole leaf blades were collected from several individual plants, and composited.

Plant tissue samples were cleaned of any foreign material, washed in distilled water, dried and lightly crushed. The dried tissue samples were analyzed for total C concentration using a Carlo Erba NA1500 CNS elemental analyzer with Atropine as an internal standard. In preparation for major and trace element analysis a portion of the dried samples were ashed at 550 °C and digested using the procedure described in Kamenov et al. (2009). Element concentrations were measured on an HR Element 2 ICP-MS with Re and Rh used as internal standards. Major element analysis was calibrated using USGS rock standards BIR-1, BCR-2 and AGV-1, and trace element analysis was calibrated using gravimetrically prepared standards purchased from QCD Analysts. The recovery of our preparation and analysis technique was checked using the external standard, Standard Reference Material 1515 (apple leaves), certified by the National Institute of Standards.

Diel Flux, Co-Precipitation, and Assimilation Calculations

The removal rate of each metal (*Me*) from the river system, i.e. the mass of metals removed from the dissolved form, referred to here as the 'observed diel flux', was calculated from the total change in dissolved mass in the water column over a 24-hour period (in *moles* m^{-2} d^{-1}) using the equation:

$$\text{Observed diel flux} = \sum_{t=1}^{24} (Me_{\max} - Me_t) \cdot Q \cdot A_B^{-1} \qquad (2\text{-}4)$$

where the difference between the maximum measured concentration (Me_{max}) and the observed diel variation (Me_t), was multiplied by river discharge (Q) at time t, and normalized to the stream-bed area (A_B = 153,000 m^2). Observed diel flux is reported per unit stream-bed area per time to be consistent with reported measures of ecosystem metabolism. The calculations of observed diel flux were compared with calculations of metal uptake by processes that may control the observed cycles in order to provide an estimate of the importance of those uptake processes relative to the magnitude of the observed diel cycles.

The amount of metals co-precipitated with authigenic calcite were estimated using the measured solution composition and distribution coefficients (D) of the partitioning reaction as defined by:

$$(Me/Ca)_{CaCO3(s)} = D\ (Me^{2+}/Ca^{2+})_{solution} \qquad (2\text{-}5)$$

Multiplying the calculated *Me*/*Ca* ratio of calcite by the corresponding Ca^{2+} concentration in the water and summing values over a complete 24 hour cycle yields the daily loss from the river due to metal partitioning in a solid solution with calcite. Upper and lower limits of estimated metal loss were calculated using a maximum and minimum distribution coefficient based on a range of values reported in the literature

(Dromgoole and Walter, 1990; Kitano et al., 1971; Lorens, 1981; Mettler et al., 2009; Tesoriero and Pankow, 1996; Zachara et al., 1991).

Metal uptake due to autotrophic assimilation was also calculated for each sampling period by multiplying the daily net primary productivity (NPP; moles-C m^{-2} day^{-1}), i.e. the net carbon flux into biomass, by the average Metal:Carbon stoichiometric ratios from both the vascular and algal tissue samples. Daily gross primary productivity (GPP; moles-C day^{-1}) in the river was determined from the diel variations in oxygen concentrations using the single station oxygen metabolism method (Odum, 1957) and corrected for reaeration based on the slope of the nighttime association between DO saturation and hourly DO changes (Owens 1974, Heffernan and Cohen, 2010). GPP was converted to NPP using the assumption that autotrophic respiration is equal to 50% of GPP (Hall and Tank, 2003); recent efforts to empirically estimate autotrophic respiration validate this assumption (Hall and Beaulieu, 2013). NPP is reported normalized to the area of the stream bed (A_B = 153,000 m^2). The Metal:Carbon stoichiometry of the vascular and algae tissue samples was converted from the measured metal concentrations in the biomass (mg-*Me*/kg-biomass) using the measured weight percent of carbon in the samples. It is assumed that the autotrophic assimilation of metals occurs in proportion to the stoichiometry measured in the tissue samples.

Results

Field Parameters, NO_3^-, Cl^-, Ca^{2+}, DOC, and DIC Concentrations, and $\delta^{13}C$ Values

Results for water temperature, solar radiation, DO concentration, pH, Cl^-, NO_3^-, and DOC concentrations, and discharge during the three sampling periods are shown in Figure 2-2. Table 2-2 summarizes the mean, amplitude, and timing of the diel cycles,

based on Eq. (2-1), for these and all other river chemical parameters. The most distinct diel cycles occurred in parameters that are directly controlled by solar radiation or plant metabolism: water temperature, pH, DO, and NO_3^- concentrations. All three sampling surveys were conducted during periods of stable discharge with no precipitation although the discharge value increased from March 2009 to May 2010 (Figure 2-2). The length of daylight increased from 11:08, 12:17, and 13:23 hrs/day in November, March and May respectively. Despite the longer length of daylight and the sun's greater altitude in March, cloudy conditions resulted in the lowest total daily solar radiation (1,999 $W/m^2/d$) of the three sampling periods, compared to November (4,345 $W/m^2/d$) and May (6,430 $W/m^2/d$).

Variations in water temperature correlated with solar radiation at both diel and seasonal frequencies. The mean daily temperature increased from November to March to May, although the smallest daily range of temperature occurred in March, reflecting the cloudy conditions (Table 2-2). The diel cycles of DO and pH were nearly in phase, although the DO peak occurred just slightly before that of pH (Figure 2-3). The lowest mean values of pH and DO concentrations occurred in March, but the smallest amplitudes occurred in November (Figure 2-2 & Table 2-2). The diel cycling of NO_3^- was 12 hours out of phase with pH and DO, reflecting the daytime consumption of NO_3^-. Similar to pH and DO concentrations, the smallest amplitude in the diel cycle of NO_3^- concentrations occurred in November and the highest in May (Figure 2-2 & Table 2-2). Cl^- concentrations showed no statistically significant diel cycling in November or March, however a slight, but significant diel cycle in Cl^- concentrations occured in May (Figure 2-3), with an amplitude of 0.02 mM (Table 2-2). DOC concentrations showed no

statistically significant diel cycle (Figure 2-3). The unexplained spikes may be a filtration artifact from DOC filter bleed.

Results for Ca^{2+} and inorganic carbon concentrations, $\delta^{13}C_{IC}$ values, and calcite saturation index ($SI_{calcite}$) over the three sampling surveys are shown in Figure 2-4. Diel cycles in all of these parameters were observed during the three sampling surveys. $\delta^{13}C_{IC}$ and calcite saturation state where in phase with each other while Ca^{2+} and inorganic carbon concentrations lagged pH by nearly 15 hours (Figure 2-3). Calcium and inorganic carbon concentrations increased overnight to plateau from 01h – 11h with a slight peak in the late morning (07h – 13h) (Figure 2-4). The morning peak was followed by a sharp decline to an afternoon low at 16h – 18h that correlated to the peak in DO concentrations and pH (Figure 2-2). The magnitude of diel variability of inorganic carbon concentrations and $\delta^{13}C_{IC}$ values increased from November to March to May, following the same seasonal trend as day length, temperature, and ecosystem GPP. Ca^{2+} concentrations varied by 0.6 mM in March and May; however concentrations in November did not exhibit a significant diel cycle (Table 2-2 & Figure 2-3).

Metal Chemistry

Of the eight metals analyzed Fe, Ba, and U exhibit statistically significant diel cycles over all three sampling surveys (Figure 2-5). Mn and Sr exhibit significant cycles only in March, however the magnitude of the Sr cycle is minor (Figure 2-5, Table 2-2). Aluminum concentrations were below detection limits. Although Zn and Cu were measured, their coefficients of variation between the ISCO and grab samples was high (15% and 52% respectively) and the analytical precision for Zn was low (Table 2-1), hence these elements are not discussed further. The metals that do display diel cycles fall into two groups defined by the phase of their diel cycles. Ba, Mn, and Sr

concentrations exhibit maxima at night, in phase with the diel cycling of Ca^{2+} and inorganic carbon concentrations (Figure 2-3). Fe and U concentrations exhibit maxima during the day and have similar phases, although they range over about 3 hours. Phases of these metals lag solar radiation by around 4 to 7 hours and are similar to the phases of water temperature, pH, and DO concentrations (Figure 2-3).

Ba, Mn, and Sr

Diel cycles in Ba concentrations occurred during all three sampling surveys. The Ba cycle displays asymmetrical diel variation, with a rapid increase in concentrations between dusk and midnight compared to a slow decline through the day. This asymmetry is not replicated by the fitted diel sine function (Eq. (2-1)), which models the peak concentration to occur around dawn (Table 2-2; Figure 2-5). The magnitude of the diel cycle varies between the three sampling surveys but follows no apparent seasonal trend when compared to any of the other field parameters.

Manganese concentrations in March also exhibit an asymmetrical diel cycle with concentrations slowly increasing overnight, reaching a plateau in the morning (08hr – 12hr) before decreasing rapidly in the afternoon. Although both Mn and Ba concentrations decrease during the day there is about a 4 hour lag between the phases of Mn and Ba (Figure 2-3) as a result of asymmetry in the Mn cycle compared to relatively symmetric Ba cycle (Figure 2-5). In November, Mn concentrations followed the same pattern of nighttime increase to midmorning plateau; however, afternoon concentrations declined little, resulting in a stair-step increase in concentration over the observation period. Because of this trend, the data were not considered to have a statistically significant diel cycle (Table 2-2). Manganese data from the May sampling is not reported because of an apparent contamination in the ISCO samples.

Sr concentrations exhibit a significant diel cycle only during the March survey; however, the diel amplitude is only 9.8 µg/L, equivalent to a 6% increase over the minimum concentration (Figure 2-5). When present the Sr cycle is in phase with that of Ba (Figure 2-3A).

Fe and U

Fe and U exhibit diel cycles during all three sampling periods (Table 2-2). All concentrations increase during the day to reach maxima in the late afternoon, and then decline overnight (Figure 2-3 and 2-5). Peak Fe concentrations in March and November occurred at 15h-16h and decline to a minimum at 01h-02h (Figure 2-5). The phase of the Fe cycle during the May sampling period is shifted forward by about 6 hours compared with the other two sampling periods, which may be an artifact of the smaller amplitude of the diel variation than the other seasons. The highest Fe concentrations and the strongest diel variation occurred in March, when concentrations increased by 4.9 µg/L, or 139% over the minimum value during the day, reaching a maximum concentration of 8.46 µg/L. The low Fe concentrations for each sampling period prevented measurements of Fe^{2+} and Fe^{3+} concentrations. Speciation estimates by PHREEQC not surprisingly suggest that Fe^{3+} comprises over 99% of the total dissolved Fe during the day, however PHREEQC does not consider reactions such as photo-reduction which could affect the speciation of Fe. U maxima occurred in late afternoon (16hr – 19hr; Table 2-2). The highest concentrations (0.86 µg/L) and highest daily variation (0.16 µg/L) occurred in May. The amplitude of the diel signal increases from November to March to May following the same seasonal trend as DO and pH (Table 2-2).

Spring Input Concentrations

The metal concentrations in the springs and the measured or estimated spring discharge were used to calculate the flow-weighted average input concentration of each metal to the river (Figure 2-5). These calculations do not consider other sources of water, such as small ungaged springs or diffuse groundwater seepage, however, these inputs are assumed to be low. The spring input concentrations of Ba and U both fall within the range of the diel cycle measured downstream. Depending on the season, the concentrations of Fe and Sr are either equal to or increase from the springs to the downstream sampling location. In contrast, Mn, and to a lesser extent Ca^{2+}, are the only metals for which the concentrations decrease from the springs to the downstream sampling location.

Plant Metabolism, Stoichiometry and Assimilation

The stoichiometry was not identical between the algae and vascular plants in the Ichetucknee River. Fe and U concentrations were both an order of magnitude greater, while Ca^{2+} and Ba concentrations were approximately twice as concentrated in the algae as the vascular plants. In contrast, Mn is approximately twice as concentrated in the vascular plants (Table 2-5). Because of these differences, metal uptake due to autotrophic assimilation was estimated using both the stoichiometry of the vascular plants and algae (Table 2-5). The fraction of ecosystem NPP from each species is unknown so the total assimilatory uptake will fall between these two estimates. Ecosystem NPP in the Ichetucknee River increased from November to March to May (0.11, 0.12, and 0.26 mol-C/m^2/d respectively), following the same seasonal trend as day length.

Discussion

The springs sourcing the Ichetucknee River control the input of solutes to the river although additional sources of solutes from diffuse seepage from the Floridan Aquifer and/or diffusion from the anoxic porewaters of the benthic sediments (Figure 2-6). Fe and Mn concentrations in the porewaters are elevated above the average river water values (~ 2000 and 30 ppb, respectively) (Kurz et al., 2009). The high porewater Fe concentrations mean that small amounts of diffusive loss from the sediments could explain the increasing Fe concentrations downstream (Figure 2-5), but since seepage does not occur at a diel frequency, this process cannot control the observed Fe cycling. In contrast, Mn concentrations in both the porewaters and the source springs are elevated above the downstream concentrations reflecting a downstream loss of Mn from the river, and sinks for Mn, as discussed below.

Diel cycles in stream chemistry can result from variations in stream flow and shifts in source water as evapotranspiration along stream banks and floodplains varies over day-night cycles (e.g. Brick and Moore, 1996). These processes seem unlikely controls for the diel cycles in the Ichetucknee River. Discharge remained constant within the sampling periods, reflecting the short-term constant discharge from the source springs (Figure 2-2). The lack of diel cycles in Cl^- concentrations, which is conservative in this setting (Martin and Gordon, 2000), during the November and March sample periods (Figure 2-2) reflects a constant spring source to the river. Even the small Cl^- cycle during the May sampling period (variation of 0.04 mM, or 12% increase in concentration; Table 2-2 & Figure 2-3) is unlikely to reflect evapotranspiration, which would require a loss of 12% of the river discharge or about 1 m^3/day. This volume, distributed across the 25 ha of the river and flood plain, would require unreasonably

high daily evapotranspiration of 35 cm. The amplitude of the Cl^- cycle is smaller than that of the other solutes, suggesting that the process(es) controlling Cl^- cycling are minor compared to those of the reactive elements. The lack of evidence for flow controlling diel cycles indicates that biogeochemical processes, including carbonate precipitation and dissolution, changes in redox state, adsorption, and autotrophic assimilation, may control diel metal cycling in the Ichetucknee River. We discuss each of these processes below.

Effects of Diel Carbonate Chemistry and Calcite Precipitation

The increase in pH of 0.38 to 0.71 pH units caused by daytime photosynthesis results in a shift in the saturation state of calcite and aragonite from around saturation at night (minimum $SI_{calcite}$ = 0.00 - 0.24; minimum $SI_{aragonite}$ = -0.17 – 0.00) to supersaturation during the day (maximum $SI_{calcite}$ = 0.55 – 0.88; maximum $SI_{aragonite}$ = 0.40 – 0.68; Figure 2-4). The increased SI_{CaCO3} values during the day correspond to decreases in Ca^{2+} concentration, reflecting calcium-carbonate precipitation during the day. The nighttime increase in Ca^{2+} concentrations appears to reflect a return to the Ca^{2+} concentrations of the spring source water rather than nighttime carbonate dissolution based on the $\delta^{13}C_{IC}$ values and $SI_{calcite}$ values equal or greater than zero (de Montety et al., 2011).

Despite the evidence for daytime calcium carbonate precipitation massive authigenic calcite has not been observed to accumulate in the river. Massive calcite would not occur if precipitation occurred on the surface of subaquatic vegetation (e.g., Hoffer-French and Herman, 1989) or biofilms and algae where high pH microenvironments can cause photosynthesis-driven cycles of carbonate mineral precipitation (Hartley et al., 1996; Shiraishi et al., 2010). The precipitate may be

sufficiently fine grained to remain in suspension and be exported out of the Ichetucknee River in colloidal or fine-grained particulate form. Fine grained precipitation would contribute to observed increases in daytime turbidity (M.J. Cohen, unpubl. data). Calcite is also biogenically precipitated as shell material, contributing to the bed load transported downstream. Regardless of the mechanism, calcite precipitation should affect metal concentration at a magnitude related to the distribution of the metal into the calcite crystalline structure or adsorbed on the surface of the calcite.

Divalent metals both adsorb onto and co-precipitate with calcium carbonate (Mettler et al., 2009; Schwartz and Ploethener, 2000; Zachara et al., 1991; Kitano et al., 1971). Zachara et al. (1991) reported calcite sorption selectivity of Cd > Zn > Mn > Co > Ni >> Ba = Sr and Mettler et al. (2009) ranked the exchange constant (K_{ex}) of Fe^{2+} with calcite between that of Cd and Zn. These affinities have been correlated with the radii of the divalent metal cations relative to Ca^{2+}, as well as the solubility product of the metal-carbonate solid (Zachara et al., 1991). The incorporation of Sr and Ba into aragonite is about two orders of magnitude greater than into calcite, as a result of the ionic radii and aragonite crystal structure (Kitano et al., 1971). Solid solution of metals in calcium carbonate, quantified by distribution coefficients (e.g., Eq. (2-5)), follows the same trend and general magnitude of the exchange constants, although they often depend on precipitation rate (Zachara et al., 1991; Kitano et al. 1971). Since the saturation indices for rhodochrosite, witherite, and siderite are negative for all three sampling periods (SI_{MnCO3} = -1.19 to -1.91, SI_{BaCO3} = -3.55 to -4.50, and SI_{FeCO3} = -2.5 to -4.3) (Figure 2-4), these minerals cannot precipitate as authigenic phases in Ichetucknee River water.

If co-precipitation with calcium carbonate is the primary control on the diel cycle of a metal, the metal cycle should be in phase with the Ca^{2+} cycles. In the Ichetucknee River the observed cycles of Mn, and to a lesser extent Ba, are in phase with Ca^{2+}, and thus may be affected by precipitation of authigenic calcium carbonate (Figure 2-3). To assess the magnitude of this control, we used Eq. (2-5), a range of published distribution coefficients, and the Metal:Ca^{2+} ratios in the river over time to estimate the amount of metal that could be removed through calcite and/or aragonite co-precipitation. This estimate is reported both as an uptake flux and as a percentage of the observed daily flux in metal concentrations (Table 2-3). For Mn, the cycle of which is almost perfectly in-phase with Ca, these estimates suggest that 30 to 400% of the observed diel cycle of Mn may result from calcite co-precipitation, depending on the value of the distribution coefficient used. The excess removal rate may explain the net downstream loss of Mn relative to the input at the springs (Figure 2-5), despite likely additional diffuse Mn inputs from the pore-waters.

Only about 2% of the Ba cycle could be the result of calcite co-precipitation, which is unsurprising given the low affinity of Ba for calcite. However, if it is assumed that the diel Ca^{2+} cycle is the product of just aragonite precipitation then co-precipitation could account for 15 - 36% of the diel Ba cycle (Table 2-3). The relative contribution of calcite vs. aragonite precipitation to the observed Ca^{2+} cycle is unknown, making it impossible to quantify the net effect of calcium carbonate co-precipitation on the Ba cycle based solely on the diel Ca^{2+} cycle. The timing of the diel cycle in carbonate solubility is constrained, indirectly, by the timing of plant metabolism but it is possible that aragonite-precipitating organisms, such as aquatic snails, take advantage of this

cycle, precipitating carbonate when geochemically favorable, thereby contributing to the magnitude of the diel Ca^{2+} and metal cycles without affecting the timing.

The diel cycles of Fe and Sr, which also have an affinity for calcite do not exhibit diel cycles in-phase with that of Ca^{2+} suggesting that the co-precipitation of these metals is limited or offset by other processes out of phase with precipitation of calcium carbonate. With respect to Fe, the observed diel cycle in total dissolved Fe), is roughly 7 hours out of phase with the cycle of Ca^{2+} (Figure 2-3). During the day, when carbonate precipitation is occurring (Figure 2-4), DO concentrations are elevated by photosynthesis, indicating dissolved Fe is likely to be predominantly in the 3+ valence state. The charge difference between Fe^{3+} and Ca^{2+} would restrict Fe substitution in the calcite structure, thereby limiting Fe-carbonate co-precipitation. Fe concentrations in the river are too low to analyze for Fe speciation so this limitation cannot be confirmed. If the total Fe concentrations were in the 2+ valence state during the day co-precipitation could account for 11 to 27% of the observed diel Fe cycle (Table 2-3).

Redox Reactions

Redox reactions could be important to Fe and Mn concentrations, which are orders of magnitude more soluble in their reduced than oxidized valence state. Other metals reported here have no variation in valence state (e.g., Ca^{2+}, Ba, Sr), or are unlikely to change valence state given high DO concentrations even at night (e.g. U). In neutral to basic streams, oxidation of soluble Fe^{2+} and Mn^{2+} to insoluble Fe^{3+} and Mn^{3+} is one of the dominant processes affecting Fe and Mn cycling (Parker et al., 2007; Scott et al., 2002). Fe^{2+} oxidation rates increase by six orders of magnitude between pH 3 and 7 in warm waters (Nimick et al., 2011 and references therein), suggesting photosynthetic production of oxygen as well as by the elevated daytime pH and

temperature would increase the in-stream oxidation of Fe. The oxidation of Fe should thus reduce concentration of total dissolved Fe, in contrast to the observed increase in daytime Fe concentrations (Figure 2-5). Mn concentrations decrease during the day as expected of photosynthetically and pH-enhanced daytime oxidation. However, the phase of the Mn cycle lags that of DO by 18, not 12 hours (Figure 2-3), reflecting the importance of calcite co-precipitation to the Mn cycle (Table 2-4, Figure 2-6).

Daytime increases in dissolved Fe concentration have been attributed to daytime photo-reduction of insoluble Fe^{3+} and hydrous ferric oxides in acidic streams where this process is rapid at pH between 2 and 4 (Gammons et al., 2005; Nimick et al., 2011; Sullivan et al., 1998). In neutral to alkaline streams, similar to the Ichetucknee River, photo-reduction of Fe has been suggested to be unimportant because of the slow reaction kinetics (Borman et al., 2010; McKnight et al., 2001; Parker et al., 2008). The phase of Fe cycling in the Ichetucknee River indicates this process could be important in neutral to alkaline streams with high clarity. Photo-reduction may be more intense in the Ichetucknee River than in temperate turbid streams, regardless of its elevated pH, considering the clarity of its water and high solar radiation in the sub-tropical setting, as reflected in the extreme productivity of the river (Heffernan and Cohen, 2012). We were unable to speciate the Fe and result this issue because of the low concentration. Photo-reduction could produce Fe^{2+} which would be incorporated into authigenic calcium carbonate. The potential for photo-reduction and carbonate precipitation should theoretically both increase with day length and solar intensity. The diel cycle of Fe is smallest in May with the greatest solar radiation would magnify both of these processes.

Adsorption Reactions

Temperature and pH-dependent adsorption to metal oxides and biofilm surfaces can cause cationic metal concentrations to decrease and anionic metal concentrations to increase during the day in neutral to alkaline streams (e.g., Gammons et al., 2005 & 2007; Nimick et al., 2003). Of the cationic metals analyzed in the Ichetucknee River, only Ba and Mn concentrations regularly decrease during the day when T and pH are elevated (Figure 2-5) as would be expected for cation adsorption. Ba cycles may be strongly controlled by adsorption (Table 2-4, Figure 2-6) since co-precipitation, even if all by aragonite, is not sufficient to explain the observed diel cycle (Table 2-3) and Ba has no variations in redox state. Since most of the Mn cycle is explained by co-precipitation, adsorption may have less control on the cycle. Adsorption could contribute to the overall downstream decrease in Mn concentration.

Total dissolved U and Fe concentrations in the Ichetucknee River increase during the day, in-phase with the cycles of temperature and pH (Figure 2-3). Although U is a cationic metal the speciation of U in the river is dominated by the anionic U-carbonate complexes $UO_2(CO_3)_3^{4-}$ and $UO_2(CO_3)_2^{2-}$. This suggests that the diel cycle in U may also be the result of surface-complexation reactions where daytime increases in pH and temperature result in desorption of the anionic U complexes and subsequent daytime increase in U concentrations. Similarly, Fe in the river could be complexed with DOC to form stable, anionic Fe(III)-DOC complexes which should desorb during the day. These colloidal complexes would pass through the 0.45 um filter used during sample collection, thereby contributing to the daytime increase in total dissolved Fe.

Autotrophic Assimilation

Metals can be micronutrients for plants, resulting in their assimilation during primary production (Sterner and Elser, 2002). This flux is particularly significant in the Ichetucknee River because of its elevated productivity (Heffernan and Cohen, 2012). We calculated assimilation of metals using river ecosystem NPP and measured stoichiometry of both algae and vascular plant tissue samples from the river and report it both as an absolute value and as a percentage of the observed diel flux, when present (Table 2-5). Ecosystem NPP in the Ichetucknee River increased from November to March to May following the same seasonal pattern as day length rather than total daily solar radiation. Consequently the magnitude of expected assimilatory uptake also increases from November to March to May, for all metals and regardless of the plant type.

The relative contribution of the vascular plants vs. the algae to the total ecosystem GPP is unknown. However, the C:N:P of the Ichetucknee River ecosystem aligns most closely with the C:N:P of the vascular plants, suggesting that vascular plant productivity dominates the GPP of the Ichetucknee River ecosystem (Cohen et al., in press) and thus possibly the assimilatory uptake. The effect of assimilation relative to the total observed diel flux, as estimated by Eq. (2-4), is greatest for Mn and Fe, the two trace elements with the highest concentration in both plant types. The assimilatory flux for Mn is the equivalent of between 24% and 44% of the observed diel flux in March for algae and vascular plants respectively. This uptake, along with carbonate co-precipitation and adsorption (Table 2-4, Figure 2-6) explains why Mn shows the greatest downstream decrease in concentrations of all the measured metals (Figure 2-5). The assimilatory flux for Fe ranges across seasons from the equivalent of 14 to 67% of the

observed diel Fe flux when calculated using the vascular plant stoichiometry, and is in excess of the observed diel Fe flux when calculated using the algae stoichiometry. The assimilatory metal flux for Ba and U is less than 5% of the observed diel flux, reflecting the low concentration of these metals in the vascular plants and algae and the limited control assimilation has on these metals. In contrast, while the assimilatory flux of Ca^{2+} is low compared to the observed diel flux (< 5%) the magnitude of Ca^{2+} removal by assimilation is the highest of all the metals (Table 2-5). This discrepancy illustrates that dominant process controlling the diel Ca^{2+} cycle in the river is the daytime precipitation of calcium carbonate.

Our calculations indicate autotrophic assimilation contributes to diel cycles of certain metals in streams. For the micronutrients such as Mn, and Fe, the flux of metal removal by autotrophic assimilation may even be on order of magnitude with other geochemical controls. The relative contribution of assimilation uptake to the observed diel metal cycles, as presented here, ignores the potential for phase-lags between the timing of assimilation and the other geochemical controls. The timing of metabolic demand and assimilatory uptake for most elements, with the exception of oxygen and carbon, is not well established. Diel variation in nutrients directly out of phase with DO suggests assimilation synchronous with photosynthesis, as has been observed for N (Heffernan and Cohen, 2010; Roberts and Mulholland, 2007). In contrast, recent observations of diel variation in SRP that significantly lags N assimilation suggests that assimilation is not intrinsically linked to the timing of photosynthesis (Cohen et al., in press). If assimilation is out of phase with the other geochemical controls, as has been demonstrated for phosphate (Cohen et al. in press), estimates based only on observed

diel cycles could over- or under-represent the controlling influence of individual processes. For example, Sr is calculated to have an assimilatory uptake that is roughly the same as the magnitude of predicted Sr removal by calcite co-precipitation (Table 2-3). The lack of diel cycling suggests that the two processes could be out of phase, implying that assimilation of Sr by plants would occur during plant respiration at night. Disentangling the relative control that each process has on the composite diel signal requires better understanding of the timing and magnitude of all processes controlling the variation but may be useful for constraining unknown parameters, such as the timing of metabolic processes driving assimilation.

Conclusions

Our results reflect the direct and indirect control that solar radiation and submerged plant metabolism have on diel variations in metal chemistry of natural, alkaline streams with low metal concentrations (Figure 2-6). Diel changes in pH and the solubility of calcium carbonate result in precipitation of carbonate minerals during the day which sequesters Mn and Ba as a solid solution. Co-precipitation of other metals with calcite is limited by differences in ionic radii from Ca^{2+} (e.g. Sr and Ba) and valence state (e.g. Fe) and obscured by overlapping signals from other diel processes (e.g. Sr). Redox changes resulting from photosynthetic production of oxygen can explain the daytime decrease in Mn, but not the daytime increases in Fe. Although typically reported only in acidic systems, the observed Fe cycle could reflect daytime photo-reduction made possible by the high clarity of the water and intense solar radiation of this sub-tropical setting. pH- and temperature-dependent adsorption could also explain the observed cycles in cationic Mn and Ba, as well as the cycles in U and Fe if present as anionic surface-complexes. The observed cycle in Fe could also be impacted by

direct assimilation by submerged plants, a process which also appears to affect Mn, Ba, U, and potentially Sr cycles. Variability in the observed metal cycles can be attributed to seasonal changes in input radiation and primary productivity affecting the competing control by these multiple processes.

This study illustrates how diel metal cycles emerge in response to multiple overlapping geochemical and biological processes, indirectly and directly the result of solar radiation and submerged plant metabolism (Table 2-4, Figure 2-6). These processes occur at an ecosystem level where biotic and abiotic forcing are mutual and reciprocal, requiring an understanding of magnitude and timing of multiple processes that may be out of phase with each other, convoluting a simple diel signal. Although the links between metal concentrations, geochemical processing, and ecosystem metabolism are complex, high resolution sampling that captures the phases and amplitudes of diel cycles can be used to assess the relative controls by various processes affecting their concentrations.

Table 2-1. Accuracy and precision of measured external standard SLRS4 relative to published standard concentrations, a combined field and analytical blank, the analytical detection limit represented by the value of the lowest calibration standard, and the average variation between ISCO storage duplicates.

Element	SLRS4: UF values (ppb)	SLRS4: Published values (ppb)	Blank (ppb)	Detection limits (ppb)	ISCO duplicates variation
Al	48 ± 16	54 ± 4	0	-	-
Mn	3.47 ± 0.11	3.37 ± 0.18	0.44	0.31	4%
Fe	105 ± 4	103 ± 5	0.33	0.40	4%
Cu	1.87 ± 0.18	1.81 ± 0.08	0.06	0.02	52%
Zn	1.29 ± 0.76	0.93 ± 0.1	0.23	0.10	15%
Sr	29.0 ± 0.5	26.3 ± 3.2	0.2	2.0	0%
Ba	12.9 ± 0.4	12.2 ± 0.6	0.04	0.10	2%
U	0.05 ± 0.005	0.05 ± 0.003	0.008	0.009	3%

Table 2-2. Summary of major field parameters, solute concentrations, and modeled diel sine function results and significance.

Parameter (units)	Sampling date	Mean	Observed diel range[a]	F-test	p-value	Significant diel cycle	Modeled diel amplitude	Modeled diel peak (hour)
Solar Radiation (W/m^2)	March '09	68.11	625.1	12.3	1.3×10^{-4}	Yes	227.4	12:00
	Nov '09	175.89	689.8	15.1	1.5×10^{-4}	Yes	552.0	12:30
	May '10	256.51	1007.0	99.1	2.2×10^{-17}	Yes	783.0	12:15
Temp (°C)	March '09	21.5	1.2	171.1	5.8×10^{-15}	Yes	1.08	17:45
	Nov '09	21.1	2.2	36.5	1.1×10^{-6}	Yes	1.85	18:00
	May '10	22.4	2.5	235.9	1.2×10^{-24}	Yes	2.44	16:45
pH	March '09	7.67	0.6	107.7	8.1×10^{-13}	Yes	0.54	16:15
	Nov '09	7.91	0.38	37.3	9.8×10^{-7}	Yes	0.36	17:00
	May '10	7.90	0.71	164.9	1.5×10^{-21}	Yes	0.67	16:00
DO (mg/L)	March '09	5.30	4.36	111.3	5.8×10^{-13}	Yes	4.00	15:45
	Nov '09	5.88	3.30	47.9	2.1×10^{-7}	Yes	3.09	16:30
	May '10	5.91	6.35	272.6	6.3×10^{-26}	Yes	6.08	15:30
NO_3^- (mg/L)	March '09	0.44	0.08	61.4	2.5×10^{-10}	Yes	0.060	05:00
	Nov '09	0.38	0.06	21.4	2.4×10^{-5}	Yes	0.051	05:15
	May '10	0.35	0.09	94.1	5.0×10^{-13}	Yes	0.084	04:00
DOC (mg/L)	Nov '09	1.15	-	0.4	6.6×10^{-1}	*No*	-	-
	May '10	2.14	-	0.0	1	*No*	-	-
DIC (mM)	March '09	2.96	0.17	82.2	1.3×10^{-11}	Yes	0.14	06:00
	Nov '09	2.91	0.10	15.6	1.6×10^{-4}	Yes	0.081	04:14
	May '10	2.88	0.22	65.4	3.1×10^{-14}	Yes	0.15	06:15
$\delta^{13}C$ (‰)	March '09	-11.03	-1.1	110.2	6.3×10^{-13}	Yes	1.12	17:45
	Nov '09	-10.81	-0.6	12.4	3.9×10^{-4}	Yes	0.64	17:00
	May '10	-10.63	-1.1	38.1	1.3×10^{-10}	Yes	1.05	17:30
Ca^{2+} (mM)	March '09	1.37	0.6	18.2	9.5×10^{-6}	Yes	0.037	07:15
	Nov '09	1.33	-	0.9	3.8×10^{-1}	*No*	-	-
	May '10	1.33	0.6	22.8	9.5×10^{-8}	Yes	0.041	06:15
Cl^- (mM)	March '09	0.17	-	0.0	1	*No*	-	-
	Nov '09	0.32	-	1.6	2.0×10^{-1}	*No*	-	-
	May '10	0.32	0.04	6.3	3.1×10^{-3}	Yes	0.013	18:45
Mn (ppb)	March '09	3.06	1.45	110.4	6.2×10^{-13}	Yes	1.35	08:45
	Nov '09	4.87	-	0.3	7.2×10^{-1}	*No*	-	-
Fe (ppb)	March '09	5.40	4.9	34.3	5.6×10^{-8}	Yes	4.04	15:30
	Nov '09	3.24	1.5	9.1	1.6×10^{-3}	Yes	0.99	16:45
	May '10	4.85	2.0	10.8	1.2×10^{-4}	Yes	0.86	12:00
Sr (ppb)	March '09	179.4	12.06	5.8	6.2×10^{-3}	Yes	3.80	03:30
	Nov '09	195.6	-	0.8	4.2×10^{-1}	*No*	-	-
	May '10	201.1	-	1.6	2.0×10^{-1}	*No*	-	-
Ba (ppb)	March '09	4.85	0.66	5.9	5.9×10^{-3}	Yes	0.35	04:30
	Nov '09	5.08	0.29	14.4	1.9×10^{-4}	Yes	0.25	03:45
	May '10	5.27	0.50	5.9	4.5×10^{-3}	Yes	0.19	03:30
U (ppb)	March '09	0.70	0.09	21.6	2.7×10^{-6}	Yes	0.049	18:45
	Nov '09	0.74	0.04	8.1	2.6×10^{-3}	Yes	0.024	15:15
	May '10	0.76	0.16	33.5	7.9×10^{-10}	Yes	0.086	16:15

[a]Diel range = $Diel_{max} - Diel_{min}$

Table 2-3. Predicted uptake of Mn, Ba, Sr, and Fe by calcite and/or aragonite co-precipitation. Only the diel cycles of Mn and Ba are in phase with that of Ca^{2+}. The speciation of Fe in the river is unknown and the diel Fe cycle is out of phase with Ca^{2+}.

	$Mn_{calcite}$		$Ba_{calcite}$		$Ba_{aragonite}$	$Sr_{calcite}$		$Sr_{aragonite}$	$Fe^{2+}{}_{calcite}$	
	Min [DW]	*Max* [L]	*Min* [TP]	*Max* [Z]	[K]	*Min* [TP]	*Max* [L]	[K]	*Min* [M]	*Max* [DW]
Log D:	0.58	1.7	-1.92	-1.22	0.00	-1.68	-1.00	0.04	-1.57	0.57
Calculated uptake ($mmol/m^2/d$):										
March	$1.4x10^{-2}$	$18x10^{-2}$	$3.0x10^{-5}$	$15x10^{-5}$	$2.5x10^{-3}$	$3.1x10^{-3}$	$15x10^{-3}$	$16x10^{-2}$	$2.0x10^{-4}$	$2.8x10^{-2}$
November	$1.2x10^{-2}$	$16x10^{-2}$	$1.7x10^{-5}$	$8.6x10^{-5}$	$1.4x10^{-3}$	$1.8x10^{-3}$	$8.7x10^{-3}$	$9.5x10^{-2}$	$6.6x10^{-5}$	$8.8x10^{-3}$
May	-	-	$3.6x10^{-5}$	$18x10^{-5}$	$3.0x10^{-3}$	$3.8x10^{-3}$	$18x10^{-3}$	$20x10^{-2}$	$1.9x10^{-4}$	$2.6x10^{-2}$
Percent of observed diel flux:										
March	29 %	400 %	0.4 %	2.2 %	36%				*(0.1 %)*	*(15 %)*
November	31 %	410 %	0.3 %	1.4 %	23%				*(0.1 %)*	*(11 %)*
May	-	-	0.2 %	1.1 %	18%				*(0.2 %)*	*(27 %)*

Sources of log D values: [DW] Dromgoole and Walter, 1990; [L] Lorens, 1981; [TP] Tesoriero and Pankow, 1996; [Z] Zachara, 1991; [K] Kitano et al., 1971; [M] Mettler et al., 2009.

Table 2-4. Processes concluded to be controlling the diel metal cycles observed in the Ichetucknee River.

	Ca^{2+}	Mn	Fe	Sr	U	Ba
Carbonate minerals interactions*	XXX	XXX	X	XX		XX
Redox state*		XX			X	
Adsorption*		XX	XX		XXX	XXX
Photo-reactions			XXX			
Assimilation*	XX	XXX	XXX	XX	XX	XX

* Directly or indirectly the result of plant metabolism.
XXX – Strong significance, XX – minor significance, X – possible but unlikely.

Table 2-5. Calculations of element uptake by autotrophic assimilation for those elements exhibiting diel cycles. Calculations based both vascular (V) and algae (A) stoichiometry. Exact contribution of vascular vs. algae productivity to ecosystem GPP is unknown.

	Ca	Mn	Fe	Sr	Ba	U
			Me in biomass (mg-*Me* kg^{-1})[a]			
Vascular	9165	319	420	36.4	5.38	0.181
Algae	24911	173	3851	37.6	11.2	1.730
			Me:C ratio in biomass (mg-*Me*/kg-C)[b]			
Vascular	22495	778	1035	89.2	13.2	0.444
Algae	60871	420	9371	91.7	27.4	4.170
			Calculated assimilatory uptake (mmol m^{-2} d^{-1})			
Vascular:						
March	0.81	2.1×10^{-2}	2.7×10^{-2}	1.5×10^{-3}	1.4×10^{-4}	2.7×10^{-6}
Nov.	0.74	1.9×10^{-2}	2.4×10^{-2}	1.3×10^{-3}	1.3×10^{-4}	2.5×10^{-6}
May	2.00	5.0×10^{-2}	6.4×10^{-2}	3.5×10^{-3}	3.3×10^{-4}	6.5×10^{-6}
Algae:						
March	2.20	1.1×10^{-2}	25×10^{-2}	1.5×10^{-3}	2.9×10^{-4}	26×10^{-6}
Nov.	1.99	1.0×10^{-2}	22×10^{-2}	1.4×10^{-3}	2.6×10^{-4}	23×10^{-6}
May	5.30	2.7×10^{-2}	59×10^{-2}	3.6×10^{-3}	6.9×10^{-4}	62×10^{-6}
			Observed diel flux (mmol m^{-2} d^{-1})			
March	98	4.6×10^{-2}	19×10^{-2}		7.0×10^{-3}	7.3×10^{-4}
Nov.	51	3.8×10^{-2}	8.0×10^{-2}		6.1×10^{-3}	3.6×10^{-4}
May	103	-	9.6×10^{-2}		17×10^{-3}	23×10^{-4}
			Assimilatory uptake as a percent of observed diel flux			
Vascular:						
March	0.8%	44%	14%		2.0%	0.4%
Nov.	1.4%	49%	31%		2.1%	0.7%
May	1.9%	-	67%		2.0%	0.3%
Algae:						
March	2.2%	24%	128%		4.1%	3.5%
Nov.	3.9%	26%	278%		4.3%	6.6%
May	5.1%	-	609%		4.2%	2.7%

[a] Average of river samples

[b] Converted from mg-*Me*/kg-biomass using measured weight % C.

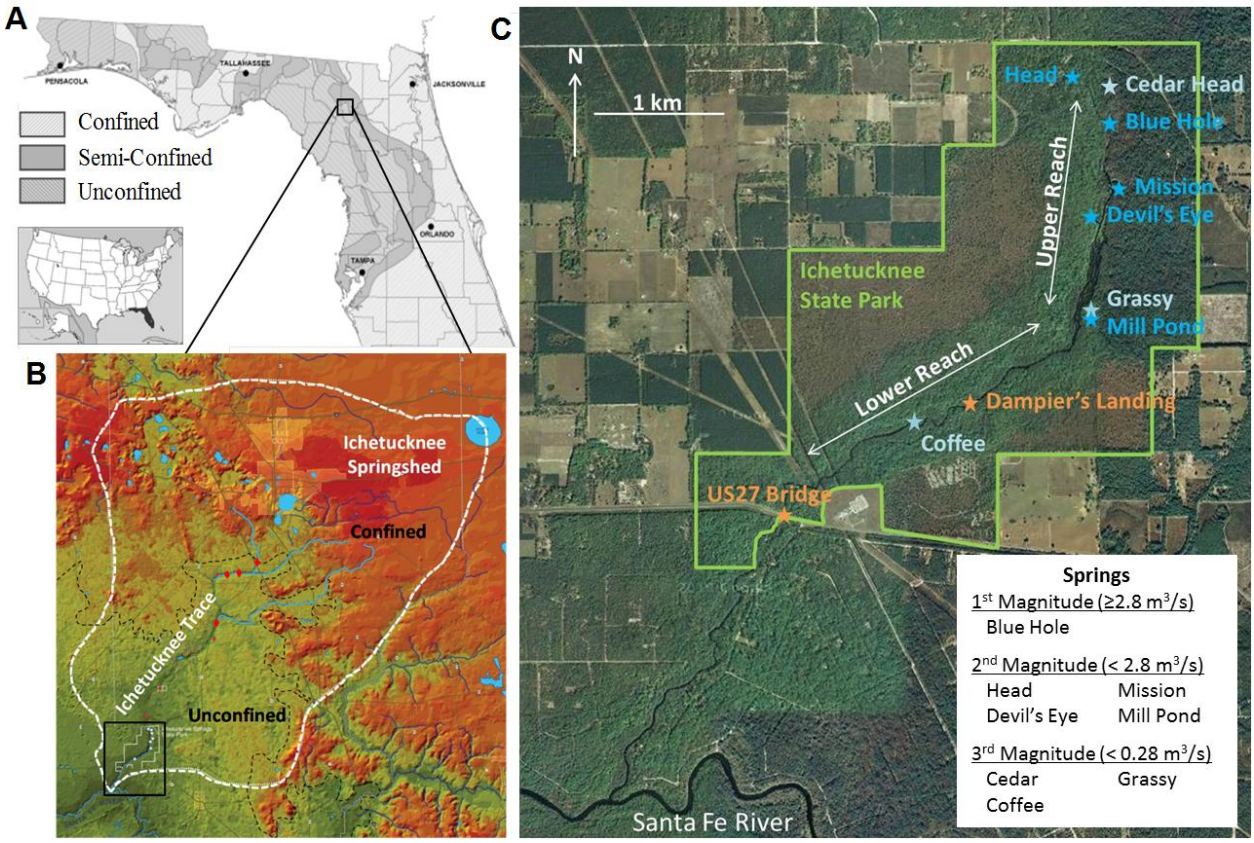

Figure 2-1. Overview of the study area. A) Map of the confined, semi-confined, and unconfined portions of the Floridan Aquifer in north Florida (FDEP, 2006; modified). B) Topographic map of the Ichetucknee springshed showing levels of confinement, three surface tributaries plus associated sinks, and the Ichetucknee Trace (SRWMD, 2007; modified). C) Google Earth image of Ichetucknee River showing the state park (green outline), 5 major springs (blue stars), 3 minor spring (light blue stars), and river gages (orange stars).

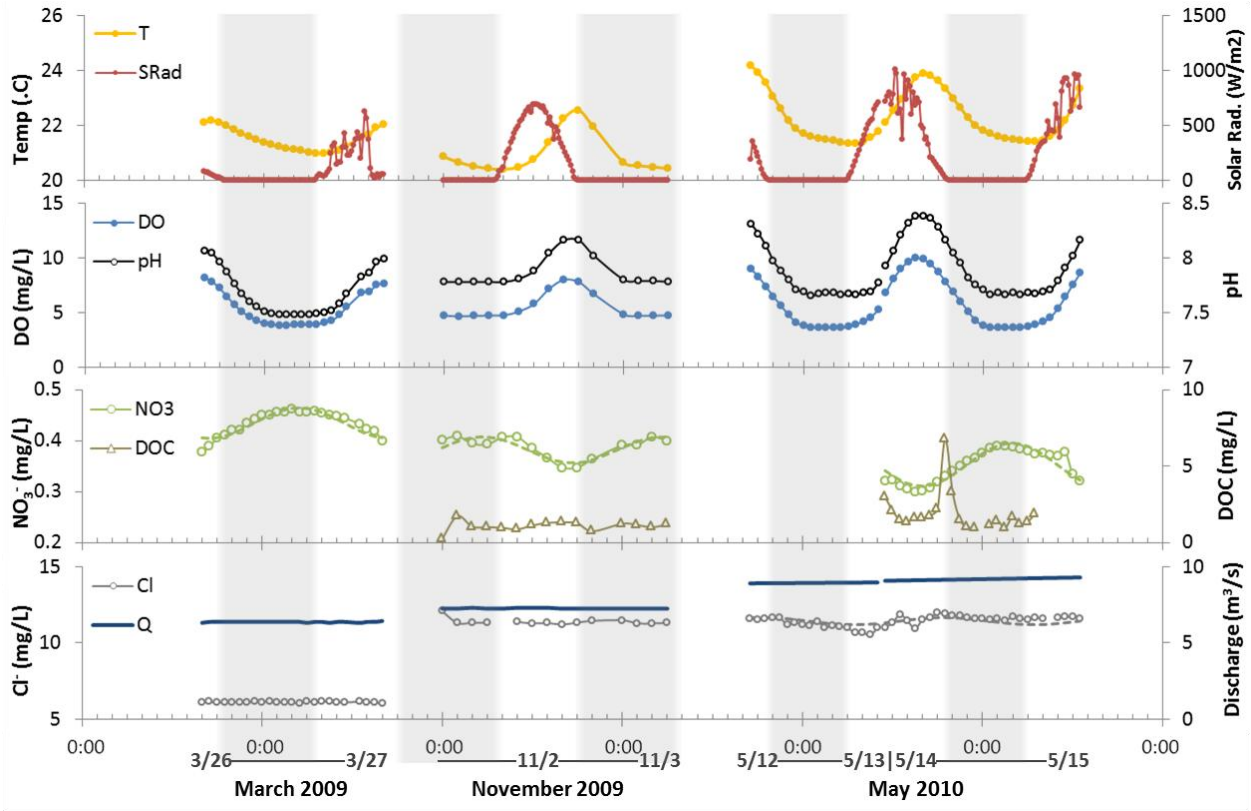

Figure 2-2. Time-series for each of the three sampling periods at the US27 Bridge: water temperature, solar radiation, DO concentrations, pH, DOC, NO_3^-, and Cl^- concentrations, and discharge. Grey bars indicate nighttime.

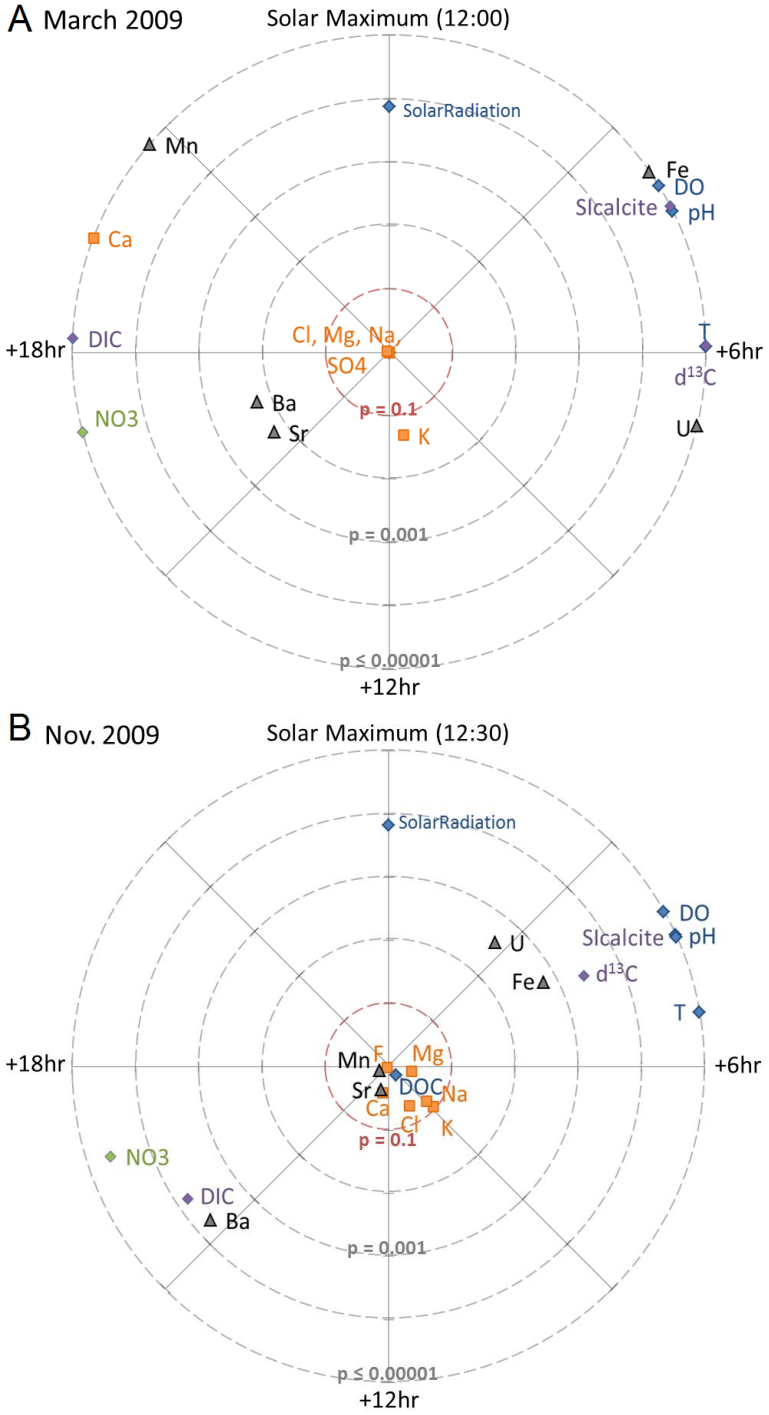

Figure 2-3. Modeled phase and diel strength plots of the observed diel cycles. A) March 2009, B) November 2009, and C) May 2010. The timing of the diel maximum, relative to the peak in solar radiation (Table 2-2), is plotted as the clockwise distance from +y axis. The distance from the origin reflects the significance of the diel cycle, plotted as the –log of the p-values of the F-test (Table 2-2). Parameters with $p > 0.1$ are not considered to have statistically significant diel cycles. Solutes with $p \leq 0.00001$ are plotted on the outer ring.

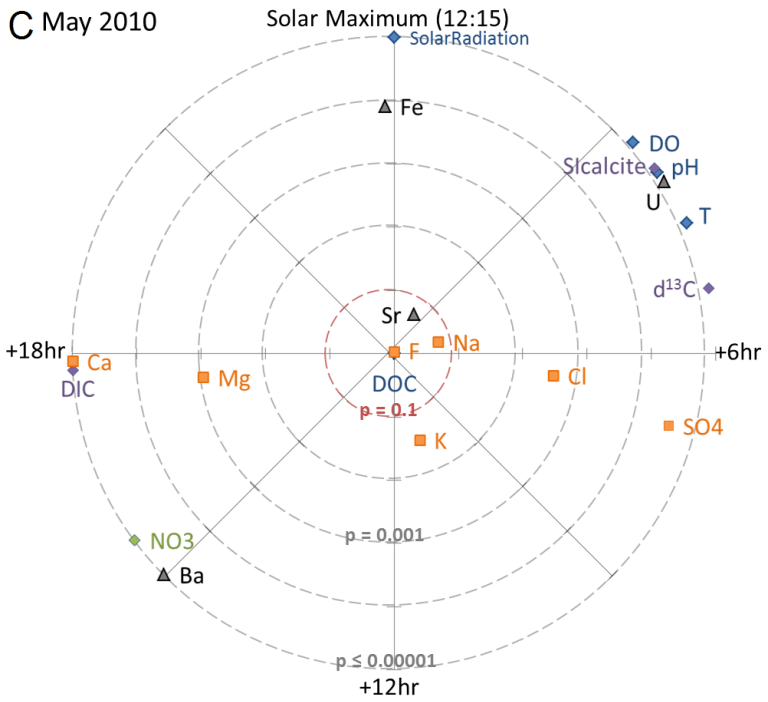

Figure 2-3. Continued

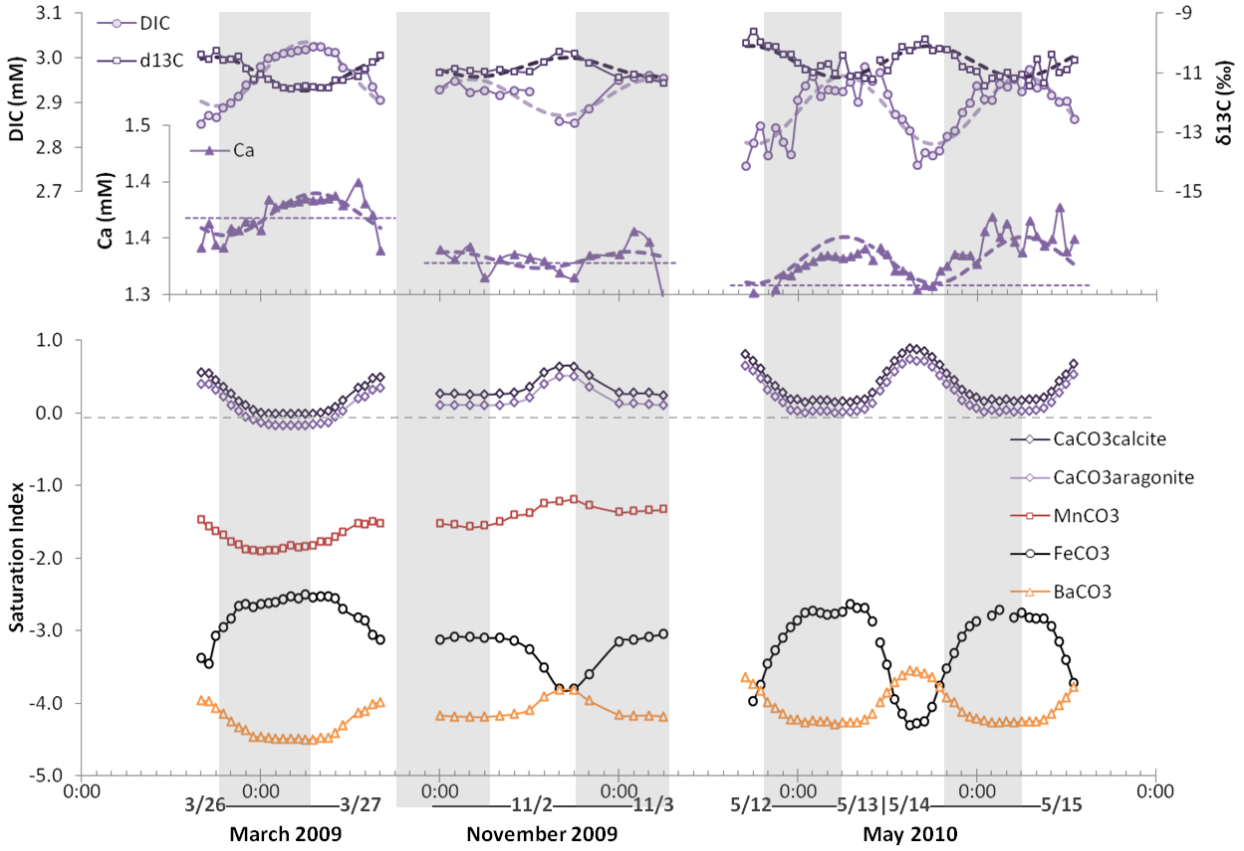

Figure 2-4. Diel carbonate cycles as seen in variability of DIC concentrations, $\delta^{13}C_{DIC}$ values and Ca^{2+} concentrations over each of the three sampling periods, as well as the saturation index of calcite, aragonite and the main metal-carbonate minerals. Diel cycles of carbonate mineral saturation co-vary with pH with the exception of $FeCO_3$ which is out of phase. The thick dashed lines indicate modeled diel fit, where significant (e.g., Figure 2-3). Grey bars indicate nighttime.

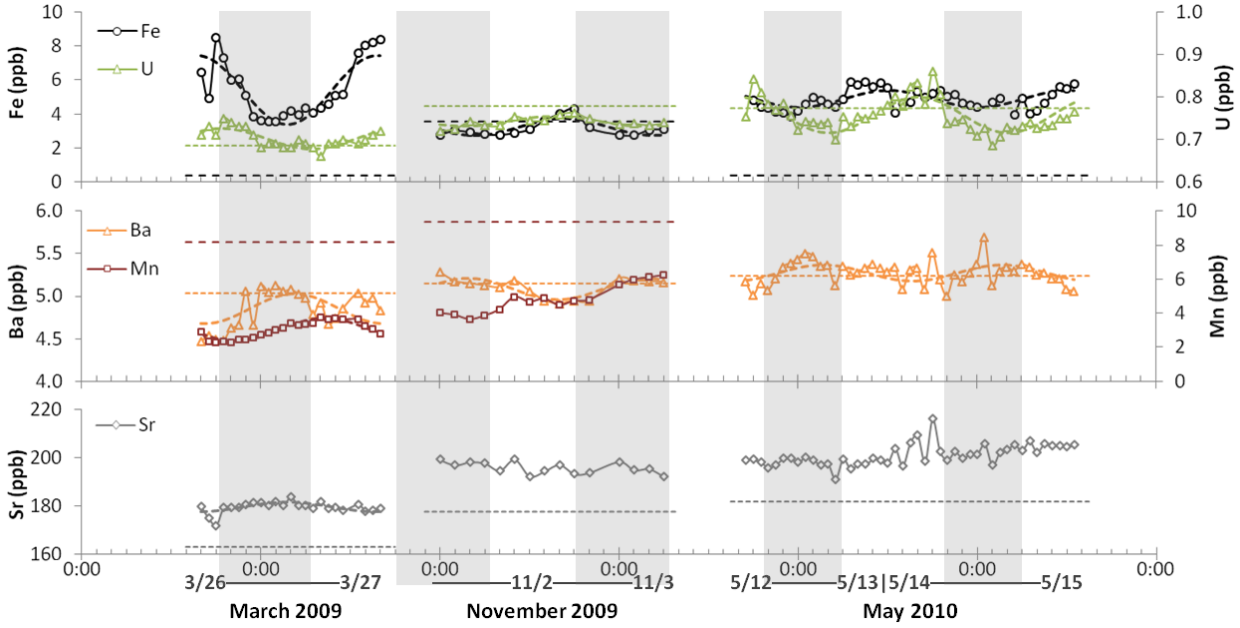

Figure 2-5. Concentrations of Fe, U, Mn, Ba, and Sr each of the three sampling periods. The thin, horizontal dashed lines indicate the flow-weighted input from the springs. The thick dashed lines indicate modeled diel fit, where significant (e.g., Figure 2-3). Fe and U exhibit similar diel trends, decreasing in the evening and increasing during the day. In contrast Mn, and Ba concentrations increase at night and decrease during the day with peak concentrations all occurring in the late afternoon. Sr concentrations exhibit little to no diel cycle. Grey bars represent night.

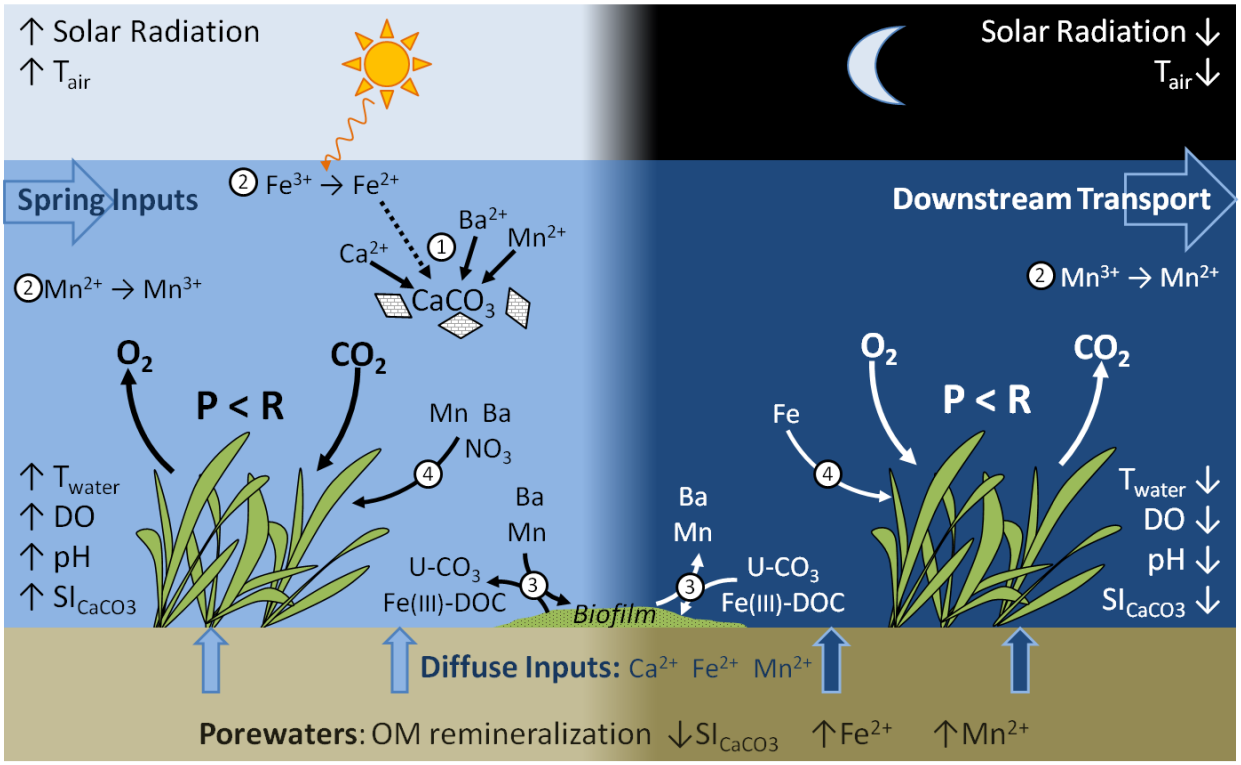

Figure 2-6. Diagram illustrating the processes concluded to be controlling the diel metal cycles observed in the Ichetucknee River. 1) Calcite co-precipitation, 2) redox reactions, 3) absorption, and 4) assimilation. Timing of assimilation is unknown. Modified from Nimick et al. (2011).

CHAPTER 3
RELATIONSHIPS BETWEEN VEGETATION STOICHIOMETRY, ASSIMILATION, AND DIEL ELEMENT VARIATION IN A SPRING-FED RIVER

Introduction

The metabolism of submerged aquatic vegetation has been shown to indirectly control the cycling of solutes in streams at diel (24-hour) frequencies. Photosynthesis and respiration alternately produce and consume oxygen and carbon dioxide, creating diel variation in dissolved oxygen (DO) concentrations and pH (Desmet et al., 2008; Odum, 1956; Simonsen and Harremoës, 1978). These changes in turn mediate elemental concentrations via the speciation of redox sensitive elements such as Fe and Mn (e.g. Scott et al., 2002), pH-dependent adsorption reactions (e.g. Nimick et al., 2003), and the saturation states of minerals (e.g. de Montety et al., 2011). Plant metabolism also directly exerts control on water composition via assimilatory uptake creating diel variation in key nutrients such as carbon (Odum 1956, Mulholland et al. 2008), nitrogen (Roberts and Mulholland, 2007; Rusjan and Mikos, 2010; Heffernan and Cohen, 2010a), and phosphorus (Vincent and Downes, 1980; Gammons et al., 2011; Cohen et al., 2013). Trace elements can be essential micronutrients (e.g. Morel and Price, 2003), suggesting their assimilatory uptake also contribute to diel variation in element concentrations in streams. If diel element variation is indicative of metabolic processing, assessing the magnitude and timing of this diel variation relative to other inorganic controls could be used to estimate the ecosystem demand for those elements, infer ecosystem function, and predict how stream ecosystems may respond to environmental change.

In theory, the relatively constant nutritional requirements of organisms should result in metabolic demand controlling both the magnitude and timing of assimilatory

element uptake (Sterner and Elser 2002). The elemental composition of organisms is strongly linked to growth (Vrede et al., 2004) due to specific material requirements of metabolic processes such as phosphorus for RNA production (Elser et al., 2003; Vrede et al., 2004), iron and magnesium for chlorophyll (Pushnik et al., 1984), and iron and molybdenum for enzyme and protein synthesis (Glass et al., 2009). Consequently, elements are required in particular proportions during growth in order for plants to maintain a compositionally homeostatic biomass, i.e., one with invariant stoichiometry of their elemental compositions (Frost et al., 2005; Kerkhoff et al., 2005).

Although strict homeostasis is observed for animals, in general autotrophs are more plastic, responding to changes in nutrient supply and light (Sterner et al., 1998). At short timescales, luxury uptake may result in assimilation of available elements beyond what is immediately required for growth (e.g. Luo and Rimmer, 1995; Sunda and Huntsman, 1995; Khoshmanesh et al., 2002). At longer timescales, organismal stoichiometry can adjust in response to ratios of environmental availability (Persson et al., 2010) as can the relative abundance of species with varying elemental requirements (Hall, 2004). The degree to which stoichiometric ratios adjust with environmental supply will control the covariation between growth and assimilation. A better understanding of the processes controlling environmental element availability and the sensitivity of the stoichiometric response to variability is therefore critical to contextualizing the relative control that assimilation has on the magnitude of diel element variation.

The timing of assimiliatory uptake should also, theoretically, reflect the timing of the metabolic process that requires the particular element; however, recent evidence suggests that the timing of assimilation is decoupled from photosynthesis for some

elements (e.g. Cohen et al., 2013). As it is unlikely that only one process, metabolic or inorganic, regulates the entire signal of diel variation (e.g. Kurz et al., in review; Nimick et al., 2011), the timing of diel variation should be assumed to be a convolution of several overlapping processes. This overlap will complicate the disentangling of assimilation relative to other drivers of diel variation and highlights the importance of assessing assimilation within the context of these other drivers.

Trace metal stoichiometry of plants, including aquatic species, has been the focus of numerous studies for a variety of reasons including understanding the role of plants in the cycling and budgets of metals in lakes (e.g., Reynolds and Hamilton-Taylor, 1992; Jackson et al., 1994; St-Cyr et al., 1994), assessing the potential of uptake and bioaccumulation as a removal mechanism for heavy metal contamination (e.g., Hozhina et al., 2001; Kamal et al., 2004; Miretzky et al., 2004; Nyquist and Greger, 2007) and as an indicator for toxicity (e.g. Wang and Dei, 2006), and determining species and spatial variability in stoichiometry (e.g. Villares et al., 2005; Watenabe et al., 2007; Gotelli et al. 2008). Despite this work, few studies have considered element assimilation on diel timescales (e.g., Kuwabara, 1992), and none appear to be comprehensive over a range of elements. The diel cycling of metals in streams has also received increasing attention in the literature (see Nimick et al., 2011 for a review) and while autotrophic assimilation, or absorption, has occasionally been suggested as a potential driver of diel metal variation (e.g., Nimick et al., 2003) Kurz et al. (in review) appears to be the first to quantify this effect for a range of elements using in-situ plant stoichiometry.

The objective of this study is to assess the relationship between the elemental requirements of submerged aquatic vegetation and the biologic and geochemical processes controlling the availability of elements in streams in a large spring-fed river (Ichetucknee River, north-central FL). This objective follows from prior work in this river (Kurz et al. in review), where they concluded geochemical processes (e.g., calcite co-precipitation) were insufficient t to explain the timing and magnitude of diel variation, and showed that autotrophic assimilation could account for a significant portion of the diel variation in some elements. In this study we expand on our evaluations of primary producer tissue stoichiometry to consider its relationship with environmental element availability, and evaluate how the magnitude and phase of diel element variation may be indicative of ecosystem function. We selected the Ichetucknee River as our study system because of its high biological productivity (Heffernan et al. 2010), which should result in high assimilatory fluxes and thus a strong signal for distinguishing assimilation from geochemical processes.

Methods

Site Description

The Ichetucknee River is an entirely spring-fed system sourced primarily from eight named springs emerging from the Floridan Aquifer, an eogenetic karst aquifer (e.g. Vacher and Mylroie, 2002). The springs drain an estimated 960 km^2 springshed (Champion and Upchurch, 2006) covering confined and unconfined portions of the aquifer. From the source springs, the river flows 8 km over the Ocala Limestone at the top of the unconfined aquifer before discharging into the tannic Santa Fe River. The springs and upper 5 km of the river are contained within Ichetucknee Springs State Park and comprise our study area (Figure 3-1).

The springs of the Ichetucknee system have distinct but stable chemistry and discharge over diel and longer time scales (Martin and Gordon, 2000). Discharge of the 6 largest springs and of the river at a site 5 km downstream of the springs (US27 Bridge; Figure 3-1) was continuously monitored by the USGS from 2002 until 2010 when all but the largest spring (Blue Hole Spring) and the river gage at US27 Bridge were discontinued. Since 2010, we have estimated discharge for the 5 unmonitored springs using the relationship between flows at each spring and flows at Blue Hole Spring from the 2002 – 2010 period. River discharge at Site 2700 has ranged from 5.7 to 14.3 m^3/s over the monitored period.

River chemistry is characterized by high water clarity (horizontal secchi distances of tens of meters; Wetland Solutions Inc, 2006), low turbidity (<1 NTU; Heffernan & Cohen, 2010), low dissolved organic carbon (DOC) concentrations (14 µmol-C L^{-1}; Duarte et al., 2010), and warm temperatures (> 19°C). These conditions result in dense submerged vegetation – both vascular plants (primarily *Sagittaria kurziana* and *Vallesnaria americana*) and filamentous benthic algae (primarily *Vaucheria* spp. and *Lyngbya wollei*), which cover up to 78% of the river bed (Kurz et al., 2004). High primary productivity relative to rivers of similar size (Heffernan et al., 2010a) results in significant diel variation in nitrate (Heffernan and Cohen, 2010), carbonate (de Montety et al., 2011), metals (Kurz et al., in review), and phosphate (Cohen et al., 2013).

Sampling Procedure

A combined survey of river and spring chemistry and submerged plant stoichiometry was conducted in May 2011 to assess the relationships between the stoichiometry of submerged vegetation, ambient water chemistry, assimilatory uptake, and diel metal cycling in the river. Submerged vegetation tissue samples were collected

at 10 sites on the river, located roughly every 500m from the source springs to Site 2700, and at five of the main springs (Head, Blue Hole, Mission, Devil's Eye, and Mill Pond springs). Tissue material was collected from the vascular plant (Sagittaria kurziana) and algal species (Vaucheria sp.) that dominated benthic cover at all sites. To the extent possible only new growth tissue was collected as this should most closely reflect current water chemistry and was the least colonized by epiphytic mineral and algal growth. For the vascular *S. kuziana,* whole leaf blades were collected from several individual plants, and composited.

Water samples from the river were collected hourly for 45 hours (5/9/11 15:00 – 5/11/11 11:00) at US27 Bridge using an ISCO autosampler in 1 L, acid-washed bottles triple rinsed before reuse. Autosampler bottles were kept chilled with ice to preserve the samples during storage in the ISCO. The sample aliquots were split, filtered and preserved for each analysis on site during the day, in the order they were collected, with a maximum delay between collection and preservation of 15 hours for the first nighttime sample. To test for concentration changes during ISCO storage a grab samples was collected and preserved simultaneously with the first nighttime ISCO sampler, which was preserved the following day after overnight storage in the ISCO (Table 3-1). Unfiltered samples for inorganic carbon (IC) and carbon stable isotope ($\delta^{13}C_{IC}$) analyses were preserved with three drops of concentrated $HgCl_2$ solution in 15 ml glass vials. Samples for major and trace element, and alkalinity analysis were filtered through a trace-metal grade 0.45 um cellulose acetate membrane and stored in 20 ml high density polyethylene (HDPE) vials. Cation and metal samples were preserved with three drops

of concentrated trace-metal grade nitric acid. All samples were kept chilled prior to their analysis.

Three in-situ sensors, recording at 15-minute intervals, were installed in the thalweg of the river at Site 2700. The field parameters (temperature, specific conductance, pH, and DO concentrations) were record using a YSI 6920 sonde (Yellow Springs Instruments, Yellow Springs, OH), nitrate (NO_3) using a SUNA submersible UV nitrate analyzer (Satlantic, Halifax, Nova Scotia), and soluble reactive phosphorus (SRP) using a Cycle-PO4 ortho-phosphate sensor (Wetlabs, Philamath, OR). The first 15 hours of Cycle-P data are omitted due to flushing effects as the instrument settles. All sensors were calibrated in the lab prior to deployment and verified in the lab after deployment.

The six main springs of the river were manually sampled on May 10, 2011 using the same methods as the high-frequency river sampling. An additional filtered sample was collected for nutrient analysis and frozen until analysis. The field parameters of the springs were measured with a calibrated YSI 556 MPS (Yellow Springs Instruments, Yellow Springs, OH). River discharge measurements at the US27 Bridge and Blue Hole Spring were obtained from USGS at 15-minute increments. Solar radiation and precipitation data, also at 15-minute resolution, was obtained from the Florida Automated Weather Network (FAWN; http://fawn.ifas.ufl.edu) for the town of Alachua, 20km from the field site.

Analytical Method: Vegetation Tissue Samples

Plant tissue samples were cleaned of any foreign material, washed in distilled water, dried and lightly crushed. A portion of the dried samples were ashed at 550 °C and digested using the procedure described in Kamenov et al. (2009) in preparation for

major and trace element analysis. Major and trace element concentrations were measured on an HR Element 2 ICP-MS with Re and Rh used as internal standards. Major element analysis was calibrated using USGS rock standards BIR-1, BCR-2 and AGV-1, and trace element analysis was calibrated using gravimetrically prepared standards purchased from QCD Analysts. The recovery of our preparation and analysis technique was checked using the external standard, Standard Reference Material 1515 (apple leaves), certified by the National Institute of Standards.

Tissue samples were also analyzed for total C, N, and P. Total C and N concentrations in the dried samples were measured using a Carlo Erba NA1500 CNS elemental analyzer with Atropine as an internal standard. Total P concentrations in the ashed samples were measured following the method described in Kenney et al. (2001), using a Technicon Autoanalyzer II with a single-channel Colorimeter and electronic data acquisition, following digestion with H_2SO_4 and $K_2S_2O_8$. Total P in the ash was converted to total P of biomass using the % loss on ignition (LOI) measurements made pre and post ashing.

Analytical Methods: Water Samples

Water samples were analyzed for alkalinity, major and selected trace element concentrations, including Cl^-, Ca^{2+}, Mg^{2+}, K^+, V, Cr, Mn, Fe, As, Sr, Ba, Pb, U and IC, and $\delta^{13}C_{IC}$. Total alkalinity was titrated within 24 hours of sampling using 30 ml of sample and 0.1 N HCl. Major element chemistry was measured with an automated Dionex DX500 Ion Chromatograph with precision of better than 4% for all runs and elements based on repeated measurements of internal standards. Charge balance errors were less than 2%. IC concentrations were measured on CO_2 extracted by acidifying samples using an AutoMate Prep Device coupled with a UIC (Coulometrics)

5011 carbon coulometer. The method was standardized with dissolved $KHCO_3$ with data precision of ±0.013 mM. $\delta^{13}C_{IC}$ samples were acidified in Labco Exetainer tubes and the liberated CO_2 analyzed using a Thermo-Finnigan GasBench II coupled with a Thermo-Finnigan DeltaPlusXL isotope ratio mass spectrometer. Dissolved $KHCO_3$ was again used for isotopic standardization, with a precision of better than 0.04‰. The isotopic data are reported in the conventional delta notation (‰) versus V-PDB. Metal concentrations were measured using a HR ICP-MS Element 2 (Thermo Finnigan). The accuracy and precision of the technique, reported in Table 3-1, were calculated by comparing multiple measurements of the external standard SLRS4 (Canadian river water standard). The speciation of the dissolved metals, as well as the saturation indexes of major metal-carbonate and metal-oxide minerals were estimated based on measured major element, trace metal and IC concentrations, and the field parameters with the analytical modeling speciation program PHREEQC (Parkhurst and Appelo, 1999).

A simple model was applied to the river time-series data to determine if statistically significant diel variation existed for each geochemical parameter and, if so, to quantify the phase, amplitude, and mean of that variation. The model fits a 24 hour periodicity sine curve of the form:

$$E_t = M + A\,[\cos(t \cdot 360 \cdot \pi \cdot 180^{-1}) - (P \cdot \pi \cdot 180^{-1})] \qquad (3\text{-}1)$$

Where t is time of day (hrs), M is the mean value of the time-series data, A is half the amplitude of the diel variation, and P is the phase of the variation as defined by the time of day at which the modeled curve peaks. The statistical significance of each diel variation was determined by calculating the F-statistic for the sine model in comparison

with a null model based only on the mean of the time series. A parameter was considered to have significant diel variation if the p-value for the F-test comparing this null model to the sine model was less than 0.1. Detailed descriptions of this statistical method are given in Kurz et al. (in review). Difference between the maximum and minimum values was integrated over a 24 hour period and this value is considered to be the loss of each element regardless of process causing the loss. We term this loss the "diel flux".

Stoichiometric Variability

The relationship between elemental stoichiometry in the vascular plant and algal tissue samples and the environmental availability of elements was evaluated by comparing the molar Carbon:Element (C:E) ratio of the vegetation samples collected in the source springs with the C:E ratio in the ambient spring water. The concentration of IC was used to calculate the C:E ratio in the water. The distinct but stable water chemistry in the source springs means that the water chemistry can be considered a reasonably strong predictor of the environment the vegetation has been growing in. An organism's degree of stoichiometric homeostasis is parameterized as H, which is calculated as 1/slope of the regression between the log of the resource (i.e. water) stoichiometry and the log of the biomass stoichiometry (Sterner and Elser, 2002). A slope of 0 (i.e., $H \rightarrow \infty$) indicates that element concentrations in the biomass are static regardless of the chemistry of the ambient water, i.e. the plant is strictly homeostatic. Conversely a slope of 1 or greater indicates that element concentrations in the biomass reflect the chemistry of the ambient water, i.e. non-homeostatic or 'plastic'.

Assimilation

The daily assimilatory uptake of elements from the river was calculated using the net carbon flux into biomass, i.e. net primary productivity (NPP), of the river ecosystem and the average measured element/carbon stoichiometry of both the vascular and algal tissue samples from the river sites. Daily gross primary productivity (*GPP*, moles-C day^{-1}) was determined from the diel variation in DO concentrations, corrected for reaeration (Heffernan and Cohen, 2010), using the single station oxygen metabolism method (Odum, 1957). This was converted to daily NPP (moles-C m^{-2} day^{-1}) by assuming autotrophic respiration is equal to 50% of GPP (Hall and Tank, 2003). NPP is reported normalized to the area of the streambed (153,000 m^2) to represent an assimilatory flux (mass/area/time). The element/carbon ratio of each tissue sample was converted from the measured elemental concentration (mg-E/kg-biomass) using the measured weight percent of carbon in the sample. It is assumed that the autotrophic assimilation of elements during growth occurs in proportion to the stoichiometry measured in the tissue samples. This explicitly neglects internal resorption, estimates of which are not possible because of the absence of senescent litter, potentially overestimating the assimilatory flux. The estimates of element removal via assimilation are presented as a percentage of the observed diel (24-hr) elemental flux, calculated as described in Kurz et al. (in review).

Results

Plant Stoichiometry

The vascular plant (*Sagittaria kurziana*) and algal (*Vaucheria* spp.) tissue samples were analyzed for 29 major and trace elements. Concentrations of C, N, and P, and of the 12 elements also analyzed in the water samples are included in Table 3-2.

Measured and published concentrations and precision for the Apple Leaf 1515 Standard are also included in Table 3-2. Complete stoichiometry of all measured elements and samples is reported in Table 3-1. Distinct differences were observed between the elemental concentrations of the vascular plant and algal tissues from the samples collected at both the river and spring locations. Major elements tend to be more concentrated in the vascular plant samples, while minor and trace elements tend to be concentrated in the algal samples (Figure 3-2). C, N, and P concentrations are nearly the same in both species although the algal tissues are slightly enriched in N and depleted in P relative to the vascular plant tissues ($C:N:P_{algae}$ = 118:14:1, $C:N:P_{vascular}$ = 80:6:1). K^-, Fe, U, and Cr concentrations exhibit the greatest difference between species, with K being an order of magnitude more concentrated in the vascular plant tissues (K_{vas} = 41315 vs. K_{alg} = 2453 mg-K/kg-biomass) and Fe, U and Cr being an order of magnitude more concentrated in the algal tissues (average concentrations in the river samples = 420 vs 3851, 0.18 vs 1.73 and 2.33 vs 24.3 mg/kg-biomass, for vascular plant and algal tissues respectively; Table 3-2). Mg^{2+} and Mn concentrations are both more than 50% greater in the vascular plant samples, while Ca^{2+}, V, Cu, and Ba concentrations are all more than 50% greater in the algal samples (Table 3-2).

Distinct differences in element stoichiometry between sampling sites was observed for both the vascular plant and algal tissues, especially in the minor and trace element concentrations (Table 3-2). For almost all elements the variability between the samples collected in the springs is higher than the variability between the samples collected in the river for both the vascular plants and algae. The relationships between the elemental stoichiometry (C:E) in the vascular plant and algal tissue samples

collected in the springs, and the IC:E ratio of the ambient spring water are show in Figure 3. The slope of the regression between the resource and biomass chemistry (i.e. 1/H) is plotted only for those elements where the regression relationship is considered significant ($p < 0.1$; e.g. Persson et al., 2010). When significant, the slope of the regression for Mn, U, and Sr is greater than 1, and for Cr is greater than 0.6, indicating the stoichiometry of these elements is relatively plastic. In contrast, the slope of the regression for N, and for K in the vascular plant tissues, is almost zero, indicating the stoichiometry of these elements is homeostatic.

Comparable river water samples were not collected at the vegetation sampling sites along the length of the river, so variability in the tissue stoichiometry of these samples cannot be compared directly to variability in ambient water. The variability between river samples may be attributed to longitudinal changes in river chemistry (e.g. Kurz et al., in review; Cohen et al., 2012; Heffernan et al., 2010) resulting from the downstream mixing of spring waters, each with its own unique compositions, diffuse additions of anoxic pore-waters that are enriched in redox sensitive elements (e.g., Fe and Mn), and in-stream chemical processing.

Diel Variation in River Chemistry

Diel variation was observed in all field parameters including pH, DO, temperature, specific conductivity, NO_3, and SRP (Figure 3-4). pH, DO concentrations and temperature all peak in the late afternoon, lagging the peak in solar radiation by 4.5 to 5.5 hours (Figure 3-5), although the maxima in pH preceded the maxima in DO and temperature by two hours. These field parameters, which all vary in direct response to either insolation or plant metabolism, have the most significant diel variation (p-values < 10^{-26}; Table 3-3). Diel variation in NO_3 and SRP concentration is almost perfectly out-

of-phase with each other (Figure 3-5). SRP declines during the day, from peak concentrations at ca. 13:00 to minimum concentrations at midnight, and NO_3 increases during the day from minimum concentrations at 16:00 (Table 3-3, Figure 3-5). All the parameters related to calcite solubility, including IC, Ca^{2+} concentrations, specific conductivity, $\delta^{13}C_{IC}$, and the saturation index of calcite ($SI_{calcite}$) exhibit significant diel variation (Figure 3-4 and 3-5). $\delta^{13}C_{IC}$ and $SI_{calcite}$ are in-phase with DO, pH and temperature while IC, Ca^{2+}, and specific conductivity are, as expected, out-of-phase.

Of the major and trace elements analyzed, significant diel variation was observed in eleven – Ca^{2+}, Mg^{2+}, K^+, V, Cr, Mn, Fe, As, Sr, Ba, and U (Figure 3-4 and 3-6) – while Na^-, Cl^-, SO_4^{2-}, and Pb concentrations exhibited no statistically significant diel variation (Table 3-3). The difference between the concentrations of Co, Cu, Zn, and Ni in the ISCO storage duplicates was greater than 10% (Table 3-1) so these data are not reported. U, As, V, Fe, Cr, Mg^{2+} and K^+ concentrations all increase during the day, approximately in phase with pH, DO and temperature (Figure 3-5), with the maxima occurring successively from U at 14:00, 4 hours ahead of diel DO variation, to K^+ at 23:00, 5 hours lagged from DO (Table 3-3). As is the closest in phase to pH, with no discernible lag, and V is closest to DO and temperature, with less than an hour lag. V and Cr had the most significant diel variation of the elements in-phase with DO, with $p < 10^{-11}$. In contrast, Sr, Ba, Ca^{2+}, and Mn concentrations all increase at night, approximately 12 hours out of phase with the timing of pH, DO and temperature. Their maxima are roughly evenly spaced from Sr at 3:00 to Mn at 8:00 with Ba being exactly 12 hours out of phase with pH. Mean concentrations of all metals are generally low,

decreasing from Sr (184 ppb),to Ba, Mn, and Fe (3-5ppb), V, Zn, and As (1-2ppb), and U, Cr, Cu, Ni, Pb, and Co (< 1ppb; Table 3-3).

Assimilation Calculations

Estimates of assimilatory uptake (mmol m^{-2} day^{-1}) were calculated using the measured stoichiometry of both the vascular plant and algae tissues for each element that displays diel variation (Table 3-4). The fraction of ecosystem GPP resulting from metabolic processes of the two species is unknown and as such the actual amount of assimilatory uptake should be between the two estimates. Large differences occur in estimated daily uptake depending on which species stoichiometry is used, reflecting differences in stoichiometry between the vascular plants and algae. Uptake was smallest for U and Co (U = 5.0 and 47 $x10^{-6}$ and Co = 7.1 and 7.3 $x10^{-5}$ mmol m^{-2} day^{-1} based on the vascular plants and algae respectively; Table 3-4), followed by Cu, Ba, V, Cr, and Sr. Except for Cr, uptake rates for all these elements are equally minor (<6%) when compared with total daily removal, based on the observed diel variation in the river. For Cr, 27% of its diel variation could be from assimilation based on the algal stoichiometry. For Ca^{2+} and Mg^{2+} the estimated assimilatory uptake is comparatively high (Ca^{2+} = 1.5 and 4.1 and Mg^{2+} = 2.3 and 0.52 mmol m^{-2} day^{-1} for vascular plants and algae respectively) but accounts for a trivial fraction (< 3%) of observed diel variation. Mn, Fe and K^{+} are the three elements where calculated assimilatory uptake is high both in absolute magnitude (Mn = 0.038 and 0.021, Fe = 0.05 and 0.45, and K^{+} = 7.0-0.41 mmol m^{-2} day^{-1}, for vascular plants and algae, respectively) and in comparison to the observed diel variation (Mn = 34 and 18%, Fe = 29 and 262%, and K^{+} = 101 and 6%, for vascular plants and algae respectively).

Discussion

The source waters of the Ichetucknee River emerge from the limestone Floridan Aquifer with chemical compositions that are unique to each spring, but are relatively stable at annual time frames (Martin and Gordon, 2000), and remain constant, well within the error of the measurements, over diel timescales. The diel variation of river solute concentrations does not result from changes in flow or evaportranspiration based on stable discharge and conservative Cl^- concentrations at the downstream 2700 sampling site (Figure 3-4) (e.g., Kurz et al., in review). This variation instead results from cumulative in-stream biogeochemical processes that occur over the 5km reach between the springs and the sampling point.

Inorganic Controls on Diel Variation in River Chemistry

The particular inorganic processes controlling the observed diel variation in river chemistry have been the topic of several previous studies and the data reported here are consistent with these. de Montety et al. (2011) demonstrated that variation in Ca^{2+}, and IC concentrations, and $\delta^{13}C_{IC}$ values can be attributed to daytime precipitation of calcite, which is indirectly controlled by daytime photosynthesis, and diurnally constant CO_2 production. Following on from this work, Kurz et al. (in review) reported the consistent presence of minor but statistically significant diel variation in Mn, Ba, Sr, and U. Co-precipitation with calcium carbonate could explain the timing and all of the magnitude of the variation in Mn, and some of the variation in Ba and Sr. The timing of diel Fe, U, Mn and Ba variation could be explained by pH- and temperature-dependent adsorption and by photo-reduction (Fe only).

Building upon these previous studies we have added the analysis of four additional elements of which three, V, Cr, and As, exhibited diel variation (Table 3-3),

generally in-phase with each other and with the diel variation in DO, temperature, pH, Fe, and U (Figure 3-5 and 3-6). Metabolically mediated pH-dependent adsorption, responsible for the diel variation in Fe and U concentration, can likely also explain the variation in As and V. Diel As variation in-phase with or lagging pH by 1-3 hours have been reported repeatedly in neutral to alkaline streams and attributed to anionic adsorption (e.g. Fuller and Davis, 1989; Nimick et al. 2005; Gammons et al., 2007). The covariance between diel As and pH variation in the Ichetucknee River are consistent with these observations. V adsorption has also been reported to decrease with increasing pH because, although V is a cationic metal, in dilute solutions the dominant V(V) species are anionic (Naeem et al., 2007; Peacock and Sherman, 2004). V speciation in the Ichetucknee River is dominated by VO_3OH^{-2} and $H_2VO_4^-$, based on the calculations by Phreeqc, suggesting that ph-dependent adsorption likely controls the observed diel variation in V.

Despite the covariance of the diel variation in Cr concentrations with DO and pH neither adsorption nor changes in redox state can clearly explain the observed diel Cr pattern. Given the pH and oxidizing conditions of the river Cr should be in the 3+ valence state and dominated by cationic species such as $Cr(OH)_2^+$. Given these conditions Cr adsorption should increase with increasing pH (Richard and Bourg, 1991), producing the opposite diel variation to what is observed. Cr(III) and Cr(VI) are both soluble, such that the diel variation in DO concentrations should not result in variation in Cr solubility.

Assimilatory Demand and Implications of Stoichiometric Variability

If we assume that assimilation occurs in proportion to tissue stoichiometry and with diel periodicity, assimilation should contribute to the observed diel variation in all

elements, to varying degrees (Table 3-4). Although contributions of the vascular plants vs. the algae to the total ecosystem GPP is unknown the C:N:P of the Ichetucknee River ecosystem aligns most closely with the C:N:P of the vascular plants, suggesting that vascular plant productivity dominates the GPP of the Ichetucknee River ecosystem (Cohen et al., 2013) and thus possibly the assimilatory uptake.

There are several elements – K^+, Cr, Fe, and to a lesser extent Mn - which exhibit marked differences in calculated assimilation between vascular plants and algae (Table 3-4). These arise from differences in the tissue stoichiometry, reported above. Concentrations of K^+ and Mn are higher in the vascular plants compared with algae, resulting in assimilation estimates for vascular plants that are 101% and 34% of the observed K and Mn diel variation vs. only 6% and 18% when based on algal stoichiometry (Table 3-4). The reverse is true for Cr and Fe which are more concentrated in the algae, resulting in assimilation estimates that are 3% vs. 27% and 29% vs. 262% of the Cr and Fe variation for vascular plants and algae respectively.

Not all elements and ions exhibit diel variation in river chemistry, e.g. Na^-, SO_4^{2-}, Cl^- and Pb and yet there is still known autotrophic demand for these elements based on their tissue stoichiometry (Table 3-2, Figure 3-2). Several processes could contribute to masking or eliminating the observable diel variation of these elements in the river. Uptake of these elements may occur continuously, especially for those which may be limiting or be internally cycled. If plant assimilation occurs with a diel variation, the magnitude of the assimilatory diel signal could be negligible relative to the precision of the measurement. Finally, the phase of the assimilatory variation could be masked by geochemical processes of equal magnitude acting out of phase. For example, Kurz et

al. (in review) showed that the magnitude of Sr removal by carbonate co-precipitation was on order with expected removal by assimilation suggesting that these two processes could be operating out of phase, effectively canceling out any visible diel Sr variation.

The Timing of Assimilatory Uptake

The timing and magnitude of the observed diel element variation in the Ichetucknee River can be partially accounted for by inorganic processes, most of which are indirectly the result of the metabolism of the submerged vegetation. A fraction of the removal should also be the direct result of assimilation; however, timing of assimilation for most elements (with the exception of oxygen and carbon) is not well established. If multiple controls (e.g., assimilation, calcite co-precipitation, or photo-reactions) are out of phase, as was inferred for phosphate (Cohen et al. 2013), estimates based on observed variation for each process could over- or under-represent the influence of individual processes.

Roberts and Mulholland (2007) and Heffernan and Cohen (2010) both report diel variation in nitrate that is exactly out of phase with DO, suggesting that N assimilation occurs synchronously with photosynthesis. If element assimilation is also synchronous with photosynthesis the resulting diel variation may overlap with variation controlled by inorganic processes which are indirectly mediated by plant metabolism (e.g. pH-dependent adsorption, carbonate precipitation/dissolution, oxidation/reduction reactions, etc.). Conversely, the timing of assimilation may be independent from photosynthesis. Cohen et al. (2013) report diel variation in SRP that significantly lags N assimilation, suggesting asynchronous assimilation of P and N. Diel variation in specific biochemical demands (e.g., proteins for N, ribosomes for P) suggests other elements may also have

diel variations in the demand for those elements. Finally, in addition to controlling the in-stream concentrations of elements, the timing of assimilation may also respond to element availability. If assimilation increasing synchronous with diel increases in concentrations in the river the diel variation resulting from assimilation will be directly out-of-phase with the diel variation resulting from other geochemical controls.

Disentangling the relative control that each process has on the composite diel signal requires better understanding of the timing and magnitude of all processes controlling the variation. As our understanding improves we can use an inverse modeling approach that considers these overlapping processes to quantitatively recreate the signal for each element and based on known parameters such as published affinities and coefficients, reaction kinetics, etc. The residuals of this model could then be used to constrain remaining unknown parameters, such as the timing of assimilatory uptake and of the metabolic processes driving that uptake.

In the Ichetucknee River the timing and/or magnitude of most of the processes controlling the diel variation not constrained well enough to definitively disentangle the assimilation signal from the other geochemical controls. Nonetheless, several inferences can be made. Diel variation in Ba, Sr, Mn, and Ca^{2+} concentrations are all 12 ±3 hours out of phase with DO and pH (Figure 3-5) suggesting the variation in these elements could be enhanced by assimilation synchronous with photosynthesis in addition to the geochemical control by calcite precipitation. In contrast, U, As, V, Fe and Cr variation is approximately in-phase (± 3 hours) with the variation of DO.

One element, K^{+}, may be controlled entirely by assimilation. Potassium has no known geologic source since limited K-bearing minerals occur in the carbonate-

dominated Ichetucknee River watershed. Furthermore, K^+ does not react in response pH or redox variation, and as such there is no obvious geochemical explanation for the small, but significant, diel K^+ variation (Figure 3-4). In contrast K has known metabolic function in autotrophs, serving a critical role in ion transport and osmotic balance (ex. Healey, 1973). Estimates based on the stoichiometry of vascular plants indicate that assimilation can account for all (101%) of the observed K^+ variation (Table 3-4), suggesting that the magnitude, and therefore also timing, of diel K^+ variation could be wholly controlled by assimilation. Assimilatory control of K^+ cycling is substantiated by the K^+ stoichiometry of the vascular samples being homeostatic (1/H = -0.02 for the samples collected in the springs; Figure 3-3) suggesting that K^+ uptake is driven by fixed metabolic demand rather than varying with environmental K^+ availability. Because the stoichiometry of K in the algal tissues is much lower than the vascular (5918 vs. 101257 mg-K^+/kg-C, respectively), the assimilatory control of K^+ holds true only if vascular GPP does in fact dominate total ecosystem GPP. The observed diel variation in K^+ is 6 hours out of phase with DO, CO_2, pH, NO_3 and PO_4 variation (Figure 3-5) suggesting that the timing of vascular plant demand for K is out of phase with photosynthesis. Potassium assimilation precedes the assimilation of IC and NO_3, possibly reflecting the need for K-based transport channels of uptake of these ions across cell walls.

Implications for Ecosystem Function

Stoichiometric differences observed between the vascular plant and algae samples, and the relationships between tissue stoichiometry and ambient water chemistry (i.e. elemental resource availability), have important implications for the biotic structure and function of spring ecosystems. The stoichiometry of two important

micronutrients, Fe and Mn, differ by an order of magnitude between the vascular and algae samples (Table 3-2). These differences suggest that changes in environmental element availability could affect the heath and/or relative abundance of algae vs. vascular plants, and conversely, that changes in relative abundance of either species should affect the cycling of metals within the ecosystem. In the case of Florida's springs and spring-fed rivers benthic algal proliferation has become increasingly common over the last 20 to 30 years; *Vaucheria* spp., the algal taxa analyzed in this study, is one of the nuisance algae found in nearly all springs (Stevenson et al., 2004). The prevailing narrative holds that N enrichment has led to algal proliferation, but a recent synthesis finds little support for that explanation (Heffernan et al., 2010b) instead arguing that a significant negative correlation of algal cover with DO might suggest grazer controls. An alternative explanation supported by these data is that changes in the availability of Mn (perhaps induced by changes in redox state of the water), but not Fe, would disproportionally inhibit the productivity and/or relative abundance of the vascular plants relative to the algae.

Evaluation of the supply of elements to the river ecosystem relative to the assimilatory demand of the submerged aquatic vegetation indicates that the supply/demand ratios for Mn, and especially Fe, in the Ichetucknee River are the closest to 1 (Table 3-5), suggesting that both Mn or Fe could potentially limit ecosystem productivity. Due to the differences in stoichiometry the vascular plants should be more sensitive to Mn limitation and the algae to Fe. Two lines of evidence refute the possibility that Fe is limiting either species. The Fe stoichiometry of neither the vascular plant nor algal tissues from the spring samples vary systematically with changes in

ambient water chemistry despite relatively significant variation in aqueous Fe concentrations between springs (Figure 3-2), indicating that both species are homeostatic with respect to Fe. Secondly, the algal cover in the river declines with distance downstream despite downstream increases in the available supply of Fe due to diffuse additions of Fe-rich anoxic pore-waters to the river (Kurz et al., 2012). Although the low Fe concentrations in the spring and river does not appear to be influencing algal productivity or abundance, the proliferation of algae could have a reciprocal effect on the cycling of Fe in the river. The assimilation of Fe can account for the equivalent of 30% to >200% of the observed diel variation in Fe (Table 3-4). The significantly higher Fe concentrations in the algal tissues mean that a relative increase in the productivity of algae in the river would increase the magnitude of assimilatory removal even further.

In contrast, Mn shows more evidence of being limiting. Mn stoichiometry is non-homeostatic in both species ($1/H_{vascular}$ = 1.0, $1/H_{algae}$ = 1.1; Figure 3-6), indicating that the tissue stoichiometry for both responds to the environmental availability of Mn. High assimilatory demand combined with the stoichiometry placticity suggests that Mn may be limiting productivity, in particular of the vascular plants. This Mn limitation is substantiated by the typical net loss of Mn seen between the source springs and the downstream river at Site 2700 (~8 ppb vs. 2-5 ppb in the flow weighted springs vs. at 2700; Kurz et al., in review), despite evidence of diffuse additions from Mn-rich pore-waters. This net downstream loss indicates that organic and inorganic processes remove Mn in excess of the hydrologic fluxes into the river system from the springs and diffuse discharge. The combined estimates of removal by assimilation and by calcite co-precipitation alone exceed the observed diel flux in Mn (assimilation = 18-34% of

observed flux, Table 3-4; co-precipitation = 30-400%, Kurz et al., in review). If the vascular plants are more sensitive to the availability Mn, declines in Mn concentrations in the river would impose greater limitation on vascular productivity over algae. Although no long-term data are available to demonstrate a decline in Mn concentrations in Florida's springs and rivers over timescales commensurate with the observed rise in benthic algae, reductions in groundwater levels and spring discharge due to drought and over-pumping would be expected to reduce both the input of Mn-rich pore-waters to the river and promote reducing conditions in the aquifer leading to lower concentrations of dissolved Mn in the springs. Each of these factors may stress vascular plant growth and enhance algal growth.

Conclusions

This study illustrates relationships between the elemental requirements of in-stream vegetation, the availability of nutrients to the aquatic ecosystem, and the magnitude and timing of diel variations in river geochemistry. Diel variation emerges in response to a number of processes both indirectly and directly controlled by the metabolism of submerged vegetation. In a biologically productive system direct autotrophic assimilation can account for a significant portion of the diel variation in river chemistry, as illustrated by K, Mn, Fe, and Cr. Although the stoichiometry of submerged vascular plants and algae in the Ichetucknee River is markedly similar to the average composition of terrestrial leaf biomass there are, nonetheless, distinct differences in stoichiometry between species and samples. Vascular plant tissues are generally enriched in major elements and depleted in trace element relative to algal tissues, with the notable exception of Fe which is an order of magnitude more concentrated in the algae. Systematic differences in the tissue stoichiometry of both species can be

correlated to changes in the ambient water chemistry. These differences suggest that the two vegetation types may respond differently to changes in elemental availability and, conversely, that changes in the relative abundance of algae vs. vascular plants will lead to corresponding changes in the magnitude of assimilatory uptake and its control on the in-stream diel variation. Determining the timing of assimilation is confounded by limited understanding of the timing of biological demand for elements. Evaluating assimilatory uptake relative to the other inorganic controls on diel variation may be useful in determining the timing of uptake and therefore of biological demand.

Table 3-1. Accuracy and precision of measured external standard SLRS4 relative to published standard concentrations, the average of the field/analytical blanks from the diel river samples, the analytical detection limit represented by the value of the lowest calibration standard, and the average coefficient of variation between ISCO storage duplicates.

Element	SLRS: UF values (µg/L)	SLRS: Published values (µg/L)	Average blanks (µg/L)	Detection limits (µg/L)	ISCO duplicates variation
V	0.331 ± 0.022	0.32 ± 0.03	0.001	0.040	3%
Cr	0.302 ± 0.010	0.33 ± 0.02	0.020	0.010	3%
Mn	3.398 ± 0.119	3.37 ± 0.18	0.350	0.305	5%
Fe	104.4 ± 5.5	103 ± 5	0.33	0.401	4%
*Co**	*0.036 ± 0.005*	*0.033 ± 0.006*	*0.032*	*0.010*	*46%*
*Ni**	*0.675 ± 0.033*	*0.67 ± 0.08*	*0.107*	*0.010*	*7%*
*Cu**	*1.817 ± 0.104*	*1.81 ± 0.08*	*0.242*	*0.020*	*16%*
*Zn**	*0.946 ± 0.198*	*0.93 ± 0.1*	*3.060*	*0.100*	*15%*
As	0.746 ± 0.063	0.68 ± 0.06	0.060	0.040	2%
Sr	28.12 ± 0.82	26.3 ± 3.2	0.52	2.01	3%
Ba	12.66 ± 0.54	12.2 ± 0.6	0.033	0.101	1%
Pb	0.077 ± 0.006	0.086 ± 0.007	0.005	0.010	1%
U	0.044 ± 0.005	0.05 ± 0.003	0.000	0.009	3%

***** Not reported in the diel river data due to ISCO storage concerns.

Table 3-2. Select major and trace element stoichiometry of dominant aquatic vascular (Sagittaria kurziana) and algal (Vaucheria spp.) species. Values are shown for each sample from the individual spring, the average, standard deviation and coefficient of variation for all the spring samples, and the average, standard deviation and coefficient of variation for the river samples. The final section reports the measured and published values and precision for the check standard 1515.

Location	C	N	P	Mg	K	Ca	V	Cr	Mn	Fe	Co	Cu	Sr	Ba	U	LOI (%)
Vascular plant (mg-Element/kg-biomass)																
Head	391000	28300	3695	9211	32793	8300	2.287	3.271	14.09	450	0.231	1.228	33.26	3.084	0.270	83.9
Blue	399100	31300	4181	6182	35670	7199	2.436	3.930	15.45	343	0.527	1.661	19.84	3.859	0.172	81.0
Mission	391800	29000	5233	4298	34741	5414	2.389	1.557	20.21	227	0.204	1.651	25.80	2.471	0.093	81.3
Devils	388900	32000	5351	6037	31303	13150	2.478	2.560	27.05	348	0.269	1.018	31.29	3.791	0.177	81.4
Mill Pond	390300	26100	3945	3509	31502	5728	3.973	0.688	6027	57	12.05	3.229	55.72	10.84	0.162	81.6
$Av_{Springs(5)}$	392220	29340	4481	5847	33202	7959	2.712	2.401	12212	285	2.66	1.757	33.18	4.808	0.174	81.8%
$StD_{Springs}$	3990	2378	761	2198	1944	3126	0.708	1.300	687	150	5.25	0.868	13.64	3.417	0.063	0.01
$CoV_{Springs}$	1%	8%	17%	38%	6%	39%	26%	54%	220%	53%	198%	49%	41%	17%	36%	1.4%
$Av_{River(6)}$	408300	32017	5010	8497	41315	9165	2.648	2.325	466	420	0.634	1.056	36.39	5.380	0.181	83.4
StD_{River}	10856	1311	907	386	4122	2724	0.467	1.230	157	175	0.440	0.264	10.17	1.894	0.053	0.01
CoV_{River}	3%	4%	16%	5%	10%	30%	18%	53%	34%	42%	69%	25%	28%	35%	30%	1.5%
Algae (mg-Element/kg-biomass)																
Head	418700	45900	3329	3112	417	34509	13.95	57.89	46.54	617	1.271	16.31	44.07	3.839	4.258	88.7
Blue	410800	47000	2672	482	82	36647	4.603	26.85	9.71	1936	0.369	2.837	26.88	3.893	0.665	78.6
Mission	402500	44200	2383	1176	78	18008	29.29	32.01	18.71	398	0.168	6.228	18.87	2.528	1.039	87.6
Devils	355900	55900	5078	1139	167	32115	3.063	23.00	620	96.9	0.918	2.965	39.38	10.25	0.245	76.3
Mill Pond	412800	46700	3233	3430	742	6978	32.08	6.091	4243	531	8.301	11.54	28.74	13.80	1.519	88.4
$Av_{Springs(5)}$	400140	47940	3339	1868	297	25652	16.40	29.17	988	716	2.205	7.974	31.59	6.862	1.545	83.9
$StD_{Springs}$	25402	4581	1048	1315	285	12730	13.33	18.77	1838	710	3.435	5.84	10.11	4.908	1.588	0.06
$CoV_{Springs}$	6%	10%	31%	70%	96%	50%	81%	64%	186%	99%	156%	73%	32%	72%	103%	14%
$Av_{River(5)}$	410480	47020	3524	1931	2453	24911	14.15	24.34	173	3851	0.664	5.223	37.55	11.22	1.725	83.6
StD_{River}	6979	2229	608	1105	2944	6735	5.868	17.41	212	1657	0.480	3.039	8.80	7.813	1.310	0.07
CoV_{River}	2%	5%	17%	57%	120%	27%	45%	72%	122%	43%	72%	58%	23%	70%	76%	8%

Table 3-2. Continued

Location	C	N	P	Mg	K	Ca	V	Cr	Mn	Fe	Co	Cu	Sr	Ba	U	LOI (%)
Standard 1515: Apple Leaf (mg-Element/kg-biomass)																
$Av_{Measured(2)}$				3029	15024	15651	0.769	0.311	50.91	74.9	0.104	5.574	25.25	48.43	0.008	
$StD_{Measured}$				19	197	35	0.003	0.014	2.5	2.9	0.003	0.156	0.23	2.38	0.0003	
$CoV_{Measured}$				0.6%	1.3%	0.2%3	0.5%	4.6%	5%	3.9%	3.1%	2.8%	0.9%	4.9%	3.8%	
Published[a]		2250	1590	2710	16100	15260	0.26	*0.3*	54 ±3	83	*0.09*	5.64	25 ±2	49 ±2	*0.006*	
(±)		±1900	±110	±80	±200	±150	±0.03			±5		±0.24				

[a] Values in *italics* reported but uncertified

Table 3-3. Summary of major field parameters, solute concentrations, and modeled diel sine function results and significance.

Parameter	Mean (*M*)	Observed data range	F-test	p-value	Significant diel cycle	Modeled amplitude (*A*)	Modeled cycle peak (*P*)
Radiation (W/m^2)	262	941	79.9	< 0.00001	Yes	822	12:30
Temp (°C)	22.5	2.57	341	< 0.00001	Yes	2.38	18:00
pH	7.40	0.8	272	< 0.00001	Yes	0.74	17:00
DO (mg/L)	5.52	5.97	648	< 0.00001	Yes	5.70	18:00
SpC (µS/cm)	333	13	215	< 0.00001	Yes	5.68	5:15
NO_3 (mg/L)	0.44	0.10	584	< 0.00001	Yes	0.092	2:45
SRP (µg/L)	1.62	0.57	116	< 0.00001	Yes	0.24	13:00
IC (mM)	2.91	0.41	180	< 0.00001	Yes	0.22	6:15
$\delta^{13}C$ (‰)	10.88	2.13	277	< 0.00001	Yes	1.86	17:45
$SI_{calcite}$	-0.04	0.80	339	< 0.00001	Yes	0.74	16:45
Ca^{2+} (mM)	1.37	0.087	43.6	< 0.00001	Yes	0.056	7:00
Mg^{2+} (mM)	0.25	0.076	8.32	0.00067	Yes	0.030	21:45
Na^{+} (mM)	0.17	0.015	0.09	0.91	No	-	-
K^{+} (mM)	0.011	0.003	8.14	0.00077	Yes	$1.2x10^{-3}$	23:15
Cl^{-} (mM)	0.18	0.018	0.28	0.75	No	-	-
SO_4^{2-} (mM)	0.15	0.013	0.32	0.71	No	-	-
V (ppb)	1.90	0.651	47.5	< 0.00001	Yes	0.36	18:30
Cr (ppb)	0.509	0.277	168	< 0.00001	Yes	0.20	20:30
Mn (ppb)	3.37	2.71	256	< 0.00001	Yes	1.92	8:15
Fe (ppb)	3.33	6.21	2.35	0.097	Yes	1.56	19:30
As (ppb)	1.18	0.332	3.85	0.025	Yes	0.092	17:00
Sr (ppb)	184	8.73	16.2	< 0.00001	Yes	3.94	3:15
Ba (ppb)	4.93	0.973	17.3	< 0.00001	Yes	0.48	5:00
Pb (ppb)	0.013	0.078	$5x10^{-15}$	1.0	No	-	-
U (ppb)	0.641	0.194	3.71	0.028	Yes	0.046	14:00

Table 3-4. Calculations of element uptake by autotrophic assimilation for those elements exhibiting diel cycles. Calculations based on both vascular and algae stoichiometry. Exact contribution of vascular vs. algae productivity to ecosystem GPP is unknown.

Type	Mg	K	Ca	V	Cr	Mn	Fe	Sr	Ba	U
					Element in biomass (mg kg^{-1})[a]					
Vascular	8497	41315	9165	2.65	2.33	319	420	36.4	5.38	0.181
Algae	1931	2453	24911	13.15	24.3	173	3851	37.6	11.2	1.73
					Element:Carbon ratio of biomass (mg-E/kg-C)[b]					
Vascular	20820	101257	22495	6.49	5.74	778	1035	89.2	13.2	0.444
Algae	4686	5918	60871	31.9	59.1	420	9371	91.7	27.4	4.17
					Calculated assimilatory uptake (mmol m^{-2} d^{-1})					
Vascular	2.3	7.0	1.5	$3.4x10^{-4}$	$3.0x10^{-4}$	0.038	0.050	$2.7 x10^{-3}$	$2.6 x10^{-4}$	$5.0 x10^{-6}$
Algae	0.52	0.41	4.1	$17x10^{-4}$	$31x10^{-4}$	0.021	0.45	$2.8 x10^{-3}$	$5.4 x10^{-4}$	$47 x10^{-6}$
					Observed diel flux (mmol m^{-2} d^{-1})					
	148	6.91	153	0.030	0.011	0.11	0.17	0.16	$9.1x10^{-3}$	$1.2x10^{-3}$
					Assimilatory uptake as a percent of observed diel flux					
Vascular	1.6%	101%	1%	1%	3%	34%	29%	2%	3%	0.4%
Algae	0.3%	6%	3%	6%	27%	18%	262%	2%	6%	4%

[a] Average of river samples; [b] Converted from mg-Me/kg-biomass using measured weight % C

Table 3-5. Calculations of the supply of elements in the river relative to the assimilatory demand. Supply is calculated based either on the flow-weighted average input from the springs, the average concentration at the down-river site US2700, or the maximum diel down-river concentration. Demand, based on either the vascular plant or algal tissue stoichiometry, was calculated by normalizing the assimilatory uptake (Table 3-4) to the benthic area of the river.

	C	N	P	Na	Mg	K	Ca	V	Cr	Mn	Fe	Co	Ni	Cu	Zn	Sr	Ba	Pb	U
								Supply (mol-E day^{-1})											
Springs	1840000	25600	998	98400	154000	6470	841000	21.6	9.7	26.2	7.2	0.1	1.2	3.1	55.6	1120	22.1	0.06	1.8
Av. @ 2700	1770000	19400	981	101000	151000	6500	830000	22.9	6.1	36.7	41.6					1280	21.9	0.04	1.6
Max. @2700	1870000	21300	1060	-	169000	7540	854000	27.2	7.6	54.8	79.8					1300	23.3	-	1.8
								Demand (mol-E day^{-1})											
Vascular	34300	2300	163	633	352	1060	230	0.05	0.05	5.86	7.58	0.01	0.05	0.02	0.18	0.42	0.04	0.0003	0.0008
Algae	34300	3370	114	23	80	63	623	0.26	0.47	3.17	69.2	0.01	0.06	0.08	0.31	0.43	0.08	0.002	0.007
								Supply/Demand											
Vascular: Sp	54	11.1	5.5	156	437	6.1	3650	413	214	4.5	1.0	10.0	26	187	315	2670	561	206	2360
R_{Av}	52	8.4	6.0	159	428	6.1	3610	437	135	6.3	5.5					3050	554	139	2120
R_{Max}	55	9.2	6.5	-	481	7.1	3710	519	169	9.4	10.5					3110	591	-	2380
Algae: Sp	54	7.6	7.9	4340	1940	103	1350	84	21	8.3	0.1	9.7	19	38	177	2600	270	35	249
R_{Av}	52	5.8	8.6	4440	1890	103	1330	88	13	11.6	0.6					2970	267	24	224
R_{Max}	55	6.3	9.3	-	2130	120	1370	105	16	17.3	1.2					3030	285	-	251

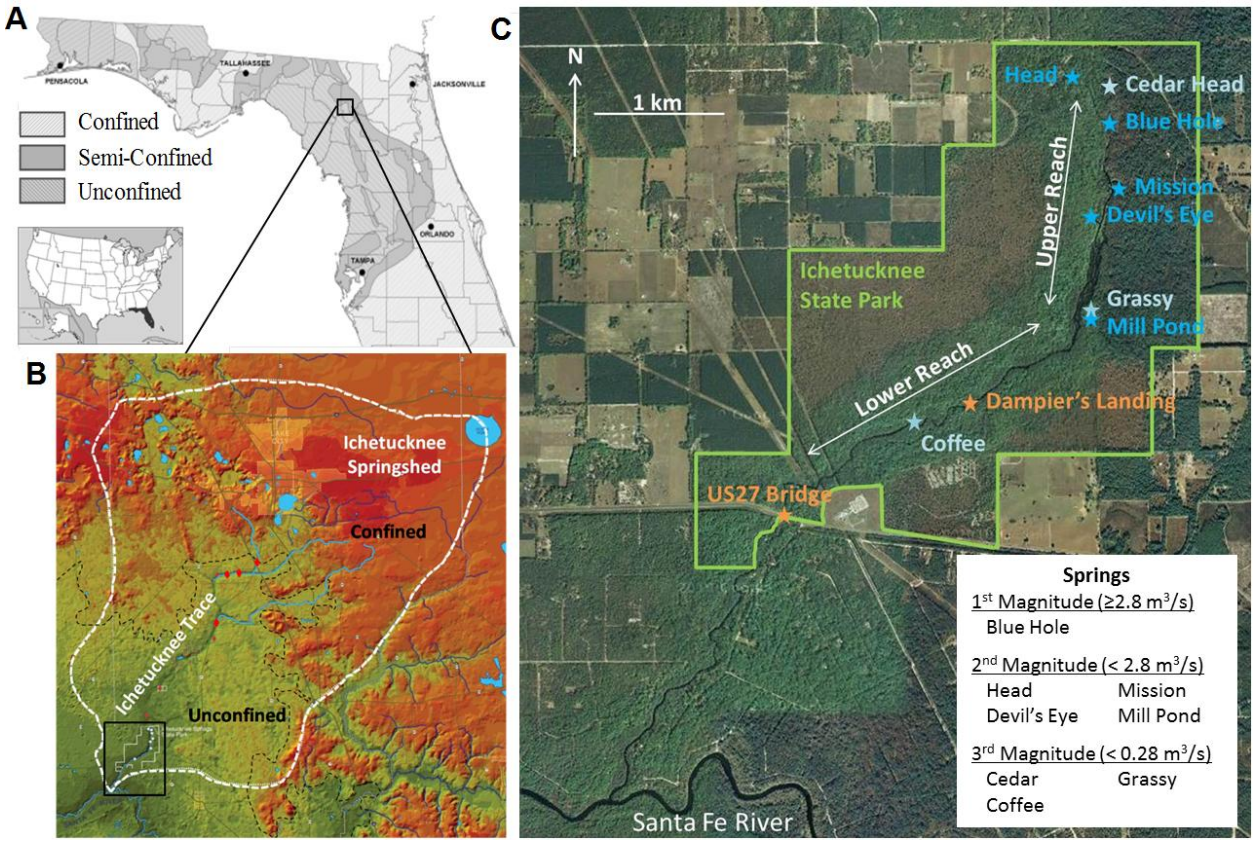

Figure 3-1. Overview of the study area. A) Map of the confined, semi-confined, and unconfined portions of the Floridan Aquifer in north Florida (FDEP, 2006; modified). B) Digital elevation model of the Ichetucknee springshed showing levels of confinement in the elevated portion, and associated surface tributaries and sinks (SRWMD, 2007; modified). C) Google Earth image of Ichetucknee River showing the state park (green outline), 5 sampled springs (blue stars), 3 minor springs (light blue stars), and USGS river gages (orange stars).

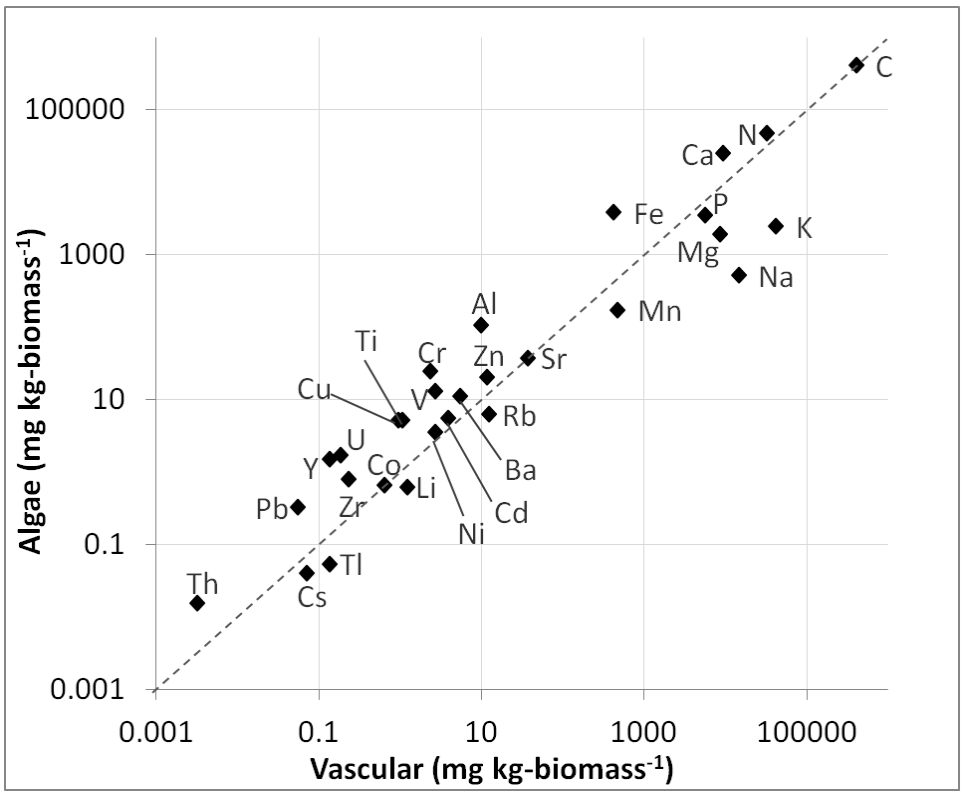

Figure 3-2. Comparison between the average elemental concentrations in the vascular and algae samples from the river sites (used in the assimilation calculations). The vascular samples are generally enriched, relative to the algae, in the major elements (especially Na and K, notable exception is Fe) while the algal samples are relatively enriched in the minor and trace elements (especially Al, Cr, Cu, Ti, U and Y). The dashed line represents identical concentrations in both species.

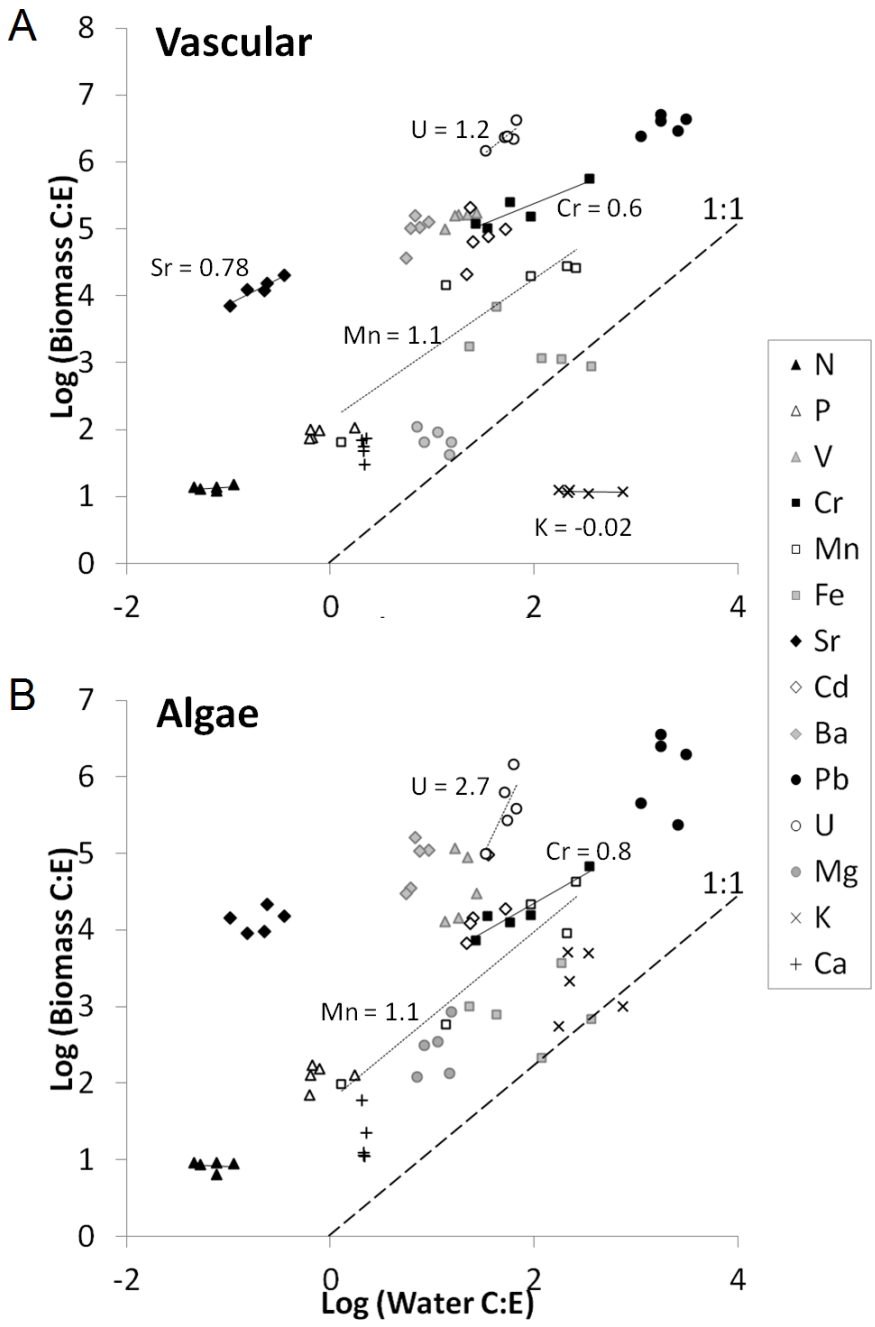

Figure 3-3. Relationship between log (C:E) in the biomass and log (IC:E) in the water for select elements. A) vascular and B) algae samples collected in the 5 main source springs of the Ichetucknee River. The slope of the relationship indicates the degree of homeostasis, and is shown (lines and values) only for elements where $p < 0.1$. $1/H = 1$ indicates no homeostasis; $1/H = 0$ indicates strict homeostasis. Large dashed line indicates the 1:1 slope.

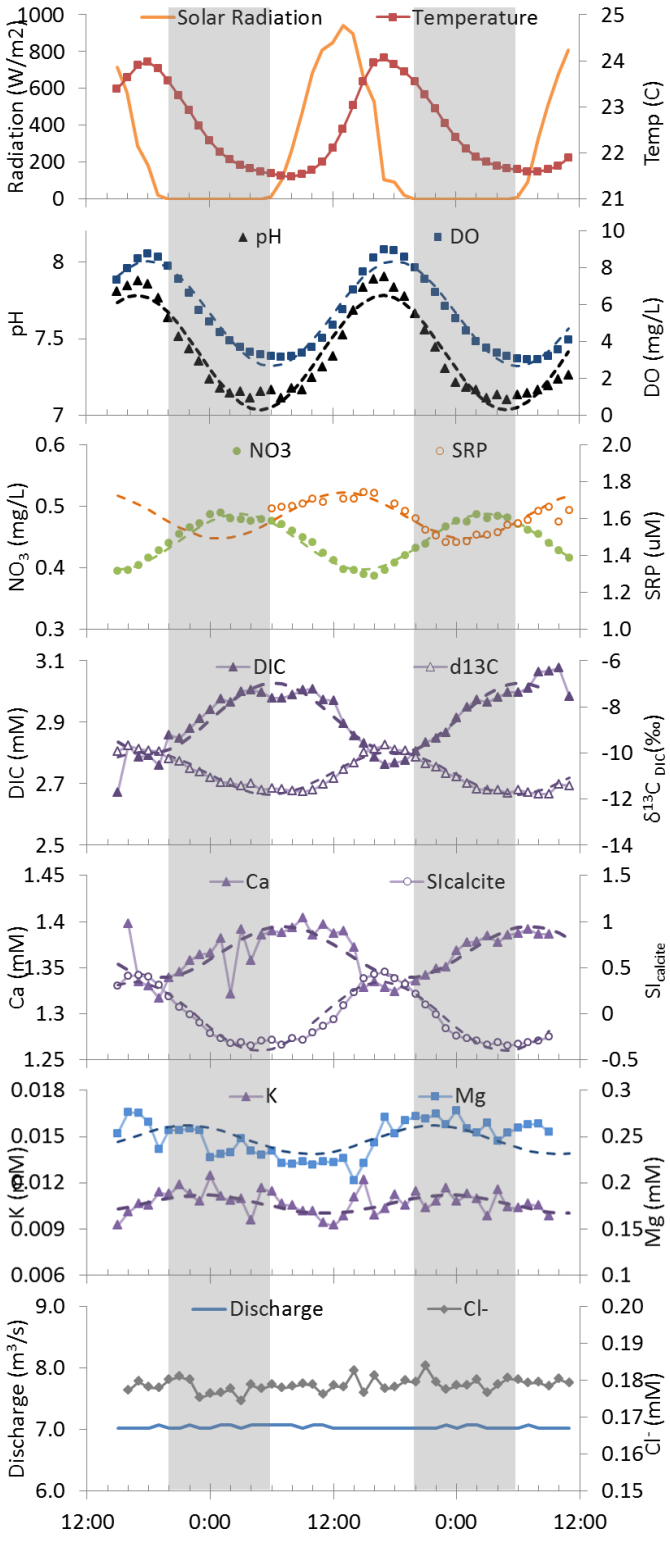

Figure 3-4. Diel cycles of select field parameters, major ions and carbonate solutes observed at site 2700. Cl concentrations and discharge, which exhibit no diel cycle, are also shown. Dashed lines represent the modeled diel fit of the respective solutes. Vertical grey bars indicate nighttime.

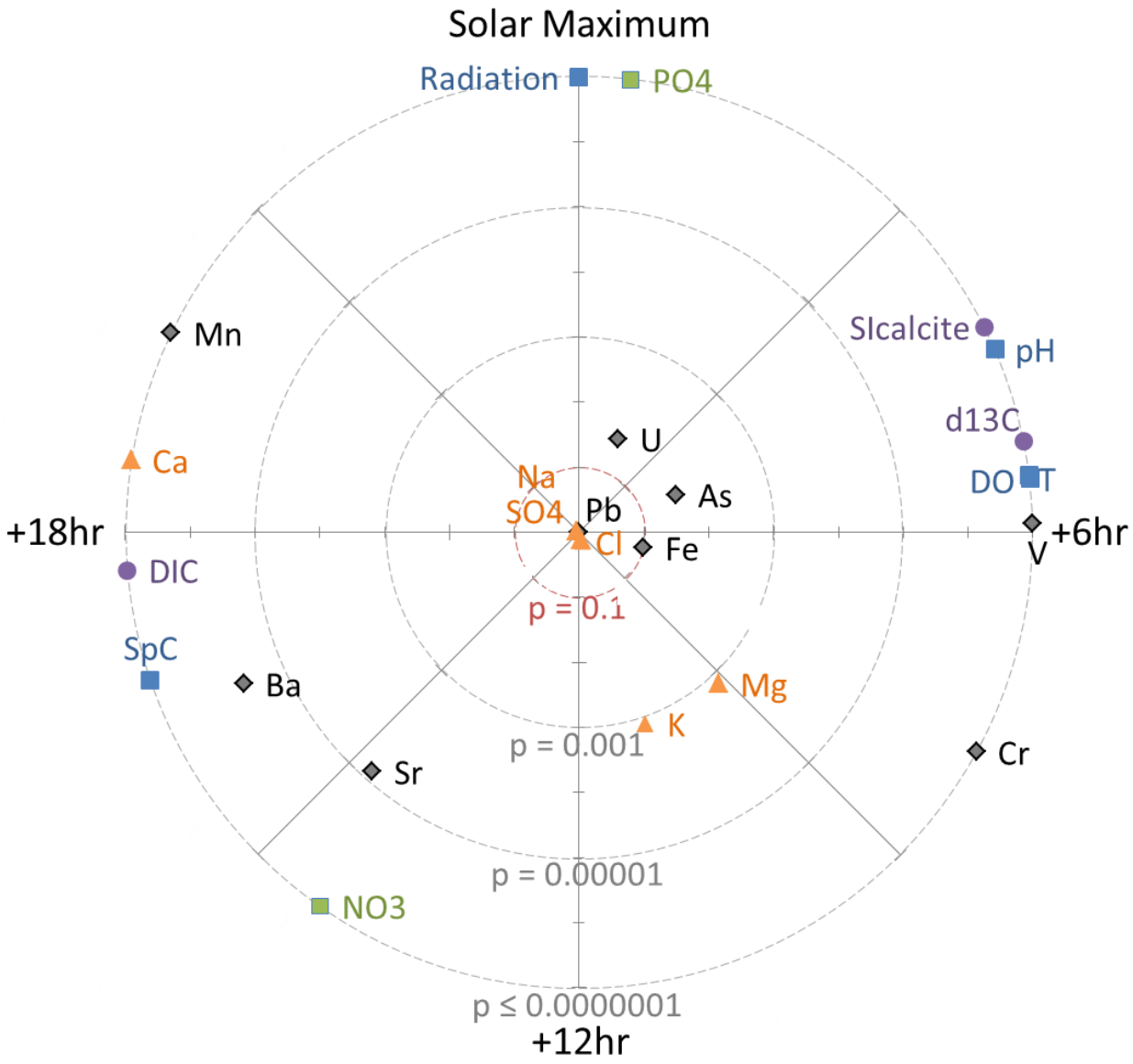

Figure 3-5. Modeled phase and diel strength plot of the observed diel cycles in river solute chemistry. The timing of elemental concentration maxima, relative to the peak in solar radiation (Table 3-3),are plotted as the clockwise distance from +y axis. The distance from the origin reflects the significance of the diel cycle, plotted as the –log of the p-values of the F-test (Table 3-3). Parameters with $p > 0.1$ are not considered to have statistically significant diel cycles. Solutes with $p \leq 0.0000001$ are plotted on the outer ring.

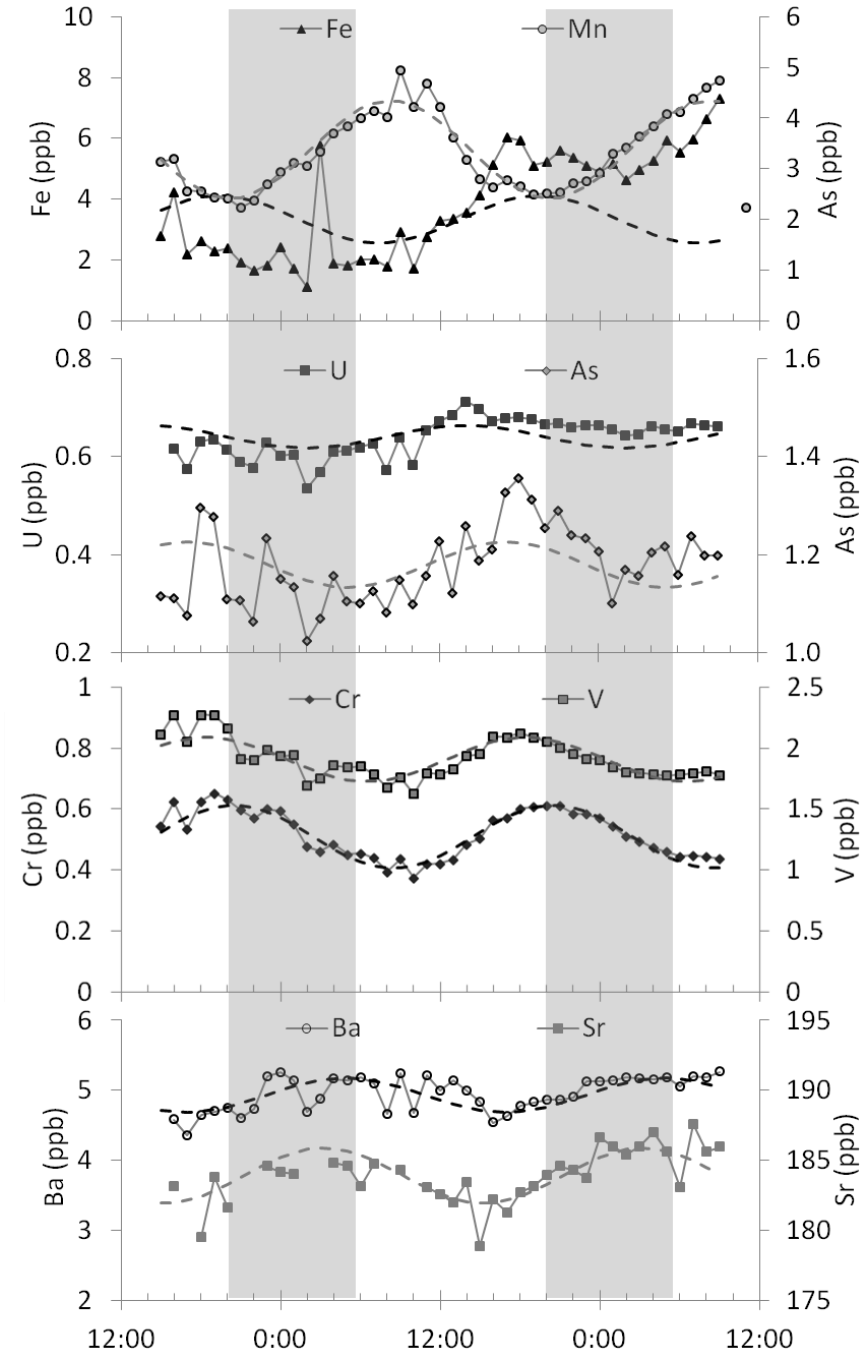

Figure 3-6. Concentrations of ten minor elements which exhibit statistically significant diel cycles. Dashed lines indicate modeled diel fit. Vertical grey bars represent nighttime.

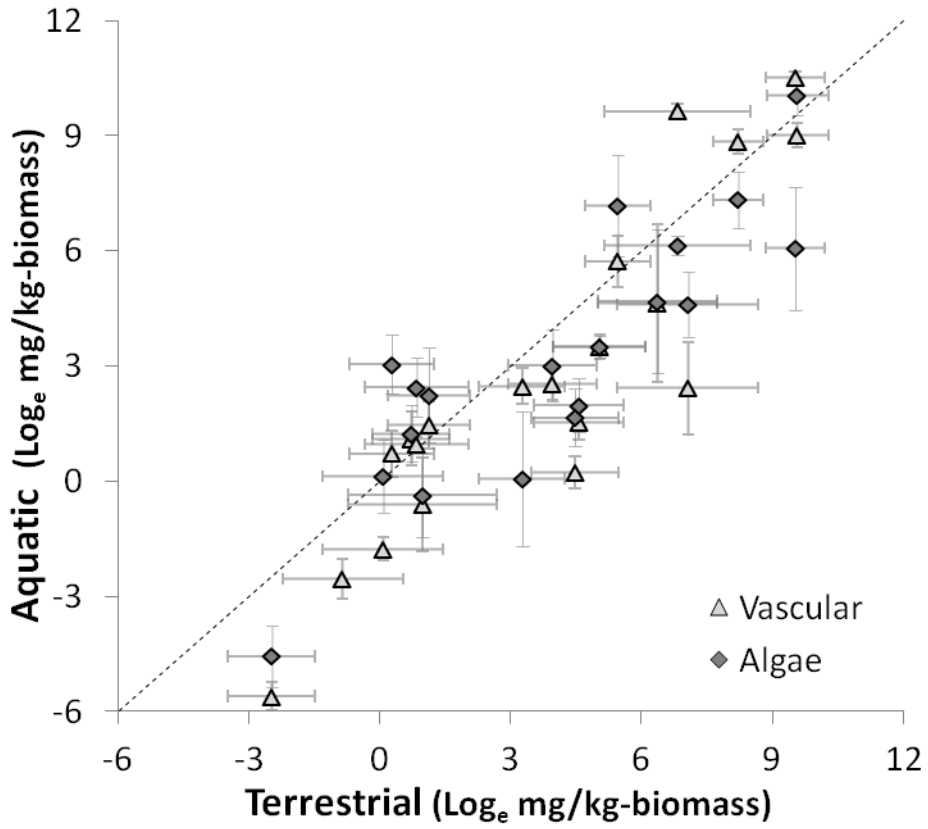

Figure 3-7. Comparison of the average elemental stoichiometry (reported as the natural log of the mg-E/kg-biomass) between a composite of terrestrial leaf tissues (Watanabe et al., 2007) and the aquatic vascular and algal tissues from the Ichetucknee River. Error bars represent standard deviation between samples.

CHAPTER 4
INTERACTIONS BETWEEN DIFFUSE GROUNDWATER DISCHARGE AND THE HYPORHEIC ZONE: IMPLICATIONS FOR ELEMENTAL AVAILABILITY TO STREAMS

Introduction

The hyporheic zone, the area within the stream bed or near-channel saturated zone where the infiltration and exfiltration of surface stream water mixes with groundwater (Bencala , 2000), is characterized by redox chemistry that differs from the surficial chemistry of the stream water. In gaining streams seepage of groundwater through the hyporheic zone can provide a source of water to streams that is chemically distinct from the water within the stream (e.g. Pretty et al. 2006, Soulsby et al., 2005; Robertson et al., 1991). In addition, chemical gradients between the streambed and water in the channel can drive diffuse fluxes of solutes from the streambed. Understanding the magnitude and composition of seepage and diffusive fluxes is critical for evaluating the control these fluxes have on solute, particularly redox sensitive nutrients and trace metals, cycling in streams, the availability of elements to the environment and the structure and functioning aquatic ecosystems.

Hyporheic flow, the chemical composition of water in the hyporheic zone, and their effects on the hydrology, biogeochemistry and ecology of streams has been to the topic of numerous studies, as described in reviews by Krause et al. (2011), Sophocleous (2002), Boulton et al. (1998), and Dahm et al. (1998). The functional significance of the hyporheic zone is primarily a function of hyporheic exchange: the mixing of infiltrating stream water and groundwater within the hyporheic zone. The rate of hyporheic exchange controls the residence time, and therefore the chemical evolution, of water within the hyporheic zone. Exchange rates can vary both spatially and temporally as the result of multiple conditions and processes operating across

scales from bedforms to catchments (e.g. Boano et al., 2007; Malcolm et al., 2005; Leek et al., 2009; Fleckenstein et al., 2006). While quantifying the flux and variability of hyporheic exchange is an ongoing pursuit (e.g. Hester and Doyle, 2008; Rosenberry, 2008; Kalbus et al., 2006) the relative contributions of surface water and groundwater is poorly known except where groundwater chemistry is distinct from the stream and hyporheic zone waters (e.g. Hayashi and Rosenberry, 2002; Hinkle et al., 2001; Triska et al., 1993a). Furthermore, the interactions and alteration of groundwater seepage during passage through the hyporheic zone is not usually considered, except for cases where nitrate is removed from contaminated groundwater by denitrification or algal uptake within the hyporheic and riparian zones (e.g. Hill et al. 1998; Robertson et al., 1991; Peterjohn and Correll, 1984). Nonetheless, the chemical alteration of groundwater seepage through the hyporheic zone may control the environmental availability of other solutes, such as Fe and Mn, which are elevated in the hyporheic zone. The effects on stream chemistry should be particularly significant, and distinguishable, in gaining streams where the underlying groundwater is not chemically distinct from the river, and where the recirculation of surface water through the hyporheic zone is minimal.

The chemistry of the hyporheic zone differs considerably across systems as a function of the residence time (e.g. Valett et al., 1996), the initial chemistry of the water entering the hyporheic zone (Triska et al., 1993a; Christensen et al., 1989), the availability of organic carbon (Holmes et al., 1996) and oxygen (Jones and Holmes, 1996), and the microbial community within the benthic sediments (Fisher et al. 1998). For example, the hyporheic zone has the ability to attenuate and mobilize nutrients as

well as trace metals (Gandy et al. 2007; Smith, 2005; Brunke and Gonser, 1997; Triska et al., 1993b). The decay of organic carbon within the hyporheic zone can produce anoxic conditions leading to denitrification and Mn and Fe reduction, and result in a hyporheic N-sink and Mn- and Fe-source. The opposite effects may result from infiltration of oxic stream water, oxygen release from aquatic plant roots (Clarke, 2002), and microbially mediated oxidation (e.g. Gandy et al. 2007; Jones and Holmes, 1996; Triska et al., 1993a). Variations in the redox state of the hyporheic zone result in variable availability of solutes across stream systems, as well as structure and health of the aquatic ecosystem.

The hyporheic zone has been increasingly recognized as significant transitional ecotone between surface water and groundwater, providing a habitat and/or refugia for aquatic organisms (Krause et al., 2011; Boulton et al., 2008). Aquatic vegetation serves as a link between the hyporheic sediments and surface water (Clarke, 2002), and is therefore sensitive to the chemistry of the hyporheic zone. Localized upwelling of water from the hyporheic zone has been shown to influence the type, distribution, and productivity of vegetation in streams. For example, upwelling of oxygen-depleted and reducing water from the hyporheic zone can be toxic to plant (Sand-Jenzen et al., 1982) as well as faunal (Soulsby et al., 2005) communities in streams. In contrast, upwelling of N- and P-rich water from the hyporheic zone result in hotspots of species richness and productivity (e.g. Mouw et al., 2009; Claret and Fontvielle, 1997; Valett et al., 1994; Grimm et al., 1991). Trace elements are essential micronutrients due to the material requirements by metabolic processes such as P for RNA production (Elser et al., 2003) and Fe for chlorophyll and protein synthesis (Glass et al., 2009; Pushnik et

al., 1984). Since the hyporheic zone can act as both a source and sink of Mn and Fe, the flux of water through the hyporheic zone may control the availability of these and other micronutrients. Hyporheic exchange may be particularly important where Mn and Fe concentrations are low in stream water, potentially limiting ecosystem productivity.

In this study we assess the effects of interactions between groundwater seepage and the hyporheic zone on the spring-fed Ichetucknee River in north-central Florida. We specifically address questions about the magnitude and chemical composition seepage to the river and the significance of these inputs to biogeochemical cycles and ecological functions within river systems. Florida's spring-fed rivers, including the Ichetucknee River, provide model systems for distinguishing the processes controlling solute sources and cycling due to the stable and easily quantifiable inputs of water and solutes from the source springs, absence of surficial inputs and minimal hyporheic exchange (Hensley and Cohen, 2012). Most solute concentrations in the Ichetucknee River exhibit large diel cycles, but these changes do not explain all observed longitudinal changes in river chemistry. Ca^{2+}, Cl^{-}, Fe, and, PO_4 concentrations in the river water are all elevated relative to the flow-weighted input from the source springs despite evidence of in-stream removal of these solutes by biotic and abiotic processes (de Montety et al., 2011; Cohen et al., 2013; Kurz et al., in review). We hypothesize that seepage, which is chemically altered during passage through the hyporheic zone, provides a chemically distinct source of water to the river, relative to the other inputs and water within the stream. We further hypothesize that this unique source mediates the availability of key nutrients, such as Fe and PO_4, in the river, thereby influencing the productivity and structure of the aquatic ecosystem. To test this hypothesis we

compare measurements of pore-water chemistry from sediments of the river bed and multi-year trends in pore-water hydraulic head to the short and long-term temporal changes in chemistry and hydrology of the river.

Methods

Study Site

The Ichetucknee River is an entirely spring-fed system in north-central Florida (Figure 4-1). The eight major, and numerous smaller springs that contribute to the river are sourced from the Floridan Aquifer, an eogenetic carbonate karst aquifer characterized by high matrix storage (e.g., Budd and Vacher, 2004; Florea and Vacher, 2007) and active conduit-matrix exchange (Martin and Dean, 2001; Bailly-Comte et al., 2010; Moore et al. 2009). The springs drain an estimated 960 km^2 springshed (Champion and Upchurch, 2006) that includes both confined and unconfined areas of the Floridan Aquifer (Figure 4-1A and B). The Ichetucknee River, in the southern, unconfined portion of the springshed, flows directly on top of the karstic Ocala Limestone that comprises the Floridan Aquifer. Consistent with the presence of abundant springs, regional potentiometric maps suggest the river is gaining from groundwater but could possibly be a partially flow through system (SRWMD, 2003).

The springs and first 5 km of the river are contained within the Ichetucknee Springs State Park, and comprise our study area. The downstream end of the park is marked by the US 27 highway bridge, which in this study is referred to as the US27 Bridge sampling site. The Ichetucknee River flows 3 km south of the park, before discharging to the Santa Fe River. Seven of the eight named springs, as well as the majority of minor springs, discharge to the river within the upper 2 km (Figure 4-1C). The springs of the Ichetucknee system have distinct but stable chemistry and discharge

(Martin and Gordon, 2000). Discharges of the 6 largest springs and of the river at the US27 Bridge were continuously monitored by the USGS from 2002 until 2010 when monitoring of all but the largest spring (Blue Hole Spring) and the river gage at US27 Bridge were discontinued. We have estimated discharge since 2010 for the 5 springs that had monitoring discontinued using the relationship between flows at each spring and flows at Blue Hole Spring during the 2002 – 2010 period. River discharge at the US27 Bridge has ranged from 5.7 to 14.3 m^3/s over the monitored period.

The river is characterized by two distinct morphologies of its channel. The upper section of the river is wider (15-100m) and shallower (0.5-2.5m) than the lower section. Sediment deposits up to 2.5m thick infill a broad bedrock channel (Hensley and Cohen, 2012). A single, sinuous river channel is incised through the sediments, with intermittent patches of bedrock exposed at the base (Figure 4-2). The majority of flow occurs both within the incised channel but also over the shallower channel margins. The deep channel and shallow margins are dominated by abundant submerged and emergent vegetation. In the lower section of the river the same infilled bedrock channel exits but flow is confined to the single narrow (20-25m), deep (2-2.5m) channel. In the lower section, river margins are characterized by low-lying floodplain dominated by bald cypress. Limestone outcrops occur along the length of the river, delineating the edge of the broad bedrock channel which underlies the river. The gradient along the entire river is less than 2 m/km. Bedrock at the base of the incised river channel is increasingly exposed with downstream distance.

Stilling Wells

A transects of shallow stilling wells was installed within the channel sediments at a site in the upper river (Figure 4-1C) known as the the Rice Marsh. Four deep wells

were installed, three in a cross-channel transect and a fourth 45 m further upstream (Figure 4-2A). The deep wells extend from above the water surface to 70 – 145 cm below the channel sediments, near the bedrock-sediment interface (Figure 4-2B). All wells were constructed of 1 ¼ inch inner-diameter polyvinyl chloride (PVC) pipe with a 30cm screened section at the base of the well made from slotted pipe with a 250um screen interval. Pump tests of each well were conducted and used to calculate the hydraulic conductivity of the sediments. Vertical hydraulic conductivity of the sediments was measured by falling head slug tests using a 3 inch PVC pipe, open only on the bottom, inserted 20 cm into the sediments.

All wells were equipped with Schlumberger conductivity, temperature and depth (CTD) sensors. An additional sensor was also installed in the river at each of the two well sites to measure the surface water conditions. The CTD calibrations were checked pre and post-deployment against a calibrated YSI 556 Multi Parameter System (Yellow Springs Instruments, Yellow Springs, OH) to correct for measurement differences between sensors. CTD measurements were recorded every 30 minutes from 12/15/2010 to 10/05/2013 at the Rice Marsh site. Several sensor failures are responsible for gaps in the CTD record. CTD pressure measurements were corrected for atmospheric pressure using data from Citizen Weather Observer Program (CWOP) station KI4ZBO located outside of Lake City, 20 km from the field site. Calculations of water depth, based on the CTD pressure measurements, were periodically compared against manually measured water depths in the wells to correct for movement of the CTD within the wells. Precipitation data, collected at the State Park, was compiled from

the Suwannee River Water Management District (Site 241) for the duration of the study period.

The design of these wells, coupled with their placement is standing water, prohibited the accurate measurement of temperature during the winter months even though the wells were constructed of low thermal-conductance PVC. Cooling of the groundwater at the top of the well during the winter by the comparatively colder adjacent river water resulted in density driven convection currents within the wells. This convection is visible as truncated diel variations in temperature in the CTD temperature records. Despite the sensors being placed at the base of the well, adjacent to the screen, the flow of water into the well was not sufficient to counter these density driven flows.

Pore and Surface Water Collection

Water samples for chemical analysis were collected from the springs, river and the pore-waters of the channel sediments. Water samples from the springs were collected at the largest six named springs in order to quantify the flow-weighted average inputs of solutes from the springs. Longitudinal changes in the chemistry of the river were assessed by collecting water samples every 500m along the length of the river from just below Head Spring to the US27 Bridge. High-resolution temporal changes in the chemistry of the downstream river were assessed by collecting water samples hourly for 24+ hours at the US27 Bridge sampling site (see Kurz et al., in review for details). Multi-samplers (Martin et al., 2003) installed next to each of the four deep wells at the Rice Marsh site allowed for collection of pore-water chemical profiles. Pumping rates from the multi-samplers varied considerably between the ports, with the time duration necessary to collect the full sample suite ranging from 15 to 50 minutes.

All water samples were filtered and preserved on site. Unfiltered samples for inorganic carbon (IC) and carbon stable isotope ($\delta^{13}C_{IC}$) analyses were preserved with three drops of concentrated $HgCl_2$ solution in 15 ml glass vials. Samples for major and trace element, nutrient and alkalinity analysis were filtered through a trace-metal grade 0.45 um cellulose acetate membrane and stored in high density polyethylene (HDPE) vials. Nutrient (N and P) samples were frozen until analysis. Cation and metal samples were preserved with three drops of concentrated trace-metal grade nitric acid in 20 ml acid-washed HDPE vials. Samples for dissolved organic carbon (DOC) analysis were filtered and stored in 40 ml ashed amber glass vials preserved with 3 drops of HCl. All samples were kept chilled prior to their analysis. The field parameters (T, pH, dissolved oxygen (DO), and specific conductance) were measured with a calibrated YSI 556 MPS (Yellow Springs Instruments, Yellow Springs, OH).

Water Sample Analysis

Samples were analyzed for alkalinity, major and selected trace element concentrations, NO_3, soluble reactive phosphorus (SRP), DOC, IC, and $\delta^{13}C_{IC}$. Total alkalinity was titrated within 24 hours of sampling using 30 ml of water and 0.1 N HCl. SRP was measured using colorometric techniques Major element chemistry, including NO_3, was measured with an automated Dionex DX500 Ion Chromatograph with precision of better than 3% for all runs and elements based on repeated measurements of internal standards. Charge balance errors were less than 3%. DOC samples were analyzed on a Shimadzu TOC-5000A total organic carbon analyzer. After sparging for 2 minutes with carbon-free air to remove inorganic C, CO_2 was measured by IR detection after high temperature catalyzed combustion. Three to five injections of a 60 µL sample were measured and the mean of the injections was reported. Replicates of each sample

had <5% coefficient of variance. Inorganic carbon concentrations were measured on CO_2 extracted by acidifying samples using an AutoMate Prep Device coupled with a UIC (Coulometrics) 5011 carbon coulometer. The method was standardized with dissolved KHCO3. Data accuracy was better than ±0.015 mM for all runs. $\delta^{13}C_{IC}$ samples were acidified in Labco Exetainer tubes and the liberated CO_2 analyzed using a Thermo-Finnigan GasBench II coupled with a Thermo-Finnigan DeltaPlusXL isotope ratio mass spectrometer. Dissolved $KHCO_3$ was again used for isotopic standardization, with a precision of better than 0.09‰ for all runs. The isotopic data are reported in the conventional delta notation (‰) versus V-PDB. Metal concentrations were measured using a HR ICP-MS Element 2 (Thermo Finnigan). The precision and accuracy of the technique were calculated by comparing multiple measurements of the external standard SLRS4 (Canadian river water standard). The speciation of the dissolved metals and the saturation indices of major metal-carbonate and metal-oxide minerals were estimated based on the field parameters and the measured major element, trace metal and inorganic carbon concentrations using the geochemical modeling program PHREEQC (Parkhurst and Appelo, 1999).

Results

Hydraulic Head and Gradients

The hydraulic head of the river and pore-waters in each of the rice marsh wells, and regional precipitation are shown in Figure 4-3A, and the difference in head between the river and each well in Figure 4-3B. Hydraulic heads in the pore-waters were, with one exception, consistently higher than water levels in the river (Δh = 1.5 – 13 cm) resulting in vertical head gradients towards the river (Figure 4-3B). The hydraulic heads in the pore-waters and river track closely with each other and exhibit little temporal

variability, responding only to major rain events (e.g. > 110 mm/day on 1/21/10, 5/1/10, 5/28/12, and 6/25-6/26/12). The hydraulic gradients exhibit more temporal variation than the heads. This variability can also be correlated to major rain events, as well as more minor ones (e.g. 2/12/10, 9/27/10, and 1/25-2/10/11). Gradients at site RM.1 are the most sensitive to precipitation, exhibiting both the largest and longest duration response to rain events. No distinguishable seasonal pattern exists in either hydraulic head or gradient over the period of record.

The most extreme response in both hydraulic heads and gradients occurred during Tropical Storm Debby which deposited a total 345 mm of rain(6/24 – 6/26/12; Figure 4-4). During, and immediately after the storm the hydraulic head in the river and at all pore-water sites rose rapidly. Gradients between the river and pore-waters increased for a day following the storm before declining as the river stage rose faster than the pore-water heads. The wells were overtopped by the river during the height of the flood (Figure 4-4). As a result, much of the head gradient record was lost at the peak of the flood, however, based on the rate of decline in gradient during the rising limb of the flood gradients may have become loosing, at least at well RM.2.

Temperature and Conductivity History

Temperature and conductivity histories of the river before and after Tropical Storm Debby are shown in Figure 4-4. Clear diel signals in river temperature are visible before Tropical Storm Debby but are missing during much of the storm and dampened following the storm. Conductivity values increase following several precipitation events in early June and peaks at almost the same time as the river stage peak following Tropical Storm Debby, before decreasing to minimum values of approximately 100 uS/cm below pre-flood conditions 23 days after the storm.

3.3 Pump tests and hydraulic conductivity

Measured values for horizontal hydraulic conductivity of the Rice Marsh sediments, calculated from the horizontal pump tests of the Rice Marsh wells, are shown in Figure 4-2. The horizontal conductivity of the sediments is quite low (0.03 to 0.34 m/day). The lowest hydraulic conductivity was observed in well RM.1, located directly east of the main incised channel, and the highest in well RM.4, located directly west of the channel. Vertical hydraulic conductivity of the sediments is presumably considerably lower, as the falling head tests for vertical hydraulic conductivity were unsuccessful due to the lack of measureable recovery in water levels during the 3 hour duration of the test.

Pore-water Chemistry

A common pattern of a maximum excursion from river water concentrations occurs at depths of approximately 10 to 40 cm below the sediment-water interface below which concentrations shift back towards river water values for all of the chemical parameters that exhibit a consistent change in concentration with depth (Figure 4-5). For example, pH and DO concentrations both decreased with depth, reaching minimum values 5 – 15cm below the surface before increasing slightly, although never to levels approaching those in the river (Figure 4-5A). Inorganic carbonate and DOC concentration both increased with depth for the upper 15-40 cm of the profile before decreasing slightly at greater depths, but, like pH and DO, never return to river water concentrations (Figure 4-5B).

Fe, Mn and SRP concentrations all increase by orders of magnitude to peak concentrations at < 30cm depth (Figure 4-5C & D). Fe concentrations in the pore-waters are 3 orders of magnitude higher than in the river, with maximum concentrations

of 1330-2510ppb. Mn and SRP concentrations both increase by about an order of magnitude, from Mn concentrations of 2ppb in the river and maximum 24-40ppb in the pore-waters, and SRP concentrations of 1.5 uM in the river and maximum 7-13 uM in the pore-waters. In contrast, the concentrations of the other major nutrient, NO_3^-, decrease with depth, from ~0.035 mM in the river to below detection limits (0.0035 mM) by 50cm below the surface (Figure 4-5D).

The final set of solutes that exhibit consistent changes with depth are Ca^{2+} concentrations and the saturation index of calcite (Figure 4-5E). Ca^{2+} concentrations increase slightly with depth, from river water concentrations of 1.26-1.30 mM to peak pore-water concentrations of 1.37-1.44mM. Concentrations of Ca^{2+} continue to generally increase with depth, unlike the majority of the other solutes. The solubility of calcite correlates with the pH of the pore-waters. Calcite solubility in the river and majority of the pore-water profile is supersaturated, however slight undersaturated conditions (minimum $SI_{calcite}$ = -0.12) occurred between 10 and 30cm depth.

Discussion

Higher gradients oriented toward the river (Figure 4-3B) reflect diffuse discharge of groundwater to the river. This diffuse discharge provides a mechanism for benthic pore-water, which is elevated with respect to Fe, Mn, PO_4 , Ca^{2+}, and Cl^- and depleted in NO_3 (Figure 4-5), to alter the chemical composition of the river water. The following sections discuss the spatial and temporal patterns of diffuse groundwater discharge through the hyporheic zone, the chemical composition of the hyporheic pore-waters, estimates of the magnitude of the solute flux and diffuse groundwater discharge to the river, and lastly the significance of this hyporheic solute source to the structure and function of the river ecosystem.

Spatial and Temporal Patterns in Hydraulic Head, Gradient, and Flow

Hydraulic gradients oriented towards the river are consistent with regional groundwater flow patterns indicated by potentiometric surface maps of the springshed (SRWMD, 2003) and with the presence of seeps and springs along the length of the river (Figure 4-1C). The hydraulic heads of both the pore-waters and river exhibit low temporal variability during the study period, only responding to large rain events, most notably the precipitation event on 1/21/10 and Tropical Storm Debby on 6/24 – 6/26/12 (Figure 4-3A). The lack of seasonal variations in head reflects a relatively constant groundwater source, similar to the constant (i.e., non-flashy) discharge observed in most of Florida's springs, including the Ichetucknee springs (Florea and Vacher, 2007).

Hydraulic gradients between the pore-water and river (Figure 4-3B) exhibit greater temporal variability than is visible in the hydraulic head record indicating that there are small variations in the hydraulic head of the pore-waters relative to the river. In general the first half of the record, roughly corresponding to the 2010 calendar year, is flashier, with more frequent and larger excursions in head. Both the annual rainfall and average daily rainfall during 2010 and 2011 are roughly the same (1297 vs. 1318 mm/year, and 3.55 vs 3.61 mm/day for 2010 and 2011 respectively). What differs between the two years is the standard deviation of the daily rainfall differs (13.6 vs. 9.9 in 2010 and 2011 respectively), suggesting that the higher variability in the first half of the gradient record is the result of precipitation being concentrated into fewer but larger bursts.

The short (typically 2-3 week long) increase in hydraulic gradient following many precipitation events reflects rapid rise in the pore-water heads relative to the river, caused by precipitation that quickly infiltrates to the aquifer rather than flowing overland

to the river. Groundwater levels therefore respond first to precipitation before these elevated levels result in a corresponding increase in groundwater discharge to the river, increase in river head and subsequent decline in hydraulic gradient. This response to precipitation reflects the highly permeable nature of the karst landscape, lack of defined surface-drainage patterns and unconfined aquifer surrounding the river (e.g. Champion and Upchurch, 2006). The increased hydraulic gradient and groundwater discharge post-precipitation events should result in corresponding temporal increases in the influence of the hyporheic chemistry on the river.

The first half of Tropical Storm Debby (6/24 – 6/26/12) provided an exception to the typical response of the system following precipitation. Relatively high precipitation in the month preceding Tropical Storm Debby, in including 114 mm on 5/28/12, meant that gradients were already increasing from background levels in early May. During the three days of the storm, the hydraulic head in both the river and pore-waters increased rapidly with the hydraulic gradients showed the typical initial increase to around 10 times the May background values (Figure 4-4). Gradients peaked on 6/27 following which the rate of increase in river head exceeded the rate of increase in the pore-water heads and the hydraulic gradients sharply declined, possibly enough to produce losing conditions, but this could not be verified due to the wells overtopping on 6/30 and 7/1. The faster response in river levels relative to the groundwater system could be the product of three processes: local overland flow into the river caused by the precipitation rate exceeding the infiltration capacity of the landscape; contributions from flooding sinking streams in the upper springshed via rapid conduit flow (e.g. Champion and Upchurch, 2006); or back-pressure from the flooded Santa Fe River.

The initial post-precipitation increase in specific conductivity that resulted from T.S. Debby (Figure 4-4) likely reflects reacted, higher conductivity, water from the aquifer matrix being flushed out in advance of the infiltrating precipitation. The subsequent decline in river conductivity, 5 days following the storm could be watertransported to the river via infiltration or swallets in the upper springshed. The magnitude of the diel temperature variation in the river also changed as the result of T.S. Debby, declining from a daily variation of between 1 and 2 °C pre-storm, to less than half a degree post-storm. This reduction in the amplitude of the diel temperature variation as a result of the storm suggests that the increase in groundwater discharge acted as a thermal buffer to the river. This relationship suggests that relative changes in the magnitude of the diel temperature variation of the river can be used as a proxy for the magnitude of groundwater recharge.

To address this suggestion we compared the diel variation in river temperature with the daily variation in the air (Figure 4-6). The temperature of discharging groundwater is constant over daily timescales; hence increased groundwater discharge should result in lower ratios of the diel temperature variation in the river relative to the air. The calculated river to air temperature ratio fluctuates with both hydraulic gradient and season. Temperature ratios degrease with increasing gradient (Figure 4-6A), and stage consistent with the previous suggestion that rapid infiltration following precipitation events results in initially elevated hydraulic gradients and increased groundwater discharge to the river. Temperature ratios are also lower in the winter months relative to the summer (Figure 4-6B) indicating that groundwater discharge to the river is lowest during the summer. Lower summer discharge could be attributed to elevated riparian

evapotranspiration reducing the groundwater heads around the stream and lowering the hydraulic gradient towards the river. Figure 4-6A confirms that gradients are generally lower in the summer, with the exception of the gradients around 0.1 which occur after Tropical Storm Debby in mid-summer.

Controls on Pore-water Chemistry

The chemical changes in the sediments of the Rice Marsh are consistent with microbial respiration and the oxidative decay of organic carbon and resulting changes in redox conditions and mineral saturation states. Organic carbon remineralization consumes oxygen and elevates DIC and pH with depth. DOC concentrations increase rather than decrease with depth, as would be expected by its remineralization, as the result of dissolution of the organic-rich sediments (Saunders, 2007). The anoxic conditions lead to decreased NO_3^- concentrations with depth indicating denitrification, which supports the inference made by Heffernan et al. (2010) that denitrification in the hyporheic zone of the river caused the high rates of N removal observed in the upper river. The elevated concentrations of Fe and Mn in the shallow pore-waters result from reduction of Fe- and Mn-oxides in this zone.

The decreased pH values in the pore-waters drive dissolution of the carbonate sediment, resulting in the increases in Ca^{2+} concentrations, alkalinity, specific conductivity, and slight undersaturation with respect to calcite. The elevated concentrations of SRP could be the result of this calcite dissolution through the release of phosphorus co-precipitated with the calcite (e.g. Cohen et al., 2013) and/or be released from the remineralized organic carbon. Both of these mechanisms provide a potential source of P to the river, and could explain the longitudinal increase in SRP concentrations reported by Cohen et al. (2013).

Diffuse Solute Fluxes

The elevated concentrations of Fe, Mn, Cl^-, Ca^{2+}, and SRP in the shallow sediments relative to the concentrations in the river indicates that diffusion of solutesr could be an important source of these solutes to the river system. This diffusional flux (F_A; Table 4-1), normalized to the area of the river bed, was estimated using the equation:

$$F_A = D_j^0 \times \left(dC/dz\right) \times A_R \quad (4\text{-}1)$$

Where D_j^0 is the diffusion coefficient at 18 °C (Li and Gregory, 1974), *dC/dz* is the concentration gradient between the maximum concentration in the pore-waters and the river, and A_R is the area of the river bed (153,000 m^2). The diffusional flux is highest for Fe (1.1 – 11 $x10^4$ ug/sec) and would create Fe concentrations in the river of 1.2 – 17.3 ug/L (Table 4-1), enough to account for 20 -200% of the observed downstream increase in Fe concentrations. The diffusional flux of Mn, and SRP is an order of magnitude smaller than Fe, but still high enough to account for 3 - 30% of the downstream increase in SRP. The flux of Ca^{2+} and Cl^-, is comparatively small, able to account for only 1% and 0.3% of the observed downstream increase, respectively.

Quantifying Diffuse Groundwater Discharge

Hydrologic estimates

Groundwater seepage to the river will impact the magnitude and temporal variability of the solute transport from the hyporheic zone into the river. The magnitude of this seepage flux was estimated based on the hydraulic conditions of each well at each well location using Darcy's Law, the measured hydraulic gradients between the pore-waters and river (Figure 4-3B) and the measured horizontal hydraulic conductivity

of the benthic sediments (Table 4-2; Figure 4-2B). These point measurements were then integrated across the area of the stream bed (153,000 m^2) to give a whole stream estimate. The average flow magnitude during period of record was estimated to be between 0.002 and 0.044 m^3/s, depending on which well site parameters were used to make the estimate (Table 4-2). The maximum flow calculated at any point in time was 0.10 m^3/s. Because our estimates of vertical hydraulic conductivity (K_V) were unsuccessful these calculations are based on measurements of vertical gradients and horizontal hydraulic conductivity. Hensley and Cohen (2012) successfully measured horizontal conductivities of 4.6 ± 1.9 m/d in the same upper section of the river, using similar methods. Repeating our calculations of flow magnitude using their K_V increases the estimated average flow to 0.35 – 0.73 m^3/s. The disparity between the measurements of K_H and K_V from seemingly similar sites in the upper river, and the sensitivity of the seepage estimates K, illustrates the heterogeneity in the river sediments and the potential for heterogeneous flow paths to the river.

Chemical estimates of seepage

The magnitude of seepage was also estimated by closing the mass balance of the four main solutes (Ca^{2+}, Cl^-, PO_4, and Fe) which exhibit downstream increases in concentration relative to the flow-weighted average input of the source springs (2-5%, 3-10%, 15-25%, and 1000+% downstream increase, respectively; Table 4-3). These increases occur despite evidence of in-stream removal of these solutes due to diel cycling (Kurz et al., in prep; in review; Cohen et al., 2013; de Montety et al., 2011). Diffuse groundwater flow (Q_{pw}) was estimated using the mass balance equation:

$$Q_{pw} = \left[Q_R\left(C_R - C_{Sp}\right) - F_A\right] \times {C_{pw}}^{-1} \quad (4\text{-}2)$$

Where Q_R is the discharge of the river, C_R is the maximum downstream solute concentrations (from Kurz et al., in prep; in review; Cohen et al., 2013), C_{Sp} is the flow-weighted input from the source springs, F_A is the diffusional solute flux in mass/time, and C_{pw} is the maximum solute concentration measured at each pore-water profile (Table 4-1).

A diffuse groundwater flow rate through the hyporheic zone of 0.11-0.84 m^3/s would be sufficient to explain the excess Ca^{2+}, PO_4 and Cl^- concentrations in the river relative to the flow-weighted spring inputs (Table 4-3). These estimates are comparable to the hydrologic-based estimate made using the K_V values from Hensley and Cohen (2012) and also with a previous estimate by de Montey et al. (2011) of 0.75 m^3/s need to close the Cl^- budget using Cl^- values from the most concentrated source spring, Mill Pond (Figure 4-1). The Fe flux associated with these seepage rates, combined with the high diffusional Fe flux, would cause the Fe concentrations of the river to exceed, by several orders of magnitude, the measured Fe concentrations. Because of the elevated DO concentrations in the river, the dissolved Fe is dominated by Fe(III) and several Fe-oxides (including FeOOH and Fe_2O_3) are supersaturated. This redox chemistry suggests that the Fe that enters the river from the pore-waters is likely oxidized and precipitated at the sediment-water interface. Micro-scale processing within this boundary zone at the the sediment-water interface, such as the formation of colloidal Fe(III)-DOC complexes, may be important in mediating what fraction of the Fe coming from the pore-waters makes it into the river.

Hyporheic exchange vs. diffuse recharge

A diffuse flow rate of 0.11 – 0.84 m3/s would be the equivalent of ~ 1-11 % of the discharge of the river (Table 4-3). During the period when the major springs were being

gauged, the difference in the spring inputs were ~11% greater than the measured discharge at the Dampier's Landing and between Dampier's and the US 27 Bridge, suggesting the river was losing water during that time period (Heffernan et al., 2010). Because head gradients are oriented toward the river (SRWMD, 2003), it seems unlikely the river would be losing water and the apparent loss likely represents a systematic overestimation of the 5 gaged source springs. Assuming our seepage calculations are correct, the apparent loss suggest an even larger error in the gauging of the springs and river.

Hyporheic exchange, i.e. the infiltration and exfiltration of stream water through the hyporheic zone, would provide a mechanism for solutes from the benthic pore-waters to be transported into the river without the addition of new water from groundwater seepage. Although the influence of hyporheic exchange on the delivery of solutes to the river cannot be completely discounted two observations suggest that significant exchange is unlikely. The strong hydraulic gradients oriented toward the river would inhibit the downwelling of stream water into the hyporheic zone. In addition, dye trace studies in the Ichetucknee River reported almost 100% mass recovery of tracer, suggesting that long-term hyporheic storage and hydraulic turnover is negligible (Hensley and Cohen, 2012).

Implications for Elemental Availability to Streams

In-stream vegetation both controls and responds to the physical and biogeochemical transport and cycling of solutes within streams (Clark, 2002). The environmental availability of elements, including Mn, Fe and P, which are required for metabolic processing and growth (Elser et al., 2003; Vrede et al., 2004) can influence the productivity, distribution and species abundance of aquatic vegetation (e.g. Valett et

al., 1994; Grimm et al. 1991). In the Ichetucknee River the assimilatory demand of the submerged vegetation for Mn, P, and, in particular, Fe is approaching the supply from the source springs (Kurz et al., in prep). In addition a number of biogeochemical processes, both directly and indirectly resulting from aquatic plant metabolism, control the in-stream removal of solutes at a diel frequency and with downstream distance (Kurz et al., in review; Cohen et al., 2013). Seepage and diffusive fluxes from the hyporheic zone into the Ichetucknee River therefore provide a critical source of these necessary solutes to the river, offsetting some of the biologic and geochemical uptake.

Conclusions

This study demonstrates the importance of groundwater seepage through the hyporheic zone as a mechanism for contributing ecologically important sources of solutes to rivers with otherwise homogenous source chemistry. Pore-water chemistry in the river sediments is dominated by a 'reaction zone' in the top 30cm where the remineralization of organic carbon results in elevate concentrations of Fe, Mn, Ca^{2+}, SRP, and Cl^- (Figure 4-5). The diffusional and seepage flux of these solutes from this reaction zone contributes to the downstream increase in river concentration. Positive gradients between the pore and river water (Figure 4-3) indicate upwards flow through the sediments, driving seepage discharge to the river. A diffuse groundwater flow rate of 0.11-0.84 m^3/s through the sediments would explain increasing solute concentrations with flow downstream from the source springs (Table 4-1). The additional hyporheic source of solutes, contributed via diffusion and advection, is particularly critical for mediating the environmental availability of macro and micronutrients, namely P, Mn, and Fe, to the river, by offsetting the removal of these solutes by in-stream diel cycling

and possibly buffering against the limitation of Mn on the productivity of the river ecosystem.

Table 4-1. Estimates of diffusional solute flux from sediments integrated over the area of the river bed (F_A), calculated using Eq. (4-1). F_A is also reported normalized to the discharge of the river (Q_R). Range in values reflects spatial variability between pore-water profile sampling sites.

	Ca^{2+} (mmol)	Cl^- (mmol)	SRP (µmol)[a]	Fe^{2+} (µg)	Mn^{2+} (µg)	
D_j^0, 18°C [a]	6.73×10^{-6}	17.1×10^{-6}	7.34×10^{-6}	5.82×10^{-6}	5.75×10^{-6}	(10^{-6} cm^2/sec)
dC/dz [b]	2.0×10^{-6} – 23×10^{-6}	0 – 1.2×10^{-6}	0.65×10^{-3} – 7.4×10^{-3}	1.24 – 0.13	1.0×10^{-3} – 19×10^{-3}	(*mass*/cm^4)
F_A	0.20 – 2.39	0 – 0.32	72 – 826	1.12×10^4 – 11.1×10^4	89 – 1690	(*mass*/sec)
$F_A \times Q_R$	2.2×10^{-5} – 37×10^{-5}	0 – 5.0×10^{-4}	0.01 – 0.13	1.2 – 17.3	0.01 – 0.26	(*mass*/L)

[a] From Li and Gregory (1974); [b] From chemical profiles (Figure 4-5).

Table 4-2. Estimates of diffuse groundwater discharge based on the hydraulic gradients (Figure 4-3) the horizontal hydraulic conductivity of the sediments (Figure 4-2B) measured at each well in the rice marsh, and integrated over the benthic area of the river (153,000 m^2).

	RM.1	RM.2	RM.4	RM.5
K_H (m/d)	0.03	0.26	0.34	0.15
Diffuse groundwater discharge (m^3/s)				
Average	0.036	0.002	0.044	0.009
Standard Deviation	0.014	0.002	0.015	0.003
Maximum	0.099	0.008	0.101	0.022
Minimum	0.000	0.000	0.024	0.000

Table 4-3. Estimates of seepage required to close the solute budgets of Ca^{2+}, Cl^-, PO_4, Fe, and Mn, calculated using Eq. (4-2). Range in spring and river values reflects temporal variation; range in pore-water values reflects spatial variation across sampling sites.

	Ca (mmol)	Cl (mmol)	PO_4 (µmol)[a]	Fe (µg)	Mn (µg)
			Concentrations in source and river waters (*mass*/L)		
Springs (C_{Sp})	1.31 – 1.36	0.17 – 0.31	1.50 – 1.58	0.38 – 0.70	8.2 – 9.4
Pore-waters (C_{pw})	1.37 – 1.44	0.26 – 0.32	7.10 – 12.7	1330 – 2510	23.8 – 29.6
River (C_R)	1.38 – 1.40	0.18 – 0.32	1.72 – 1.77	7.2 – 7.3	3.8 – 5.0
			Solute mass transfer in and out (*mass*/sec)		
Springs ($x10^3$)	8.70 – 12.2	1.2 – 2.8	10.9 – 14.1	2.4 – 26.3	59.6 – 59.9
Diffusion (F_A)	0.20 – 2.39	0 – 0.32	72 – 826	$1.12x10^4$ – $11.1x10^4$	89 – 1690
River ($x10^3$)	9.00 – 12.7	1.1 – 3.0	13.4 – 17.5	30.7 – 57.1	24.1 – 38.2
			Seepage required to close the chemical budgets (m^3/day)		
	0.11 – 0.42	0 – 0.84	0.08 – 0.46	0 – 0.03	0
			Fraction of seepage relative to river discharge		
	1.4% – 4.5%	0% – 11.5%	1.1% – 5.0%	0% – 0.4%	0%

[a] From Cohen et al. (2013), corrected for overlapping signals in assimilation and calcite co-precipitation

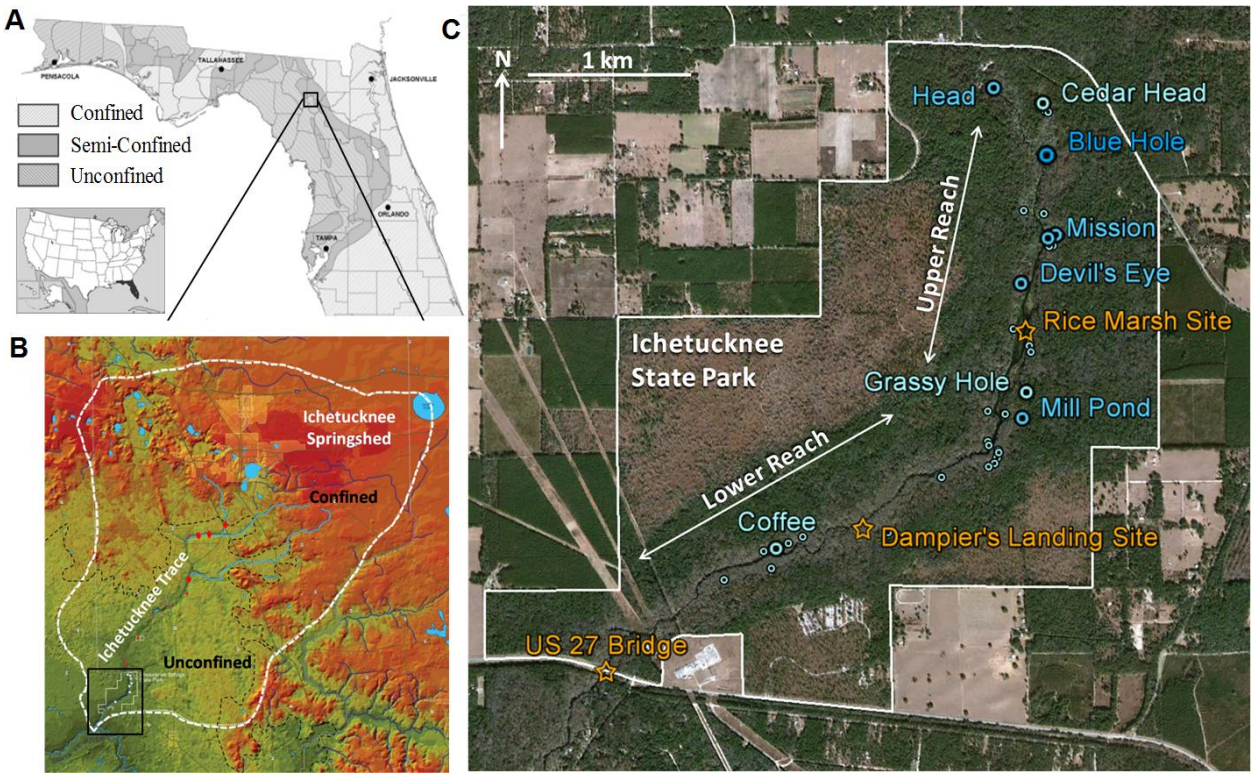

Figure 4-1. Overview of the study area. A) Map of the confined, semi-confined, and unconfined portions of the Floridan Aquifer in north Florida (FDEP, 2006; modified). B) Topographic map of the Ichetucknee springshed showing levels of confinement, three surface tributaries plus associated sinks, and the Ichetucknee Trace (SRWMD, 2007; modified). C) Google Earth image of Ichetucknee River showing the state park (green outline), named major springs (large dots), unnamed minor springs (small dots), and the well and sampling sites (orange stars).

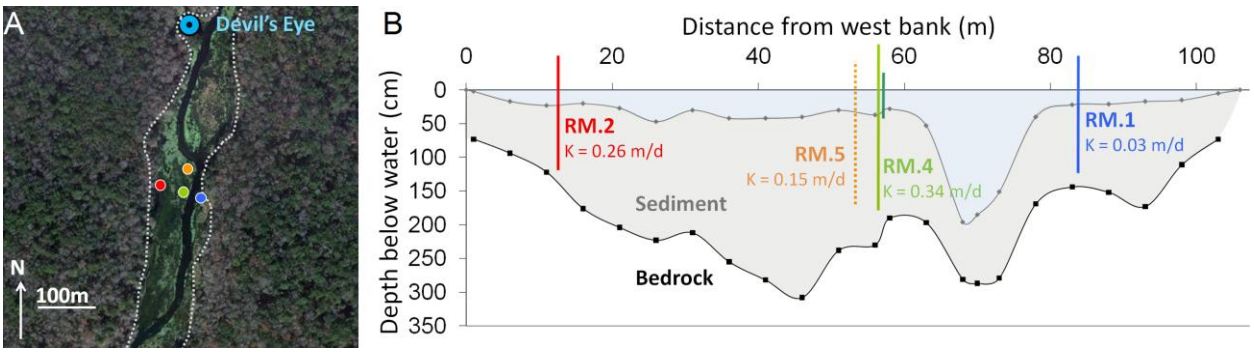

Figure 4-2. Location of the wells at the Rice Marsh site (Figure 4-1C) in the upper river. A) Map view. The dashed grey line delineates the edge of the channel (image by Google Earth). B) Placement of wells relative to the water-sediment (grey line) and sediment-bedrock (black line) interfaces. K values indicate the horizontal hydraulic conductivity measured at each well. The dashed line represents well 5 which is located approximately 45 m north of the transect.

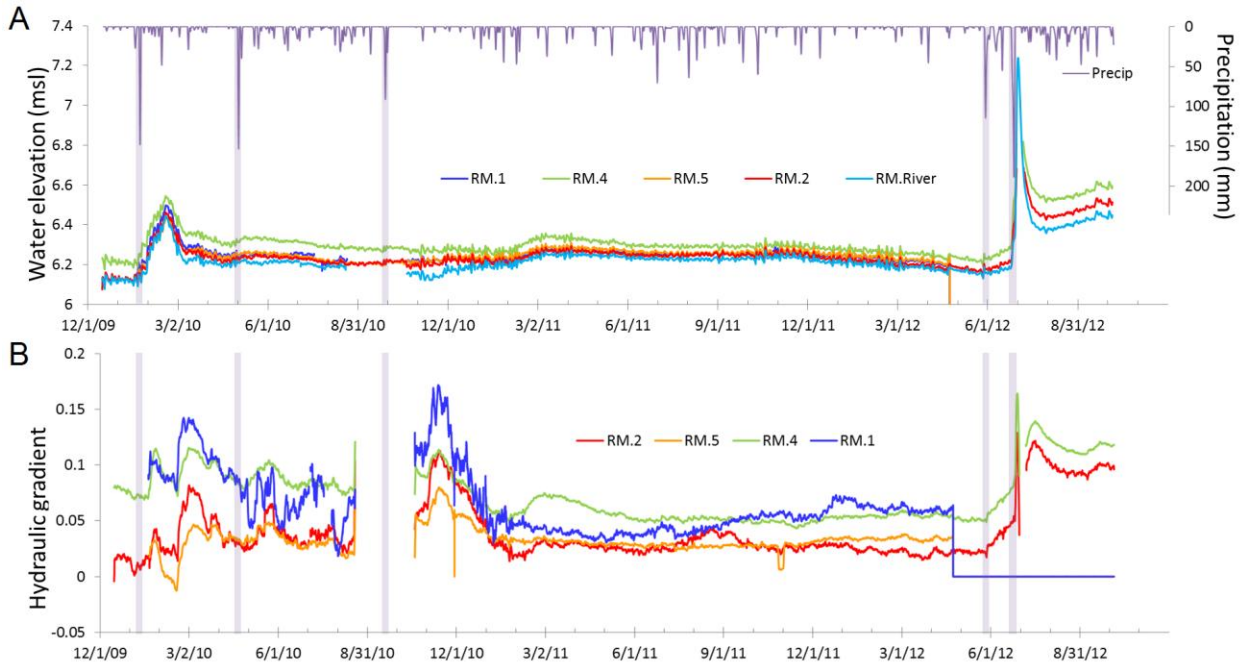

Figure 4-3. Hydrologic record of the river and pore-waters. A) Daily average hydraulic head and total daily precipitation. B) Daily average vertical hydraulic gradients between the river and Rice Marsh pore-waters. Vertical bars highlight precipitation events of over 90 mm/day.

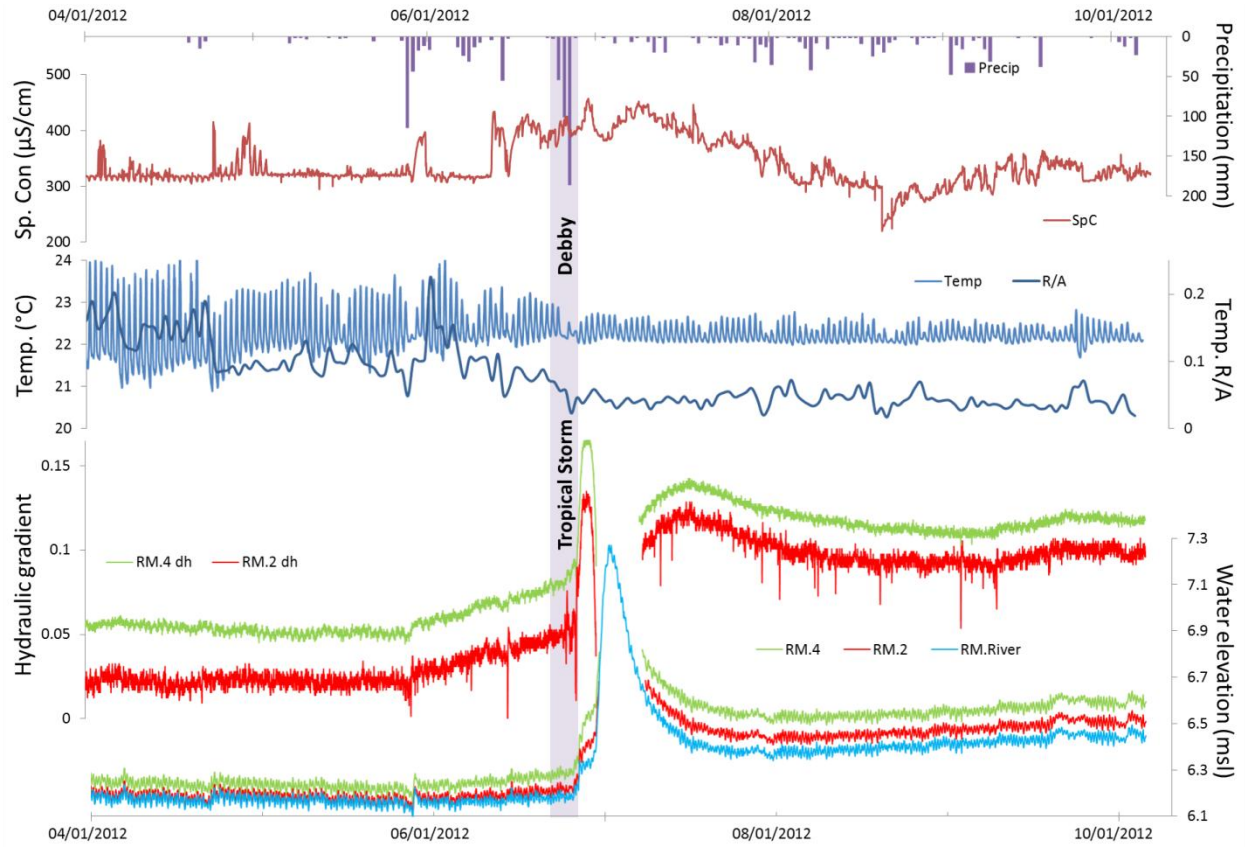

Figure 4-4. Detail of hydrologic and chemical parameters of the river and pore-waters at the Rice Marsh site in the months preceding and following Tropical Storm Debby (6/24 - 6/26/12): Precipitation, river specific conductivity, river temperature, the ratio of the diel temperature range in the river relative to the air, hydraulic gradient, and hydraulic head.

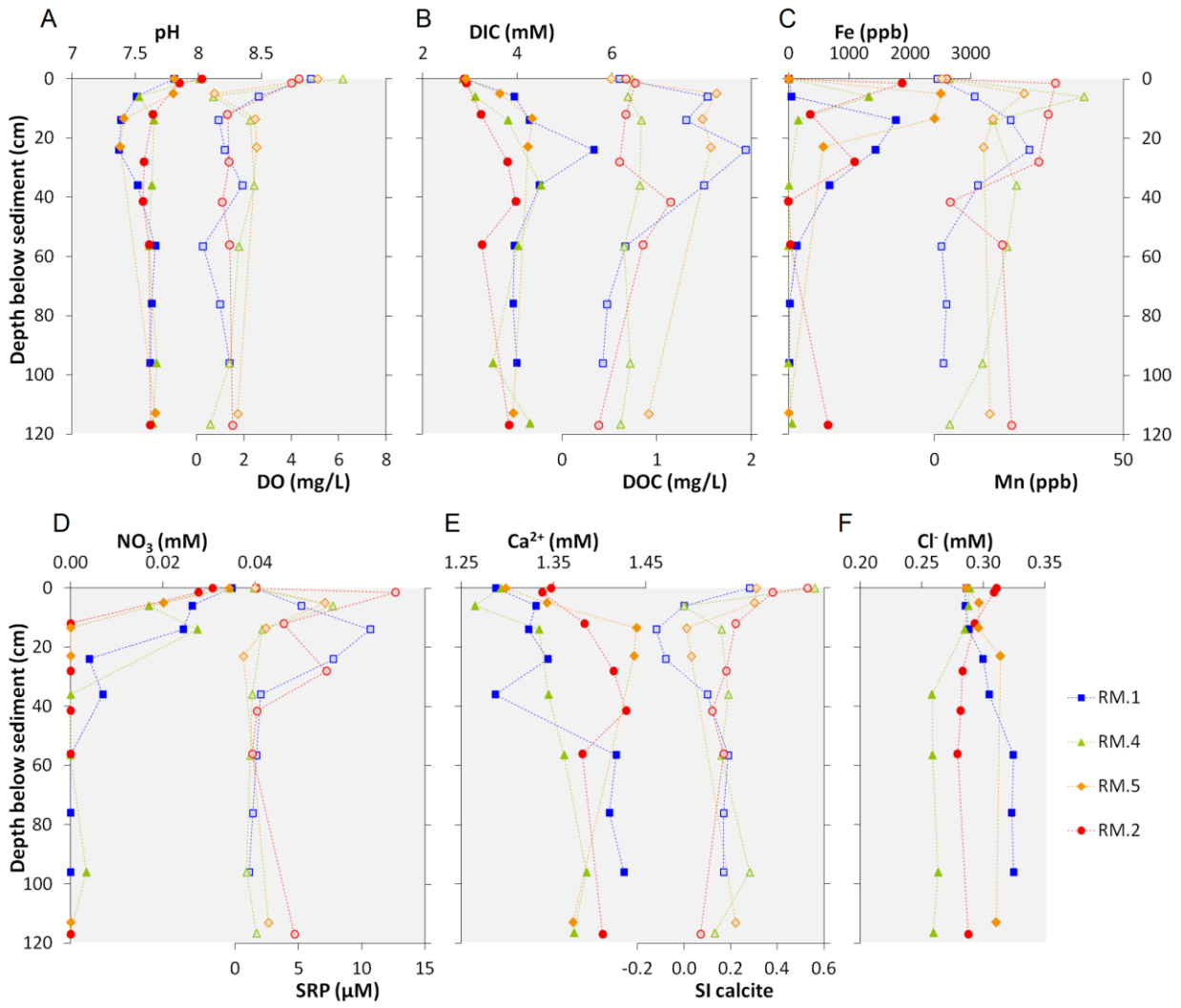

Figure 4-5. Chemical profiles of select parameters from the porewaters at the Rice Marsh site in the upper river. A) pH and DO, B) DIC and DOC, C) Fe and Mn; D) NO_3^- and SRP; E) Ca^{2+} and $SI_{calcite}$; and F) Cl^-.

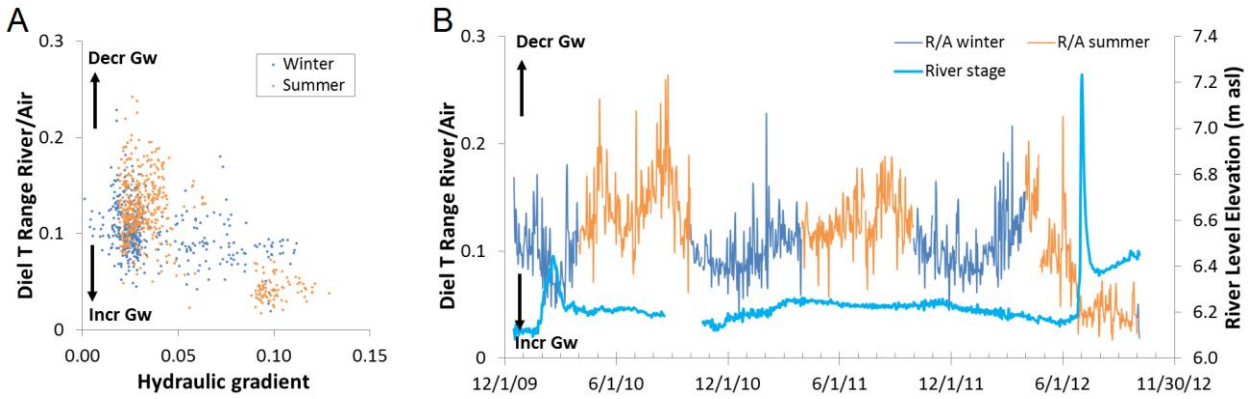

Figure 4-6. Diel temperature range. A) Ratio of the diel temperature range in the river relative to in the air vs. the hydraulic gradient from RM.2. B) Diel temperature ratio and river water levels over the length of the record. Both plots differentiate between the summer months (April – September; orange) and winter months (October – March; blue). Lower diel temperature ratios are indicative of increased groundwater discharge. Ratios indicate groundwater discharge increases with hydraulic gradient and during the winter months.

CHAPTER 5
SUMMARY AND CONCLUSIONS

This dissertation research illustrates the reciprocal interactions between the sources and cycling of solutes in streams and the metabolism of submerged aquatic vegetation. Multiple overlapping geochemical and biological processes, indirectly and directly the result of diel variations in solar radiation and submerged plant metabolism control the diel variation of solutes in the Ichetucknee River. In contrast, diffuse groundwater discharge through the hyporheic zone provides a mechanism for transporting solutes, enriched in the anoxic subsurface pore-waters, into the river, partially offsetting the in-stream removal by diel processes and contributing to downstream increases in some solute concentrations. Both the hyporheic sources and in-stream cycling of solutes therefore mediate the availability of solutes to the stream ecosystem, affecting the composition, and potentially the productivity and functioning, of the aquatic vegetation.

The effects of these hydro-biogeochemical controls on solute source and cycling in the Ichetucknee River are particularly well exemplified with Mn. Multiple diel processes, including carbonate co-precipitation, adsorption, and autotrophic assimilation contribute to the removal of dissolved, bio-available Mn from the river resulting in downstream decreases in Mn concentrations. This removal is in part offset by the delivery of Mn from the Mn-enriched hyporheic pore-waters into the river by groundwater discharging diffusely through the hyporheic zone. Mn is an important micronutrient, although the metabolic demand for Mn appears to be an order of magnitude higher for the vascular aquatic vegetation than for the benthic algae. This

behavior suggests that the abundance and productivity of the vascular vegetation would be more sensitive to the availability of Mn in the river.

Although the links between solute availability, geochemical processing, and ecosystem metabolism are complex, understanding the timing and magnitude of in-stream diel variations relative to the timing of known processes, can be used to distinguish which biogeochemical processes control solute concentrations. However, if multiple controls (e.g., assimilation, calcite co-precipitation, or adsorption) are out of phase with each other and solar radiation, estimates based on observed variation for each process could over- or under-represent the influence of individual processes. Disentangling the individual processes controlling diel variation in streams therefore requires better understanding of the timing and magnitude of all processes controlling the elemental cycling. In particular, future work is needed to constrain the timing of assimilatory uptake of elements, and if and how this timing is controlled by factors such as the metabolic process(es) utilizing the elements, species type, or whether the element is limiting.

Understanding the biogeochemical processes controlling the in-stream sources and cycling of solutes has implications for river systems even where diel variation is not visible. With increasing residence time and distance downstream, diel processes that control an individual element will begin to lag so that the cycles will become increasingly dampened. Hence the lack of observable diel variation within a river does not imply that these processes are not occurring. Moreover, with distance downstream the cumulative effects of these processes may become more important, especially for those processes, such as assimilation, which result in the net-removal of solutes from the river.

Understanding how observable diel variations evolve with distance downstream, residence time, and mixing of different source waters, and scaling the relative significance of these diel processes to larger stream systems, and those with significant upstream drainage networks is another area for future research.

The overlapping of diel signals and the net downstream removal of solutes can also complicate the construction of stream solute budgets and quantifying the magnitude of solute additions to stream systems by processes such as hyporheic exchange and diffuse groundwater discharge, as was illustrated with Mn in the Ichetucknee River. Quantifying these diffuse inputs may also be complicated by geochemical processes mediating the transport of solutes across the sediment-water interface and into the main water column. For example, it was shown that the flux of Fe from the hyporheic zone far exceeded the concentration of Fe in the river, suggesting that additional processes, are further mediating Fe availability in the river. Investigations into the micro-scale chemical changes and controlling processes acting at the benthic surface are other areas for future research.

LIST OF REFERENCES

Anastasiou, C.F., 2006. Investigation of the spatial and temporal trends in water clarity: Rainbow River, FL. Report, Southwest Florida Water Management District, Brooksville, Florida, pp. 63.

Ashworth, J., Coese,l S., Lee, A., Armbrust, E.V., Orellana, M.V., Baliga, N.S., 2013. Genome-wide diel growth state transitions in the diatom Thalassiosira pseudonana. PNAS 110, 7518-7523.

Bailly-Comte, V., Martin, J. B., Jourde, H., Screaton, E. J., Pistre, S., Langston, A., 2010. Water exchange and pressure transfer between conduits and matrix and their influence on hydrodynamics of two karst aquifers with sinking streams. J. Hydrol. 386, 55-66.

Bencala, K.E., 2000. Hyporheic zone hydrological processes. Hydrological Processes 14, 1085-1099.

Boano, F., Revelli, R., Ridolfi, L. 2007. Bedform-induced hyporheic exchange with unsteady flows. Advances in Water Resources 30, 148-156.

Borman, C.J., Sullivan, B.P., Eggleston, C.M., Colberg, P.J.S., 2010. Is iron redox cycling in a high altitude watershed photochemically or thermally driven? Chem. Geol. 269, 33-39.

Boulton, A.J., Findlay, S., Marmonie,r P., Sanley, E.H., Valett, H.M., 1998. The functional significance of the hyporheic zone in streams and rivers. Annual Review of Ecology and Systematics 29, 59-81.

Brick, C.M., Moore, J.N., 1996. Diel variation of trace metals in the upper Clark Fork River, Montana. Environ. Sci. Tech. 30, 1953-1960.

Brunke, M., Gonser, T., 1997. The ecological significance of exchange processes between rivers and groundwater. Biology 37, 1-33.

Budd, D.A., Vacher, H.L., 2004. Matrix permeability of the confined Floridan Aquifer, Florida, USA. Hydrogeology Journal 12, 531-549.

Carling, G.T., Fernandez, D.P., Rudd, A., Pazmino, E., Johnson, W.P., 2011. Trace element diel variations and particulate pulses in perimeter freshwater wetlands of Great Salt Lake, Utah. Chemical Geology 283, 87-98.

Champion, K.M., Upchurch, S.B., 2006. Delineation of spring-water source areas in the Ichetucknee springshed. Tampa, Florida, Report Prepared for the Florida Department of Environmental Protection. SDII Global Corporation, pp. 39.

Christensen, P.B., Nielsen, L.P., Revsbech, N.P., Sorensen, J., 1989. Microzonation and denitrification activity in steam sediments as studied with a combined oxygen and nitrous oxide microsensor. Appl. Environmental Microbiology 55, 1234-1241.

Cicerone, D.S., Stewart, A.J., Roh, Y., 1999. Diel cycles in calcite production and dissolution in a eutrophic basin. Environ. Toxicol. Chem. 18, 2169-2177.

Claret, C., Fontvielle, D., 1997. Characteristics of biofilm assemblages in two contrasted hydrodynamic and trophic contexts. Microbial Ecology 34, 49-57.

Clarke S.J., 2002. Vegetation growth in rivers: Influences upon sediment and nutrient dynamics. Processes in Physical Geography 26, 159-172.

Cohen, M.J., Kurz, M.J., Heffernan, J.B, Martin, J.B., Douglass, R.L., Foster, C.R., Thomas, R.G., in press. Diel phosphorus variation and the stoichiometry of ecosystem metabolism in a large spring-fed river. Ecological Monographs. http://dx.doi.org/10.1890/12-1497.1.

Dahm, C.N., Grimm, N.B., Marmonier, P., Valett, H.M., Vervier, P., 1998. Nutrient dynamics at the interface between surface waters and groundwaters. Freshwater Biology 40, 427-451.

de Montety, V., Martin, J.B., Cohen, M.J., Foster, C., Kurz, M.J., 2011. Influence of diel biogeochemical cycles on carbonate equilibrium in a karst river. Chem. Geol. 283, 31-43.

Desmet, N. J. S., Van Belleghem, S., Seuntjens, P., Bouma, T.J., Buis, K., Meire, P., 2008. Quantification of the impact of macrophytes on oxygen dynamics and nitrogen retention in a vegetated lowland river. Physics and Chemistry of the Earth, Parts A/B/C In Press, Corrected Proof.

Dromgoole, E.L., Walter, L.M., 1990. Iron and manganese incorporation into calcite: Effects of growth kinetics, temperature and solution chemistry. Chem. Geol. 81, 311-336.

Drysdale, R., Lucas, S., Carthew, K., 2003. The influence of diurnal temperature on the hydrogeochemistry of a tufa-depositing stream. Hydrological Processes 17, 3421-3441.

Duarte, C.M., Prairie, Y.T., Frazer, T.K., Hoyer, M.V., Notestein, S.K., Martinez, R., Dorsett, A., Canfield, D.E., 2010. Rapid accretion of dissolved organic carbon in the springs of Florida: the most organic-poor natural waters. Biogeosciences 7, 4051-4057.

Eglin, I., Roeck, U., Robach, F., Tremolieres, M., 1997. Macrophyte biological methods used in the study of the exchange between the Rhine river and the groundwater. Water Research 31, 503-514.

Elser, J.J., Acharya, K., Kyle, M., Cotner, J., Makino, W., Markow, T., Watts, T., Hobbie, S., Fagan, W., Schade, J., Hood, J. Sterner, R. W., 2003. Growth rate–stoichiometry couplings in diverse biota. Ecology Letters 6, 936–943.

FDEP, 2006. Water quality study of the Ichetucknee River. Florida Department of Environmental Protection Bureau of Laboratories. Tallahassee, FL, pp. 26.

Fisher, S.G., Grimm, N.B., Marti, E., Holmes, R.M. Jones, J.B., 1998. Material spiraling in stream corridors: A telescoping ecosystem model. Ecosystems 1, 19-34.

Fleckenstein, J.H., Niswonger, R.G., Fogg, G.E., 2006. River-aquifer interactions, geologic heterogeneity and low-flow management. Groundwater 44, 837-852.

Florea, L. J., Vacher, H.L., 2006. Springflow hydrographs: Eogenetic vs. telogenetic karst. Ground Water 44, 352-361.

Frost, P.C., Evans-White, M.A., Finkel, Z.V., Jensen, T.C., Matzek, V., 2005. Are you what you eat? Physiological constrains on organismal stoichiometry in an elementally imbalanced world. Oikos 109, 18-28

Gammons, C.H., Babcock, J.N., Parker, S.R., Poulson, S.R., 2011. Diel cycling and stable isotopes of dissolved oxygen, dissolved inorganic carbon, and nitrogenous species in a stream receiving treated municipal sewage. Chemical Geology 283, 44-55.

Gammons, C., Milodragovich, L., Belanger-Woods, J., 2007. Influence of diurnal cycles on metal concentrations and loads in streams draining abandoned mine lands: an example from High Ore Creek, Montana. Environ. Geol. 53, 611-622.

Gammons, C.H., Nimick, D.A., Parker, S.R., Cleasby, T.E., McCleskey, R.B., 2005. Diel behavior of iron and other heavy metals in a mountain stream with acidic to neutral pH: Fisher Creek, Montana, USA. Geochim. Cosmochim. Acta 69, 2505-2516.

Gandy, C.J., Smith, J.W.N, Jarvis, A.P., 2007. Attenuation of mining-derived pollutants in the hyporheic zone: A review. Science of the Total Environment 373, 435-446.

Glass, J.B., Wolfe-Simon, F., Anbar, A.D., 2009. Coevolution of metal availability and nitrogen assimilation in cyanobacteria and algae. Geobiology 7, 100-123.

Gotelli, N.J., Mouser, P.J., Hudman, S.P., Morales, S.E., Ross, D.S., Ellison, A.M., 2008. Geographic variation in nutrient availability, stoichiometry, and metal concentrations of plants and pore-water in ombrotrohic bogs in New England, USA. Wetlands 28, 827-840.

Grimm, N.B., H.M. Valett, E.H. Stanley, Fisher, S.G., 1991. Contribution of the hyporheic zone to stability of an arid-land stream. Internationale Vereiningung für Theoretische und Angewandte Limnologie, Verhandlungen. 24, 1595-1599.

Hall, S.R., 2004. Stochiometrically-explicit competition between grazers: species replacement, coexistence and priority effects along resource supply gradients. American Naturalist 164,157-172.

Hall, R.O., Beaulieu, J.J., 2013. Estimating autotrophic respiration in streams using daily metabolism data. Freshwater Science 32, 507-516.

Hall, R.O., Tank, J.L., 2003. Ecosystem metabolism controls nitrogen uptake in streams in Grand Teton National Park, Wyoming. Limnology and Oceanography 48, 1120-1128.

Hartley, A.M., House, W.A., Leadbeater, B.S.C., Callow, M.E., 1996. The use of microelectrodes to study the precipitation of calcite upon algal biofilms. J. Colloid Interface Sci. 183, 498-505.

Hayashi, M., Rosenberry, D.O., 2002. Effects of ground water exchange on the hydrology and ecology of surface water. Ground Water 40, 309-316.

Healey, F.P., 1973. Inorganic nutrient uptake and deficiency in algae. Critical Reviews in Microbiology 3, 69-113.

Heffernan, J. B., Cohen, M. J., 2010. Direct and indirect coupling of primary production and diel nitrate dynamics in a large spring-fed river. Limnol. Oceanogr. 55, 677-688.

Heffernan, J.B., Cohen, M.J., Frazer, T.K., Thomas, R.G, Rayfield, T.J., Gulley, J., Martin, J.B., Delfino, J.J., Graham, W.D., 2010a. Hydrologic and biotic influences on nitrate removal in a subtropical spring-fed river. Limnol. Oceanogr. 55, 249-263.

Heffernan, J.B., Liebowitz, D.M., Frazer, T.K., Evans, J. M., Cohen, M.J., 2010b. Algal blooms and the nitrogen-enrichment hypothesis in Florida springs: evidence, alternatives, and adaptive management. Ecological Applications 20, 816-829.

Hensley, R.T., Cohen, M.J., 2012. Controls on solute transport in large spring-fed rivers. Limnology and Oceanography 57, 912-924

Hester, E.T., Doyle, M.W., 2008. In-stream geomorphic structures as drivers of hyporheic exchange. Water Resources Research 44, W03417, doi:10.1029/2006WR005810.

Hill, A.R., Labadia, C.F., Sanmugadas, K., 1998. Hyporheic zone hydrology and nitrogen dynamics in relation to the streambed topography of a N-rich stream. Biogeochemistry 42, 285-310.

Hinkel, S.R., Duff, J.H., Triska, F.J., Laenen, A., Gates, E.B., Bencala, K.E., Wentz, D.A., Silva, S.R., 2001. Linking hyporheic flows and nitrogen cycling near the Willamette River – a large river in Oregon, USA. Journal of Hydrology 244, 157-180.

Hoffer-French, K.J., Herman, J.S., 1989. Evaluation of hydrological and biological influences on CO2 fluxes from a karst stream. J. Hydrol. 108, 189-212.

Holmes, R.M., Jones, J.B., Fisher, S.G., Grimm, N.B., 1996. Denitrification in a nitrogen-limiting stream ecosystem. Biogeochem 33, 125-146.

Hozhina, E.I., Khramov, A.A., Gerasimov, P.A., Kumarkov, A.A., 2001. Uptake of heavy metals, arsenic, and antimony by aquatic plants in the vicinity of ore mining and processing industries. Journal of Geochemical Exploration 74, 153-162.

Jackson, L.J., Rasmussen, J.B., Kalff, J., 1994. A mass-balance analysis of trace metals in two weedbeds. Water, Air and Soil Pollution 75, 107-119.

Jones, J.B., Holmes, R.M., 1996. Suface-subsurface interactions in stream ecosystems. Trends Ecol.Evol. 11, 239-242.

Jones, C.A., Nimick, D.A., McCleskey, R.B., 2004. Relative effect of temperature and pH on diel cycling of dissolved Zn and As in Prickly Pear Creek, Montana. Water Air Soil Poll. 153, 95–113.

Kamal, M., Ghaly, A.E., Mahmoud, N., Cote, R., 2004. Phytoaccumulation of heavy metals by aquatic plants. Environment International 29, 1029-1039.

Kamenov, G.D., Brenner, M., Tucker, J.L., 2009. Anthropogenic versus natural control on trace element and Dr-Nd-Pb isotope stratigraphy in peat sediments of southeast Florida (USA), ~1500 AD to present. Geochimica et Cosmochimica Acta 73:3549-3567.Kitano, Y., Okumura, M, Idogaki, M., 1980. Abnormal behabiours of copper (II) and zinc ions in parent solution at the early stage of calcite formation. Geochem. J. 14, 167-175.

Kenney, W.F., Schelske, C.L., Chapman, A.D., 2001. Changes in polyphosphate sedimentation: a response to excessive phosphorus enrichment in a hypereutrophic lake. Can J Fish Aquat Sci 58, 879¬887.

Kerkhoff, A.J., Enquist, B.J., Elser, J.J., Fagan, W.F., 2005. Plant allometry, stoichiometry and the temperature-dependence of primary productivity. Global Ecology and Biogeography 14, 585-598.

Khoshmanesh, A., Hart, B.T., Duncan, A., Beckett, R., 2002. Luxury uptake of phosphorus by sediment bacteria. Water Research 36, 774-778

Kitano, Y., Kanamori, N., Oomori, T., 1971. Measurments of distribution coefficients of strontium and barium between carbonate precipitate and solution – Abnormally high values of distribution coefficients measured at early stages of carbonate formation. Geochemical Journal 4, 183-206.

Krause, S., Hannah, D.M., Fleckenstein, J.H., Heppell, C.M., Kaeser, D., Pickup, R., Pinay, G., Robertson, A.L., Wood, P.J. 2011. Interdisciplinary perspectives on processes in the hyporheic zone. Ecohydrology 4, 481-499.

Kurz, M.J., deMontety, V., Martin, J.B., Cohen, M.J., Foster, C., In revision. Controls on diel metal cycles in a biologically productive carbonate-dominated river. Chemical Geology.

Kurz, M.J., Martin, J.B., Cohen, M.J., Douglass, R.L. Foster, C.R., In prep. Relationships between vegetation stoichiometry, assimilation, and diel element variation in a spring-fed river.

Kurz, M.J., Martin, J.B., de Montety, V., 2009. Pore-water chemistry in a spring-fed river: Implications for hyporheic control of nutrient cycling and speleogenesis. Geol. Soc. Am. Abstracts with Programs 41, 469.

Kurz, R.C., Woithe, D., Notestein, S.K., Frazer, T.K., Hale, J.A., Keller, S.R., 2004. Mapping and monitoring submerged aquatic vegetation in Ichetucknee springs. Report, Suwannee River Water Management District, Live Oak, Florida, pp. 135.

Kuwabara, J.S., 1992. Associations between benthic flora and diel changes in dissolved arsenic, phosphorus, and related physicochemical parameters. Journal of the North American Benthological Society 11, 218-228.

Leek, R., Wu, J.Q., Wang, L., Hanrahan, T.P., Barber, M.E., Qiu, H., 2009. Heterogeneous characteristics of streambed saturated hydraulic conductivity of the Touchet River, south eastern Washington, USA. Hydrol. Process. 23, 1236–1246.

Li, Y., Gregory, S., 1974. Diffusion of ions in sea water and in deap-sea sediments. Geochimica et Cosmochimica Acta 38, 703-714.

Liu, Z., Li, Q., Sun, H., Liao, C., Li, H., Wang J., Wu, K., 2006. Diurnal variations of hydrochemistry in a travertine-depositing stream in Baishuitai Yunnan, SW China. Aquatic Geochem. 12, 103-121.

Liu, Z., Liu, X., Liao, C., 2008. Daytime deposition and nighttime dissolution of calcium carbonate controlled by submerged plants in a karst spring-fed pool: insights from high time-resolution monitoring of physico-chemistry of water. Envir. Geol. 55, 1159-1168.

Lorens, R.B., 1981. Sr, Cd, Mn and Co distribution coefficients in calcite as a function of calcite precipitation rate. Geochim. Cosmochim. Acta 45, 553-561.

Luo, Y., Rimmer, D.L., 1995. Zinc copper interaction affecting plant growth on a metal-contaminated soil. Environmental Pollution 88, 79-83.

Malcolm, I.A., Soulsby, C., Youngson, A.F., Hannah, D.M., 2005. Catchment-scale controls on groundwater-surface water interactions in the hyporheic zone: implications for salmon embryo survival. River Research and Applications 21, 977-989.

Martin, J.B., Hartl, K., Corbett, R., Swarzenski, P., Cable, J.E., 2003. A multi-level pore water sampler for permeable sediments. Journal of Sedimentary Research 73, 128-132.

Martin, J. B., Dean, R.W., 2001. Exchange of water between conduits and matrix in the Floridan aquifer. Chem. Geol. 179, 145-165.

Martin, J. B., Gordon, S. L., 2000. Surface and ground water mixing, flow paths, and temporal variations in chemical compositions of karst springs. In Groundwater Flow and Contaminant Transport in Karst Aquifers. (I.E. Sasowsky and C. Wicks). Rotterdam, A.A. Balkema, 65-92.

McKnight, D.M., Kimball, B.A., Bencala, K.E., 1988. Iron photoreduction and oxidation in an acidic mountain stream. Science 240, 637-640.

McKnight, D.M., Kimball, B.A., Runkel, R.L., 2001. pH dependence of iron photoreduction in a rocky mountain stream affected by acid mine drainage. Hydrol. Proc. 15, 1979-1992.

Mettler, S., Wolthers, M., Charlet, L., von Guten, U., 2009. Sorption and catalytic oxidation of Fe(II) at the surface of calcite. Geochim. Cosmochim. Acta 73, 1826-1840.

Miretzky, P., Saralegui, A., Cirelli, A.F., 2004. Aquatic macrophytes potential for the simultaneous removal of heavy metals (Buenos Aires, Argentina). Chemosphere 57, 997-1005.

Moore, P.J., Martin, J.B., Screaton, E.J., 2009. Geochemical and statistical evidence of recharge, mixing and controls on spring discharge in an eogenetic karst aquifer. Journal of Hydrology 376, 443-455.

Morel, F.M.M., Price, N.M., 2003. The biogeochemical cycles of trace metals in the oceans. Science 300, 944-947.

Morris, J.M., Farag, A.M., Nimick, D.A., Meyer, J.S., 2006. Light-mediated Zn uptake in photosynthetic biofilm. Hydrobiologia 571, 361-371.

Morris, J.M., Nimick, D.A., Farag, A.M., Meyer, J.S., 2005. Does biofilm contribute to diel cycling of Zn in High Ore Creek, Montana? Biogeochemistry 76, 233-259.

Mouw, J.E.B., Stanford, J.A., Alaback, P.B., 2009. Influences of flooding and hyporheic exchange on floodplain plant richness and productivity. River Research and Applications 25, 929-945.

Naeem, A., Westerhoff, P., Mustafa, S., 2007. Vanadium removal by metal (hydr)oxide adsorbants. Water Research 41, 1596-1602.

Neal, C., Watts, C., Williams, R.J., Neal, M., Hill, L., Wickham, H., 2002. Diurnal and longer term patterns in carbon dioxide and calcite saturation for the River Kennet, south-eastern England. Sci. Total Environ. 282-283, 205-231.

Nimick, D.A., Cleasby, T.E., McCleskey, R.B., 2005. Seasonality of diel cycles of dissolved trace metal concentrations in a Rocky Mountain stream. Environ. Geol. 47, 603-614.

Nimick, D.A., Gammons, C.H., Cleasby, T.E., Madison, J.P., Skaar, D., Brick C.M., 2003. Diel cycles in dissolved metal concentrations in streams: Occurrence and possible causes. Water Resour. Res. 39, doi:10.1029/2002WR001571.

Nimick, D.A., Gammons, C.H., Parker, S.R., 2011. Diel biogeochemical processes and their effect on the aqueous chemistry of streams: A review. Chem. Geol. 283, 3-17.

Nyquist, J. Greger, M., 2007. Uptake of Zn, Cu, and Cd in metal loaded Elodea canadensis. Environmental and Experimental Botany 60, 219-226.

Odum, H. T., 1956. Primary production in flowing waters. Limnol. Oceanogr. 1, 102-117.

Odum, H. T., 1957. Trophic structure and productivity of Silver Springs, Florida. Ecological Monographs 27, 55-112.

Owens, M., 1974. Measurements on non-isolated natural communities in running waters. In A Manual on Methods for Measuring Primary Production in Aquatic Environments (ed. R. A. Vollenweider). Blackwell Scientific Publications. pp. 111-119.

Parker, S.R., Gammons, C.H., Fernando, L.P., Wood, S.A., 2008. Diel changes in metal concentrations in a geogenically acidic river: Rio Agrio, Argentina. J. Volc. Geothermal Res. 178, 213-223.

Parker, S.R., Gammons, C.H., Poulson, S.R., DeGrandpre, M.D., 2007. Diel variations in stream chemistry and isotopic composition of dissolved inorganic carbon, upper Clark Fork River, Montana, USA. Applied Geochem. 22(7), 1329-1343.

Parkhurst, D. L., Appelo, C.A.J., 1999. User's guide to PHREEQC (Version 2)-A computer program for speciation, reaction path, 1D-transport, and inverse geochemical calculations., U.S. Geological Survey Water-Resources Investigation Report 99-4259.

Peacock, C.L., Sherman, D.M., 2004. Vanadium(V) adsorption onto goethite (a-FeOOH) at pH 1.5 to 12: A surface complexation model based on ab initio molecular geometries and EXAS spectroscopy. Geochim. et Cosmochim. Acta 68, 1723-1733.

Perrin, J., Jeannin, P.-Y., Cornaton, F., 2007. The role of tributary mixing in chemical variations at a karst spring, Milandre, Switzerland. Journal of Hydrology 332, 158-173.

Persson, J., Fink, P., Goto, A., Hood, J.M., Jonas, J., Kato, S., 2010. To be or not to be what you eat: regulation of stoichiometric homestasis among autotrophs and heterotrophs. Oikos 119, 741-751.

Peterjohn, W.T., Correll, D.L., 1984. Nutrient dynamics in an agricultural watershed: Observations on the role of a riparian forest. Ecology 65, 1466-1475.

Pushnik, J.C., Miller, G.W., Manwaring, J.H., 1984. The role of iron in higher plant chlorophyll biosynthesis, maintenance and chloroplast biogenesis. Journal of Plant Nutrition 7, 733-758.

Reynolds, G.L. Hamilton-Taylor, J., 1992. The role of planktonic algae in the cycling of Zn and Cu in a productive soft-water lake. Limnology and Oceanography 37, 1759-1769.

Richard, F.C. Bourg, A.C.M., 1990. Aqueous geochemistry of chromium: A review. Water Research 25, 807-816.

Roberts, B.J., Mulholland, P.J., 2007. In-stream biotic control on nutrient biogeochemistry in a forested stream, West Fork of Walker Branch. Journal of Geophysical Research 112, G04002, doi:10.1029/2007JG000422

Robertson, W.D., Cherry, J.A., Sudicky, E.A., 1991. Ground-water contamination from two small septic systems on sand aquifes. Groundwater 29, 82-92.

Rosenberry, D.O., 2008. A seepage meter designed for use in flowing water. Journal of Hydrolog 359, 118-130.

Rosenberry, D.O., Striegl, R.G., Hudson D.C., 2000. Plants as indicators of focused ground water discharge to a northern Minnesota lake. Ground Water 38, 296-303.

Rusjan, S. Mikos, M., 2010. Seasonal variability or diurnal in-stream nitrate concentration oscillations under hydrologically stable conditions. Biogeochemistry 97, 123-140.

Salehin, M., Packman, A.I., Worman, A., 2003. Comparison of transient storage in vegetated and unvegetated reaches of a small agricultural stream in Sweden: seasonal variation and anthropogenic manipulation. Advances in Water Resources 26, 951-964.

Sand-Jenzen, K., Prahl, C., Stokholm, H., 1982. Oxygen release from roots of submerged aquatic macrophytes. Oikos 38, 349-354.

Saunders T. J., 2007. Multi-scale analysis of benthic biogeochemical properties and processing in a spring-fed river and estuary. Ph.D. thesis. Univ. of Florida.

Schwartz, M.O., Ploethner, D., 2000. Removal of heavy metals from mine water by carbonate precipitation in the Grootfontein-Omatako canal, Namibia. Environ. Geol. 39, 1117-1126.

Scott, D.T., McKnight, D.M., Voellker, B.M., Hrncir, D.C., 2002. Redox processes controlling manganese fate and transport in a mountain stream. Environ. Sci. Tech. 36, 453–459.

Shiraishi, F., Okumura, T., Takahashi, Y., Kano A., 2010. Influence of microbial photosynthesis on tufa stromatolite formation and ambient water chemistry, SW Japan. Geochim. Cosmochim. Acta 74, 5289-5304.

Shope, C.I., Xie, Y., Gammons, C.H., 2006. The influence of hydrous Mn-Zn oxides on diel cycling of Zn in an alkaline stream draining abandoned mine lands. Applied Geochemistry 21, 476-491.

Simonsen, J. F., Harremoës, P., 1978. Oxygen and pH fluctuations in rivers. Water Research 12, 477-489.

Smith, J.W.N., 2005. Groundwater-surface water interactions in the hyporheic zone. Environment Agency Science report SC030155/SRI.

Sophocleuous, M., 2002. Interactions etween groundwater and surface water: the state of the science. Hydrogeology Journal 10, 52-67.

Soulsby, C., Malcolm, I.A., Youngson, A.F., Tetzlaff, C.N., Gibbons, C.N., Hannah, D.M., 2005. Groundwater-surface water interactions in upland Scottish rivers: hydrologica, hydrochemical and ecological implications. Scottish Journal of Geology 41, 39-49.

Spiro, B., Pentecost, A., 1991. One day in the life of a stream - A diurnal inorganic carbon mass balance for travertine-depositing stream (Waterfall Beck, Yorkshire). Geomicrobiol. J. 9, 1-11.

SRWMD, 2003. Geostatistical analysis of water-level and water-quality data for the Ichetucknee springshed. Suwannee River Water Management District. Live Oak, FL, pp. 14.

SRWMD, 2007. Ichetucknee Springs Basin Map. Florida, Suwannee River Water Management District.

St-Cyr, L., Campbell, P.G.C., Guertin, K., 1994. Evaluation of the role of submerged plant beds in the metal budget of a fluvial lake. Hydrobiologia 291, 141-156.

Sterner, R.W., Clasen, J., Lampert, W., Weisse, T., 1998. Carbon:phosphorus stoichiometry and food chain production. Ecology Letters 1, 146-150.

Sterner, R. W., Elser, J.J., 2002. Ecological stoichiometry: the biology of elements from molecules to the biosphere. Princeton University Press.

Stevenson, R., Pinowska, A., Wang, Y.K. 2004. Ecological condition of algae and nutrients in Florida springs. WM858, Florida Department of Environmental Protection, Tallahassee, Florida, USA.

Stumm, W., Morgan, J.J., 1996. Aquatic Chemistry, third ed, Wiley Interscience, New York.

Sullivan, A.B., Drever, J.I., McKnight, B.N., 1998. Diel variation in element concentrations, Peru Creek, Summit County, Colorado. J. Geochem. Explor. 64, 141-145.

Sullivan, A.B., Drever, J.I., 2001. Spatiotemporal variability in stream chemistry in a high-elevation catchment affected by mine drainage. J. Hydrol. 252, 237–250.

Sunda, W.G. Huntsman, S.A., 1995. Iron uptake and growth limitation in oceanic and coastal phytoplankton. Marine Chemistry 50, 189-206.

Sunda, W.G., Huntsman, S.A., 1994. Photoreduction of manganese oxides. Mar. Chem. 46, 133–152.

Tesoriero, A.J., Pankow, J.F., 1996. Solid solution partitioning of Sr2+, Ba2+, and Cd2+ to calcite. Geochim. Cosmochim. Acta 60, 1053–1063.

Toth, D.J., Katz, B.G., 2006. Mixing of shallow and deep groundwater as indicated by the chemistry and age of karstic springs. Hydrogeology J. 14, 827-847.

Triska, F.J., Duff, J.H., Avanzino R.J., 1993a. The role of water exchange between a stream channel and its hyporheic zone in nitrogen cycling a the terrestrial-aquatic interface. Hydrobiology 251, 167-184.

Triska, F.J., Duff, J.H., Avanzino, R.J., 1993b. Patterns of hydrological exchange and nutrient transformations in the hyporheic zone of a gravel-bottom stream: examining terrestrial-aquatic linkages. Freshwater Biology 29, 259-274.

Triska, F.J., Kennedy, V.C., Avanzino, R.J., Zellweger, G.W., Bencala, K.E., 1989. Retention and transport of nutrients in a third-order stream: Channel processes. Ecology 70, 1877-1892.

Usdowski, E., Hoefs, J., Menschel, G., 1979. Relationship between 13C and 18O fractionation and changes in major element composition in a recent calcite-depositing spring – A model of chemical variations with inorganic CaCO3 precipitation. Earth and Planetary Science Letters 42, 267-276.

Vacher, H.L., Mylroie, J.E., 2002. Eogenetic karst from the perspective of an equivalent porous medium. Carbonates and Evaporites 17, 182-196.

Valett, H.M., Fisher, S.G., Grimm, N.B., Camill, P., 1994. Vertical hydrologic exchange and ecological stability of a desert stream ecosystem. Ecology 75, 548-560.

Valett, H.M., Morrice, J.A., Dahm, C.N., Campana, M.E., 1996. Parent lithology, surface-groundwater exchange, and nitrate retention in headwater streams. Limnol. Oceanogr. 41, 333-345.

Villares, R., Carral E., Puente, X., Carballeira, A., 2005. Metal levels in estuarine macrophytes: Differences among species. Estuaries 28,948-956.

Vincent, W.F. Downes, M.T., 1980. Variation in nutrient removal from a stream by watercess (Nasturtium officinale R. Br.). Aquatic Botany 9, 221-235

Vrede, T., Dobberfuhl, D.R., Kooijman, S., Elser, J.J., 2004. Fundamental connections among organism C:N:P stoichiometry, macromolecular composition, and growth. Ecology 85, 1217-1229.

Wang, W., Dei, R.C.H., 2006. Metal stoichiometry in predicting Cd and Cu toxicity to a freshwater green alga Chlamydomonas reinhardtii. Environmental Pollution 142, 303-312.

Wetland Solutions Inc., 2006. Ichetucknee River, Florida Ecosystem Evaluation and Impairment Assessment. Work Plan Report, 76 pp.

Zachara, J.M., Cowan, C.E., Resch C.T., 1991. Sorption of divalent metals on calcite. Geochim. Cosmochim. Acta 55., 1549-1562.

BIOGRAPHICAL SKETCH

Marie Kurz was born in Los Angeles, CA and tagged along with her scientist parents from there to Tucson, AZ, and on to Munich, Germany, before returning to the United States for university. Marie earned a Bachelor of Science (B.S.) in geology, environmental concentration, with a minor in anthropology from The College of William & Mary in 2007. While at W&M Marie worked with Professor Greg Hancock on a senior research thesis entitled *Looking for 'Landscape Knickzones' in the Virginia Piedmont: Evaluating Landscape Disequilibrium Through GIS-Based Analysis of Hillslopes and Channels*. After listening to a particularly eye-opening presentation on salt water intrusion at the 2006 Geological Society of America Fall Meeting Marie decided to leave geomorphology for hydrology and subsequently started her Ph.D. at the University of Florida in the fall of 2007. In addition to her doctoral studies and research Marie also participated in a National Science Foundation funded Integrated Graduate Education and Research Traineeship (IGERT) on the theme of Adaptive Management of Water, Watersheds and Wetlands. This IGERT program is largely responsible for the interdisciplinary direction Marie's research has taken.